Characterization of Human and Swine IFITM-Mediated Restriction of Influenza A Virus

---

Dissertation

zur

Erlangung der naturwissenschaftlichen Doktorwürde

(Dr. sc. nat.)

vorgelegt der

Mathematisch-naturwissenschaftlichen Fakultät

der

Universität Zürich

von

Caroline Lanz

von

Rütschelen BE

Promotionskommission

Prof. Dr. Silke Stertz (Vorsitz)

Prof. Dr. Alexandra Trkola

Prof. Dr. Christian Münz

Dr. Nicolas Ruggli

Zürich, 2017

Table of Contents

Research summary

Influenza A virus (IAV) is the causative agent of “influenza”, a febrile respiratory illness in humans. Yearly influenza epidemics impose a huge burden on human health and economy. Besides humans IAV also infects other species such as pigs and ducks and zoonotic spillovers of IAV into the human population can give rise to devastating pandemics.

To protect itself from viral invasion and to contain viral replication, a cell produces antiviral proteins that inhibit the virus at different stages of its life cycle. IFITM proteins are such antiviral proteins that have been described to potently block cellular entry of IAV as well as many other viruses in humans and mice. Since very little was known on IFITM proteins present in other species that are often infected by IAV we studied the IFITM proteins present in swine (swIFITMs), as described in Chapter 2. We identified two homologues of IFITM1 and one of IFITM2 and IFITM3 respectively in porcine cells, and all of them were found to be upregulated upon interferon(IFN)-stimulation or IAV infection. Furthermore, overexpression of swIFITMs potently restricted the replication of IAV strains of human and porcine origin in human as well as porcine cells. Importantly, knockdown of endogenous swIFITMs strongly diminished the antiviral activity of IFN in porcine cells. Thus, our study demonstrates the relevance of swIFITM proteins as potent mediators of the antiviral IFN response in porcine cells.

In Chapter 3 we present our studies on how IFITM proteins contribute to the cellular antiviral defense beyond their described function of blocking viral entry. We show that upon budding, IFITM3 is incorporated into IAV virions and VLPs and that this incorporation is associated with a decrease in viral/VLP HA levels. IAV VLPs produced in the presence of IFITM3 were reduced in their entry efficiency, an effect that could be counteracted in a dose-dependent manner by increasing amounts of HA. While the infectivity of IAV virions was not impaired by the presence of IFITM3 in virus producer cells, they showed increased neutralization sensitivity to an HA-directed antibody which might be to the virus’ detriment in an *in vivo* situation. Hence, we provide evidence that in addition to blocking viral entry, IFITM3 contributes to the antiviral defense during late stages of IAV infection by increasing the virus’ neutralization sensitivity.

In summary, the here presented studies establish swIFITM proteins as potent and relevant antiviral restriction factors and identified a role for IFITM3 during late stages of the IAV life cycle.

Zusammenfassung

Der Influenza A Virus (IAV) ist der Erreger der Grippe (med. Influenza), einer fiebrigen Erkrankung der Atmungsorgane des Menschen. Jährlich wiederkehrende Grippeepidemien belasten sowohl die menschliche Gesundheit als auch die Wirtschaft. IAV zirkuliert nicht nur im Menschen sondern auch in verschiedenen Tierarten, wie beispielsweise Schweinen und Enten. Dabei können sogenannte zoonotische Infektionen, Infektionen von Menschen mit einem Virus tierischen Ursprungs, verheerende Pandemien auslösen.

Um sich vor Viruserkrankungen zu schützen, und um die Virusreplikation im Falle einer Infektion einzudämmen, werden in der Zelle sogenannte antivirale Proteine produziert. Diese hemmen verschiedene Stadien des viralen Lebenszyklus. IFITM Proteine sind solche antiviralen Proteine, die das Eindringen von IAV, aber auch diversen anderen Viren, in Menschen – oder Mauszellen zu verhindern. Da nur sehr wenig bekannt war über IFITM Proteine in anderen Spezies, die oft von IAV infiziert werden, haben wir die IFITM Proteine im Schwein (swIFITMs) untersucht, wie in Kapitel 2 beschrieben. Dabei identifizierten wir in Schweinezellen zwei Homologe von IFITM1, und je eines von IFITM2 und IFITM3, die alle durch Interferon-Stimulation oder IAV Infektion induziert wurden. Zudem konnten wir zeigen, dass die Replikation von IAV Stämmen menschlichen oder porcinen Ursprungs durch die Überexpression von swIFITMs in humanen als auch porcinen Zellen gehemmt wurde. Bedeutenderweise führte das Stilllegen endogener swIFITM Proteine zu einer starken Verminderung der antiviralen Aktivität von Interferon in porcinen Zellen, womit diese Studie die Relevanz von swIFITM Proteinen als wichtige Bestandteile der Interferonantwort in porcinen Zellen demonstriert.

In Kapitel 3 beschreiben wir, wie IFITM3 zur zellulären antiviralen Abwehr jenseits der Hemmung des viralen Eintritts in die Zelle beiträgt. Wir zeigen, dass IFITM3 sowohl in Influenza virusähnliche Partikel (VLP), als auch in IAV Partikel eingebaut wurde, und dass dieser Einbau mit einer Reduktion des Hemagglutinin (HA) Levels einherging. Wurden VLPs in der Gegenwart von IFITM3 produziert, reduzierte sich dadurch ihre Infektiösität. Dem konnte jedoch durch Erhöhung der HA Level in VLP-produzierenden Zellen in dosisabhängiger Weise entgegengewirkt werden. Während, im Gegensatz zu VLPs, die Infektiösität von IAV Partikeln durch die Gegenwart von IFITM3 in Virus-produzierenden Zellen nicht gemindert wurde, waren diese IAV Partikel anfälliger für neutralisierende, gegen HA gerichtete Antikörper, was dem Virus *in vivo* potentiell nachteilig sein könnte. Somit konnten wir zeigen, dass IFITM3 zusätzlich zur Hemmung des viralen Eintritts in die Zelle, durch die Erhöhung der Empfindlichkeit des Virus gegenüber neutralisierenden Antikörpern, zur antiviralen Abwehr während späten Stadien des viralen Lebenszyklus beiträgt.

Zusammengefasst demonstrieren die hier präsentierten Studien die Relevanz von swIFITM Proteinen als wirksame antivirale Faktoren und offenbaren eine Rolle für IFITM3 während späten Stadien des viralen Lebenszyklus.

Abbreviations

25HC	25-hydroxycholesterol
BlaM1	β-lactamase-M1
BSA	bovine serum albumin
CARD	caspase-recruitment domain
CH25H	cholesterol-25-hydroxylase
CME	clathrin-mediated endocytosis
COPI	coat protein I
CPZ	chlorpromazine
CRM1	chromosome maintenance region 1
cRNA	complementary RNA
CT	cytoplasmic tail
DC	dendritic cell
DMEM	Dulbecco's Modified Eagle's Medium
EGFR	epidermal growth factor receptor
EIF2α	eukaryotic translation initiation factor 2α
Env	envelope glycoprotein
ER	endoplasmic reticulum
FCS	fetal calf serum
Fig.	figure
FPPS	farnesyl diphosphate synthase
FRAP	fluorescence recovery after photobleaching
GAF	IFN-γ activation factor
GAP	GTPase activating protein
GAS	gamma-activated sequence
GPI	glycophosphatidylinositol
HA	hemagglutinin
HCMV	human cytomegalovirus
HCoV-OC43	human coronavirus OC43
HIV	human immunodeficiency virus
HL	hemagglutinin-like
HPAI	highly pathogenic avian influenza
HTBE	human tracheobronchial epithelial cell
IAV	influenza A virus

IFITM	interferon-induced transmembrane protein
IFN	interferon
IFNAR	IFN-α receptor
IFNGR	IFN-γ receptor
IFNLR	IFN-λ receptor
IRF	IFN-regulatory factor
ISG	IFN-stimulated gene
ISRE	IFN-stimulated response elements
JAK	Janus kinase
JSRV	Jaagsiekte sheep retrovirus
LBPA	lysobisphosphatidic acid
LPAI	low pathogenic avian influenza
LRR	leucine-rich repeats
M1	matrix 1 protein
M2	matrix 2 protein
MAPK	mitogen-activated protein kinase
MAVS	mitochondrial antiviral-signaling protein
MDCK cells	Madin Darby canine kidney cells
MOI	multiplicity of infection
MTOC	microtubule organizing centre
Mx	myxovirus resistance protein
NA	neuraminidase
NEP	nuclear export protein
NES	nuclear export signal
NL	neuraminidase-like
NLRP	NOD-like receptor Family Pyrin Domain
NLS	nuclear localization signal
NP	nucleoprotein
NPC	nuclear pore complex
NPTr cells	newborn pig trachea cells
NS1	non-structural protein 1
NS2	non-structural protein 2
NSK cells	newborn swine kidney cells
OA	oleic acid
OAS	oligoadenylate synthetase

ORF	open reading frame
OSBP	oxysterol-binding protein
p.i.	post infection
p.i.DMEM	post infection Dulbecco's modified Eagle's medium
PAMP	pathogen-associated molecular patterns
PBSi	infection PBS
pDC	plasmacytoid DC
PEI	polyethylenimine
PK15 cells	porcine kidney 15 cells
PKR	protein kinase R
poly(I:C)	polyinosinic:polycytidylic acid
PRR	pattern-recognition receptors
Rack1	protein C kinase 1
RIG-I	**r**etinoic acid-inducible gene I
Rr	Pearson correlation coefficient
RSV	respiratory syncytial virus
RTK	receptor tyrosine kinase
SeV	Sendai virus
sialic acid	N-acetylneuraminic acid
SNP	single nucleotide polymorphism
STAT	Signal Transducers and Activators of Transcription
suppl.	supplementary
swIFITM	swine interferon-induced transmembrane protein
TEM	transmission electron microscopy
TGN	trans-Golgi network
TLR	Toll-like receptor
TMD	transmembrane domain
TYK	tyrosine kinase
VAPA	vesicle-membrane protein-associated protein A
VLP	virus-like particle
vRNP	viral ribonucleoprotein
w/v	weight per volume
WSN	A/WSN/33
wt	wild type

Chapter 1

INTRODUCTION

1.1 INFLUENZA VIRUS – A GENERAL INTRODUCTION

„Influenza“ or shortly „the flu“ describes a febrile respiratory illness in humans caused by influenza viruses [1]. Historical reports describing the occurrence of influenza-like diseases in humans and animals date back to the middle ages [2], suggesting that influenza viruses have been circulating for centuries. They impose a huge burden on human health and economy by causing seasonal epidemics that lead to the hospitalization of over 200’000 and the death of 30’000-50’000 people in the U.S. every year [4].

Based on their genome and protein composition influenza viruses can be classified into types A, B and C [1]. While type A has been shown to infect a wide variety of species such as humans, birds, pigs, seals, horses and dogs [7], type B and C have been found to be primarily human viruses [1].

Influenza A virus (IAV) strains are categorized into different subtypes according to their envelope glycoproteins hemagglutinin (HA) and neuraminidase (NA), their main antigenic determinants. Aquatic birds are the natural reservoir for IAV, and currently there are 16 different HA and 9 different NA subtypes circulating [1, 8]. Recently, IAV-like virus sequences were isolated from Central and South American bat species. The high seroprevalence of these IAV-like viruses in multiple bat species suggests that bats may represent another reservoir for influenza viruses [9, 10]. Interestingly, the bat HA-like (HL) H17 and H18 proteins lack sialic-acid binding, while bat NA-like (NL) N10 and N11 proteins lack neuraminidase function [11]. HL17NL10 and HL18NL11 have recently been rescued from synthetically derived cDNA and await their further characterization [12]. First studies performed with chimeric viruses harboring six bat IAV-like genes and HA and NA genes from a prototypic IAV strain showed no reassortment between bat IAV-like and prototypic IAV strains, suggesting that zoonotic IAV transmissions from bats to humans are not very likely to occur [13]. In contrast, reassortment between avian or porcine and human IAV strains does occur. The introduction of novel HAs into IAV strains circulating in humans can lead to pandemics due to the lack of protecting antibodies present in the population. This is exemplified by the “swine flu” pandemic in 2009/2010 that was caused by a reassortant H1N1 IAV that harbored an HA gene from swine IAV.

Currently IAV are kept in check by protective vaccination and, in case of infection, antiviral therapy. However, vaccination, as well as antiviral therapy have their shortcomings. Due to the high mutation rate in influenza viruses vaccinations need to be adapted every season to match the currently circulating virus strains. Current antiviral drugs include M2 ion channel inhibitors and neuraminidase inhibitors. However, resistance against ion channel inhibitors is widespread and can also arise against

neuraminidase inhibitors given the high mutation rate observed in IAV [14], highlighting the need for further understanding of the interplay between influenza viruses and their hosts to develop additional strategies to combat these viruses.

1.2 Classification & Architecture of Influenza A virus virions

IAV belongs to the family of *Orthomyxoviridae*, whose members are characterized by their single-stranded segmented RNA genome of negative sense [15]. Unlike most other RNA viruses, IAV genome transcription and replication take place in the nucleus of infected cells [16-18]. As a consequence, the virus benefits from access to the cellular splicing and 5'-cap machinery which increases its coding capacity [19].

The genome of IAV consists of 8 viral RNA segments, each of which is associated with an RNA-dependent RNA polymerase complex composed of PB1, PB2 and PA. The viral RNA itself is encapsidated by the nucleoprotein (NP). Viral RNA segments associated with their RNA polymerase and bound by NP are referred to as viral ribonucleoproteins (vRNPs) [20]. IAV is an enveloped virus that derives its membrane from its host cell upon budding. On the inside of the virions this membrane is lined by the viral matrix protein M1, as depicted in Figure 1 [15]. The only viral proteins exposed on the virion's surface are the hemagglutinin (HA), neuraminidase (NA) and matrix 2 (M2) proteins. While HA is responsible for the attachment of the virus to its cellular receptor sialic acid, NA cleaves the binding between HA and sialic acid and thus enables the release of budding viruses from the sialic acid containing surface of the virus-producing cell. M2 is a transmembrane protein forming ion channels in the viral membrane that allow the acidification of the virion core as the virus travels along the endocytic route. This acidification is thought to be required to weaken electrostatic interactions between M1 and vRNPs, thus facilitating the cytosolic release of vRNPs upon membrane fusion [21, 22].

Besides the structural proteins the virus also codes for several non-structural proteins that are expressed upon viral infection. mRNA transcribed from the NS segment is translated to the non-structural protein 1 (NS1) if unspliced, while the spliced mRNA gives rise to the non-structural protein 2 (NS2), also described as nuclear export protein (NEP). NS1 plays important roles in antagonizing the host's antiviral immune response, both by limiting the induction of the interferon (IFN) response and by blocking the antiviral proteins PKR and OAS. Furthermore, NS1 is involved in a plethora of different functions such as inhibition of cellular mRNA processing and export and activation of PI3K

[23]. NS2/NEP is required for the nuclear export of vRNPs [24]. In addition, it has been shown to regulate viral RNA transcription and replication [25].

The +1 reading frame of the PB1 gene segment gives rise to PB1-F2, a short peptide whose interaction with mitochondria leads to cytochrome c release and apoptosis in infected cells [26, 27]. Furthermore, PB1-F2 has been associated with an increase in inflammation and secondary bacterial infection in infected mice [28]. PB1 N40 is the third open reading frame (ORF) known to be translated from the PB1 mRNA to date. PB1 N40 arises through differential usage of start codons, resulting in a truncated version of PB1 that lacks its first 40 amino acids. PB1 N40 interacts with PB2 and PA, but fails to reconstitute a functional polymerase complex. It is non-essential for the virus but its loss can impair viral replication [29].

Spliced mRNA transcribed from the PB2 gene segment is translated to PB2-S1. Harboring an internal deletion, this form of PB2 localizes to mitochondria and has been reported to interfere with viral polymerase activity and the RIG-I-induced induction of IFN signaling. However, viruses lacking PB2-S1 show normal growth kinetics and immunopathology [30].

Apart from the RNA polymerase component PA, the PA gene segment has been reported to give rise to 3 additional viral proteins. The PA-X protein, consisting of the PA N-terminal and an alternative C-terminal domain results from ribosomal frameshifting. PA-X has been described to be involved in host-cell shutoff and viral immunopathology [31]. Usage of alternative in-frame AUG start codons yields PA-N155 and PA-N182. These truncated forms of PA do not show polymerase activity, however, in their absence viruses grow slower in tissue culture and show decreased pathogenicity in mice [32].

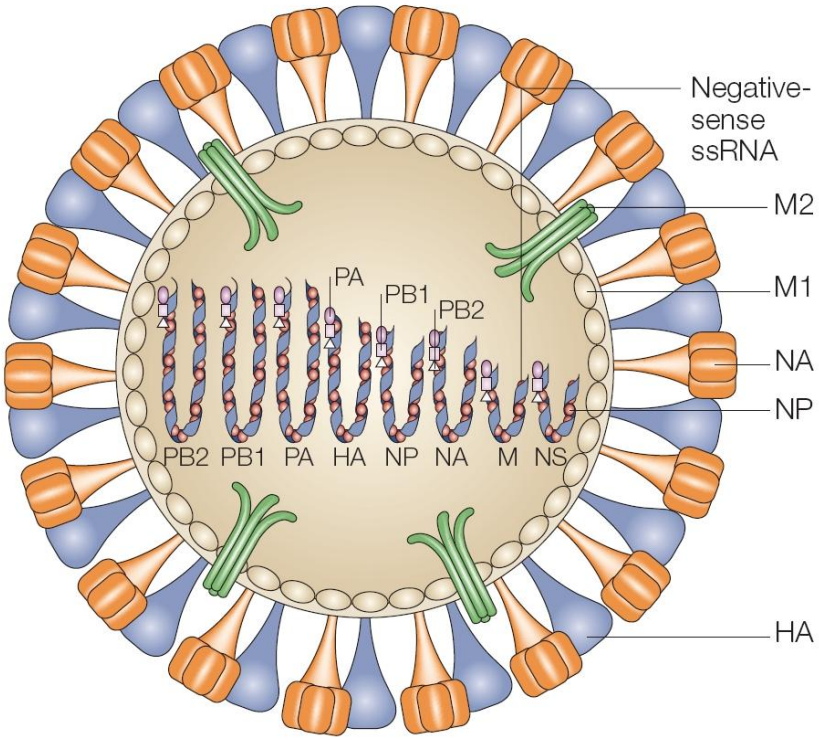

Figure 1: The structure of an IAV virion. IAV is enveloped by a host-cell-derived lipid membrane that harbors the surface glycoproteins HA and NA and the M2 ion channel. The segmented RNA genome of negative sense is tightly bound by NP proteins and associated with the polymerase complex consisting of PA, PB1 and PB2. M1 lines the inside of the virion, interacting with vRNPs and the viral envelope. [5]

1.3 THE INFLUENZA A VIRUS LIFE CYCLE

1.3.1 IAV BINDING TO HOST CELLS

The viral entry process is initiated upon engagement of HA glycoprotein trimers with their cellular receptor N-acetylneuraminic acid (sialic acid) [15, 33]. Sialic acids are typically linked to galactose and terminate oligosaccharide chains attached to cellular proteins [34]. While human IAV isolates preferentially bind to α2,6-linked sialic acids that are displayed in the human upper respiratory tract [35, 36], avian isolates show predominant binding to glycans displaying α2,3-linked sialic acids that are found in the gastrointestinal tract of birds [35, 37, 38].

HA is translated from HA mRNA as HA0, the uncleaved HA precursor. HA0 trimerizes in the endoplasmic reticulum (ER) before being routed to the cellular surface via the Golgi apparatus [39]. To become fusogenic, HA0 needs to be cleaved into its subunits HA1 and HA2 [40]. While HA1 harbors receptor-binding moieties, HA2 carries a hydrophobic fusion peptide at its N-terminus which is inserted into the target cell membrane upon fusion [41]. Cleavage of HA0 occurs at a specific arginine residue and is exerted by proteases present in either the trans-Golgi network, such as TMPRSS2, or on the cellular surface, as for example HAT [41]. The presence or absence of suitable proteases able to cleave HA0 affects virus tropism and systemic spread [40].

1.3.2 IAV ENDOCYTOSIS AND ENDOSOMAL TRAFFICKING

There are several ways for viruses get endocytosed into their target cells. Pinocytosis, the cellular uptake of extracellular fluid and its contents, can be divided into four distinct processes: clathrin-mediated endocytosis (CME), caveolae-mediated endocytosis, clathrin – and caveolae independent endocytosis and macropinocytosis [42]. CME describes the process of invagination of clathrin-coated pits at the plasma membrane that pinch off into the cytoplasm giving rise to clathrin-coated vesicles [43]. Caveolae-mediated endocytosis occurs at caveolin-1-enrichted domains of lipid rafts [44]. CME as well as caveolae-mediated endocytosis are dependent on dynamin, a GTPase that mediates scission of vesicles off the plasma membrane [45, 46]. In addition, several clathrin – and caveolin-independent endocytosis pathways have been described but their characterization remains challenging due to lack of suitable protein markers [47]. Stimulation of cells (for example by growth factors) can lead to “membrane ruffling”consisting of actin-driven protrusions of membranes. When collapsing onto and fusing with the plasma membrane, these protrusions engulf extracellular material, a process referred to as micropinocytosis [42].

Early electron microscopy experiments provided evidence that IAV can enter target cells via CME. However, the same studies also observed IAV present in uncoated vesicles and cell surface invaginations, suggesting IAV also uses pathways other than CME for cellular entry [48]. Indeed, blocking CME by treating cells with the CME inhibitor chlorpromazine or introducing a dominant-

negative mutant of a protein needed for CME (Eps15) did not inhibit IAV infection. Furthermore, IAV infection was left largely unaffected when caveolin-mediated endocytosis was prevented by treating cells with cholesterol-sequestering drugs (nystatin, methyl-β-cyclodextrin) [49]. A recent study corroborates the involvement of macropinocytosis in IAV cellular entry. In the presence of fetal calf serum IAV entry is completely abolished only if both, CME and macropinocytosis, are blocked by either chemical inhibitors or dominant-negative mutants [50].

For viruses entering via CME it has been observed that clathrin-coated pits form de novo at the site of viral attachment [51]. Epsin1, an adaptor protein able to interact with clathrin, ubiquitin and phospholipids has been shown to be recruited to these viral attachment sites and identified as essential for CME of IAV but not for other substrates of CME [52]. This suggests that viral cues are necessary for a successful entry process. However, how viral attachment is sensed and how the uptake of the virus is triggered remains elusive. Nevertheless, several studies provided evidence that downstream signaling processes do play a role in the uptake of IAV. The protein and lipid kinase PI3K is involved in several cellular processes such as growth, metabolism and survival. Interestingly, PI3K seems to regulate early steps of viral infection. Blocking PI3K with its inhibitor wortmannin prior to or early in infection reduced viral titers, while titers remained largely unaffected upon PI3K blockage later in infection [53]. IAV binding and PI3K activation might be linked through the activation of receptor tyrosine kinases (RTKs). Indeed, tyrosine kinase activity has been shown to be required for IAV uptake [54] and the RTK epidermal growth factor receptor (EGFR) was found to be involved in IAV uptake. Since the multivalent binding of IAV to target cells was found to lead to the clustering of lipid rafts, and EGFR is localized to those, the authors of this study speculated that lipid raft clusters might serve as signaling platforms activating RTKs required for viral uptake [54].

The endosomal system regulates the cellular distribution of vesicles and can be divided into three compartments: early endosomes, late endosomes and lysosomes. The early endosomes, localized close to the plasma membrane, are primarily responsible for protein sorting. Endosomal cargo can either be routed back to the plasma membrane via recycling endosomes (often happening for receptors displayed at the plasma membrane) or be sent along the endosomal pathway towards late endosomes and lysosomes localized in nuclear proximity [55]. Specificity of vesicular transport is ensured by Rab proteins. These monomeric GTPases selectively bind to specific vesicular membranes and mediate their transport and fusion. While Rab5 is associated with early endosomes, Rab7 is a marker for late endosomes [43]. Experiments performed with dominant-negative forms of Rab5 and Rab7 showed that IAV infection requires Rab5 as well as Rab7, confirming that IAV moves via early to late endosomes [56]. As endosomes mature travelling along the endocytic route their internal pH is

continuously decreased by V-ATPases that pump protons across their membrane [57]. IAV need to reach late endosomes where they are exposed to a low pH triggering conformational changes in HA that lead to fusion of the viral with the endosomal membrane [48, 58, 59].

1.3.3 IAV FUSION AND UNCOATING

When exposed to the acidic pH occurring in late endosomes, cleaved HA undergoes an irreversible conformational change that leads to the insertion of its hydrophobic fusion peptide (the N-terminal part of HA2) into the target cell membrane [39, 60-62]. To induce fusion between the viral and the target cell membrane HAs tilt, bringing the two membranes into close proximity [63]. Finally, membranes start to fuse and it is thought that a ring of fusogenic HA trimers locally limiting lipid flux allows for the opening of a fusion pore through which vRNPs are delivered to the cytoplasm [39, 64].
Acidification of endosomes is not only required to trigger HA-mediated fusion, but also to weaken interactions between vRNPs and M1. The M2 ion channel pumps protons into the viral lumen, inducing a conformational change in M1 that leads to its dissociation from vRNPs. Free vRNPs can then be delivered to the cytoplasm and this process is called uncoating [65-68].

1.3.4 vRNP NUCLEAR IMPORT

As a nuclear-replicating virus, IAV needs to deliver its genome into the host cell's nucleus for successful viral replication [16]. While small proteins can pass the nuclear membrane via passive diffusion, larger proteins and complexes need to interact with the nuclear import machinery to be funneled through nuclear pore complexes [19]. It has been shown that naked IAV RNA is no substrate for nuclear translocation but needs to be bound by NP to get imported into the nucleus. NP harbors nuclear localization signals (NLS) that mark it as substrate for nuclear import [69]. Importantly, these NLS are masked by binding of M1 to NP, highlighting the importance of the uncoating process [19]. The other components of the vRNP, PB1, PB2 and PA, have also been shown to harbor NLS [70-72]. However, to date it is not known whether those also contribute to vRNP import.

1.3.5 TRANSCRIPTION AND REPLICATION OF THE IAV GENOME

Once inside the nucleus, the viral genome is transcribed into mRNA in a process called primary transcription. Due to its RNA genome of negative polarity IAV cannot make use of the host cell's transcription machinery, but relies on its RNA-dependent RNA polymerase complex composed of PB1, PB2 and PA [73]. Deficient in mRNA 5'-capping, IAV performs the so-called "cap-snatching" to get access to 5'-capped mRNA primers. While PB2 and PA have both been shown to bind to host-derived 5'-capped mRNA, endonuclease function necessary to cleave off 5'-capped mRNA primers has been mapped to PA [73-75]. PB1 in turn has been found to be responsible for mRNA chain elongation and harbors the actual RNA polymerase function [76]. It is thought that the polymerase

complex remains associated with the 5’ end of the viral RNA, while the template is funneled through the PB1 active site in the 3’-5’ direction, giving rise to nascent mRNA. Once the polyU sequence, encoded approximately 16 nucleotides from the vRNA 5’ end, reaches the PB1 active site, the template cannot be funneled any further due to sterical hindrance. Template slipping on the polyU sequence subsequently leads to the addition of a polyA tail to the viral mRNA [73]. Although not resolved entirely, there is evidence for viral mRNAs using the normal host cell machinery for splicing, nuclear export and translation [77].

To generate a template for viral genome replication, vRNA is first transcribed into complementary RNA (cRNA). cRNA lacks a 5’-cap as well as a polyA tail and is thus distinct from viral mRNA [73]. Although still under debate, there is strong evidence for a model explaining the switch from mRNA to cRNA production. In this model, vRNA is transcribed to mRNA by the incoming polymerase associated with the viral RNA during infection, while cRNA production is mediated by newly produced polymerase complexes [78, 79]. Fittingly, de novo synthesis of viral proteins has been found necessary for viral genome replication [80]. Interestingly, other studies also highlight the importance of viral protein synthesis for genome replication, but they hypothesize that cRNA is rapidly degraded by endonucleases if not stabilized by NP and the polymerase complex [81].

1.3.6 Late stages of the IAV life cycle

After successful genome replication vRNPs need to be transported out of the nucleus and trafficked to the plasma membrane where virus assembly takes place. Similarly, viral structural proteins and envelope glycoproteins need to be localized to virus assembly sites to allow the formation of new IAV particles and their budding from the plasma membrane. Current knowledge on late stages of the IAV life cycle and the interplay between IAV and its host is summarized in chapter 5 in the review from Pohl, M.O., Lanz, C. and Stertz, S. *Late stages of the influenza A virus replication cycle – a tight interplay between virus and host*. J Gen Virol, 2016 that I contributed to [82].

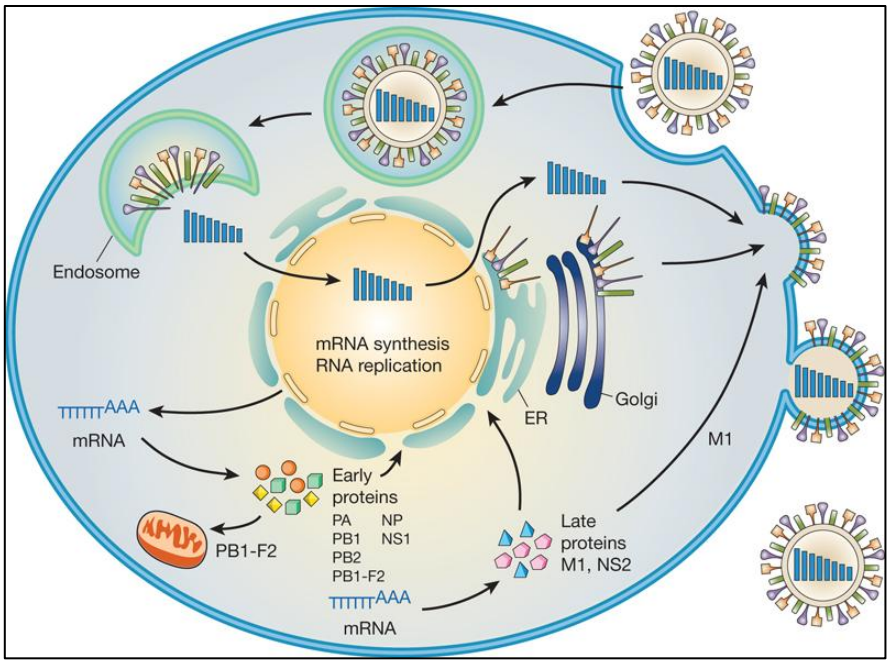

Figure 2: The IAV life cycle. After receptor-mediated endocytosis, IAV travels along the endocytic route. Upon acidification in late endosomes HA undergoes a conformational change, leading to fusion between the viral and the endosomal membrane. vRNPs are subsequently released into the cytoplasm and trafficked to the nucleus, where primary transcription and replication take place. Early proteins are translocated to the nucleus where they are involved in genome replication and vRNP assembly. Finally, vRNPs and viral proteins are trafficked to the plasma membrane, where new IAV virions bud from lipid rafts [3].

1.4 THE ZOONOTIC POTENTIAL OF INFLUENZA A VIRUS

IAV has been shown to infect various animal species such as birds, swine, dogs, horses and bats [7]. Although IAV strains are highly adapted to their hosts in terms of receptor binding, host factor usage and counteraction of the immune system (among others), occasional "jumps" of IAV from one species to another occur [7, 83]. Due to their segmented genome IAV strains can reassort when infecting the same cell [15, 84]. Invading viruses can thus swap gene segments with viruses already circulating in and thus adapted to the host [85, 86]. Together with the fact that IAVs harbor an error-prone RNA-dependent RNA polymerase [87] this facilitates and accelerates the emergence of IAV strains adapted to replicate in a new host [85, 86].

Historically, this proved especially fatal when IAV crossing the species barrier displayed HAs the population was immunologically naïve to [7]. From 1918-1919, the pandemic known as "The Spanish Flu" caused by an avian-like H1N1 IAV strain killed approximately 50 million people. While the pandemic potential of this virus can be explained by the lack of protecting antibodies circulating in the population, its unprecedented severity remains a matter of study [3]. Since then, the human population repeatedly suffered from pandemics caused by human/avian or human/avian/swine IAV reassortants [3, 7].

Pigs have been hypothesized to play a crucial role in giving rise to human IAV pandemics. They have been shown to display α2,3 – as well as α2,6-linked sialic acid residues in the trachea, which renders them susceptible to infection with avian IAV strains that preferentially bind to α2,3-linked sialic acid, as well as human IAV strains showing preferential binding to α2,6-linked sialic acid [88]. This is exemplified by the pandemic H1N1 IAV strain that started to circulate in the human population in 2009 . IAV from porcine, avian and human origin gave rise to a triple-reassortant virus maintained in pigs. Further reassortment with an avian-like swine IAV finally yielded an IAV strain able to ignite a pandemic in humans (Fig. 3) [3]. Importantly, reassortment in pigs does not seem to be a prerequisite for avian or swine IAV to infect humans, as several direct transmission events suggest [89-94]. However, none of those resulted in sustained IAV human-to-human transmission [7]. Concludingly, to detect potentially pandemic zoonotic IAV strains as early as possible, careful monitoring of the circulating IAV strains is necessary [95]. Nevertheless, since vaccine production may take too long and antiviral drugs may not be effective or sufficiently available in case of a pandemic, research focusing on a vaccine that induces broadly-neutralizing antibodies against IAV is driven forward [3, 96].

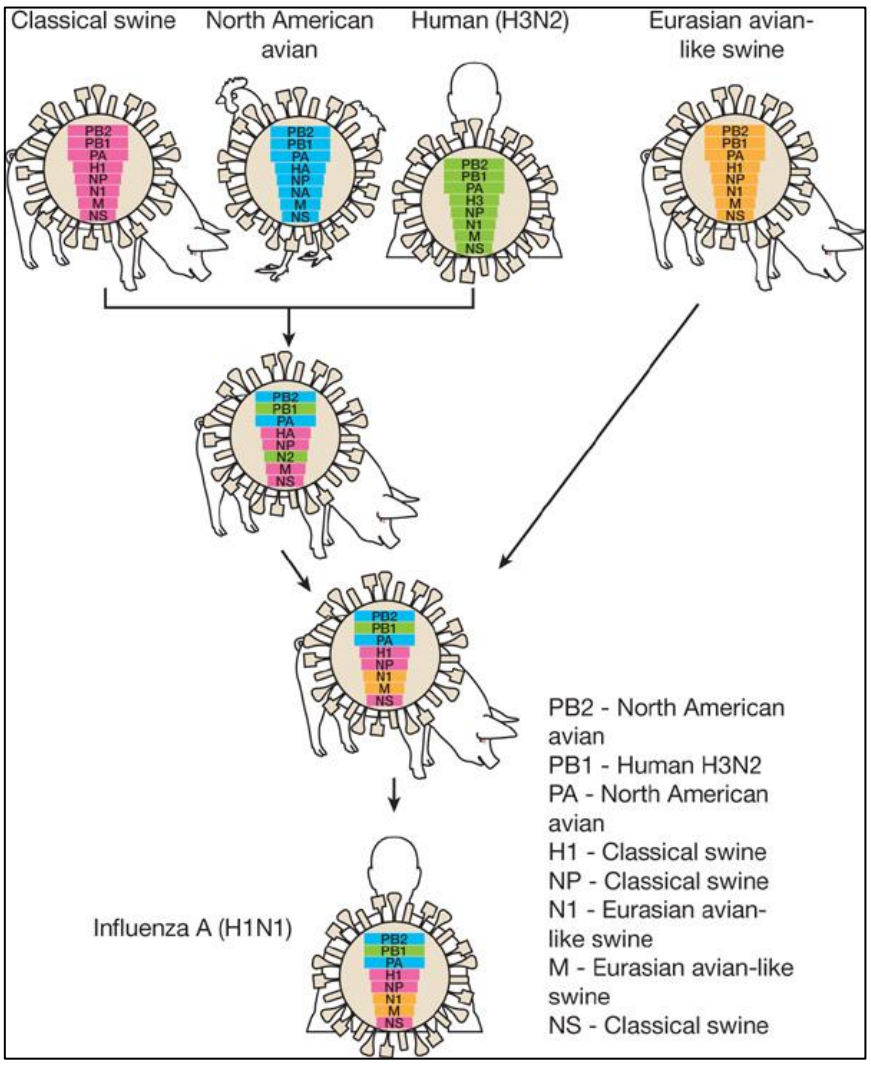

Figure 3: The source of swine-origin 2009 pandemic H1N1 IAV. IAV strains from porcine, avian and human origin gave rise to a triple-reassortant IAV strain in pigs. Subsequent reassortment with an Eurasian avian-like IAV strain yielded the 2009 pandemic H1N1 IAV strain. [3]

1.5 THE INTERFERON SYSTEM

1.5.1 INTRODUCTION

The concept of “viral interference”, the observation that infection of a bacterial, plant or animal cell with a virus can protect this cell from further viral infection [97] led the foundation for the discovery of the interferon system. Groundbreaking work performed by Isaacs and Lindenmann [98, 99] in the 1950s led to the discovery of interferon (IFN), described as a factor released from chick chorio-allantoic membrane upon incubation with heat-inactivated IAV that could interfere with IAV infection in a fresh piece of chorio-allantoic membrane. Further studies showed that IFNs are proteins secreted by one cell upon detection of pathogen-associated molecular patterns (PAMPs) and sensed by another through binding to specific receptors. IFN signaling results in the transcription of interferon-stimulated genes (ISGs) that induce an antiviral state, but also affects numerous cellular processes such as motility, proliferation and immunological responses [100, 101]. Based on their receptor usage, IFNs can be divided into three classes: type I, type II and type III IFNs. Type I IFNs signal through the IFN-α receptor 1 (IFNAR1)/IFN-α receptor 2 (IFNAR2) heterodimeric receptor complex and comprise IFN-α, IFN-β, IFN-ε, IFN-κ and IFN-ω in humans [6]. These different IFN subclasses induce distinct cellular functions thought to be mediated at least partially by differential receptor affinity and stability of the IFN/IFNAR complexes [102, 103].

The homodimeric IFN-γ, signaling through the IFN-γ receptor (IFNGR), is the only member of type II IFN known to date. IFN-γ is mainly produced by immune cells, but can be sensed by a wide variety of target cells, especially in epithelial tissues [104].

Type III IFNs comprise IFN-λ1, IFN-λ2, IFN-λ3 and IFN-λ4 [105-107]. Distantly related to the IL-10 family of interleukins, type III IFNs signal through heterodimeric complexes of IL-10R2 and IFN-λ receptor 1 (IFNLR1) [105, 106]. Only epithelial cells have been found to be responsive to IFN-λ, possibly protecting the host from pathogens infecting through mucosal surfaces [108].

1.5.2 IFN SIGNALING

All types of IFN rely on the Janus kinases (JAKs) and the Signal Transducers and Activators of Transcription (STATs) to translate the binding of IFN receptors by their ligands into a cellular response, as depicted in Figure 4. JAKs involved in IFN signaling comprise JAK1, JAK2 and tyrosine kinase 2 (TYK2) and are associated with the cytoplasmic portion of IFN receptor chains [6]. All STATs known to be expressed in mammals (STAT1, STAT2, STAT3, STAT4, STAT5a, STAT5b and STAT6) seem to participate in innate immune signaling [109]. However, mainly STAT1 and STAT2 have been found to be involved in IFN signaling.

Upon binding of IFN to its receptor, the individual receptor chains are brought closely together, resulting in the juxtaposition of the associated JAKs that subsequently undergo transphosphorylation

and thus activation [110, 111]. Activated JAKs phosphorylate their IFN receptor chains, generating a binding interface for SH2-domains on STAT proteins. Binding of STAT proteins to the IFN receptor chains brings them into close proximity of and leads to their phosphorylation by JAKs. Phosphorylated STATs form homo – or heterodimers that translocate to the nucleus where they drive the expression of IFN-stimulated genes (ISGs) [110, 112].

More precisely, signaling via type I and type III IFN leads to the formation of phospho-STAT1/phospho-STAT2 heterodimers that recruit the IFN-regulatory factor 9 (IRF9), combining into the IFN-stimulated gene factor 3 (ISGF3). ISGF3 translocates to the nucleus and binds to IFN-stimulated response elements (ISRE) that are localized upstream of ISGs. In contrast, type II IFN signaling leads to the formation of homodimers of phospho-STAT1 called IFN-γ activation factor (GAF). GAF also translocates to the nucleus, but instead of binding to ISRE it binds to gamma-activated sequence (GAS) promoters that drive the expression of GAS-responsive ISGs [6].

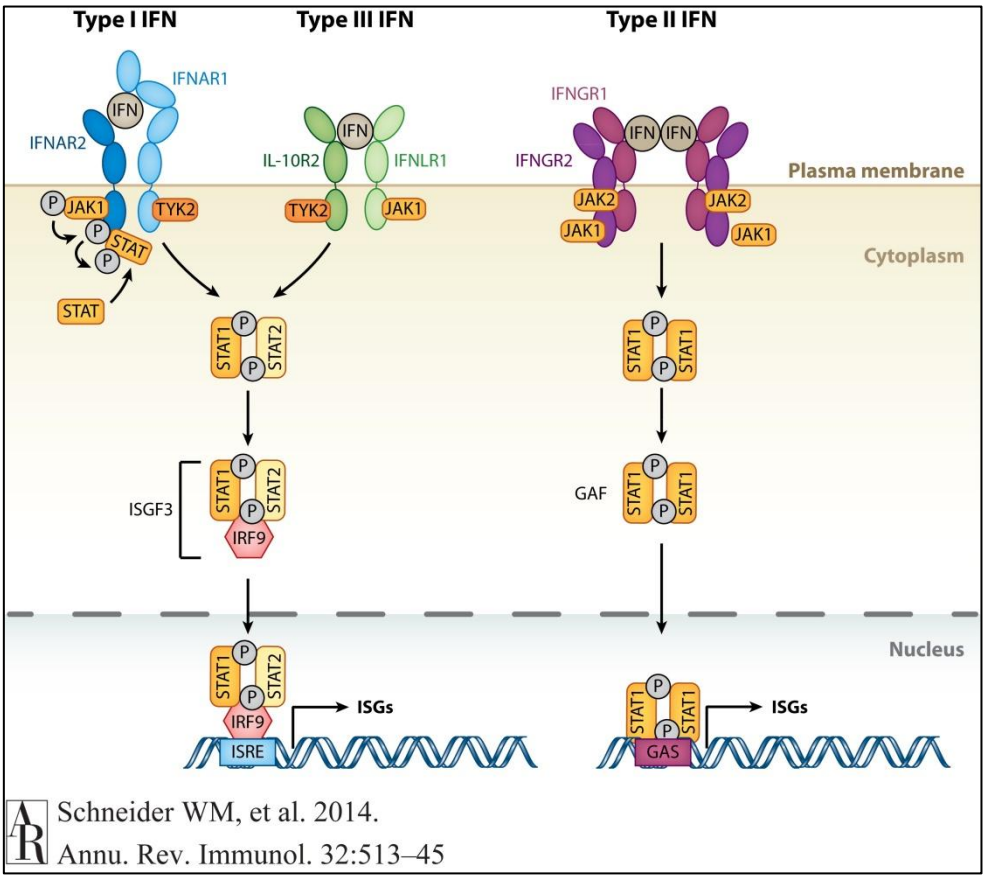

Figure 4: The interferon (IFN) signaling pathway. Type I, II and III IFN bind to and signal via specific IFN receptors. Binding of IFNs to their cognate receptors triggers the autophosphorylation of receptor-associated kinases that in turn phosphorylate specific receptor residues, enabling the recruitment and phosphorylation of STAT proteins. Type I and III IFN signaling results in the formation of phosphorylated STAT1-STAT2 heterodimers that associate with IRF9 to translocate to the nucleus to initiate ISRE-mediated transcription of ISGs. In contrast, type II IFN signaling results in the formation of phosphorylated STAT1 homodimers that drive GAS-mediated transcription of ISGs. [6]

Importantly, the interferon signaling cascade described here is simplified. Some examples for more elaborate mechanisms include IRFs recognizing parts of ISREs, cooperation of STATs with other transcription factors (such as IRFs) and epigenetic modifications of DNA stretches accessed by STATs. This drastically increases the complexity but also the potential for fine-tuning of the system [113].

1.5.3 Innate immune signaling upon IAV infection

To sense invading pathogens cells are equipped with so-called pattern-recognition receptors (PRRs) that induce immune signaling upon detection of non-self motifs, called pathogen-associated molecular patterns (PAMPs) [114]. These PAMPs include for example the lipopolysaccharides displayed on the membrane of Gram-negative bacteria or dsRNA present during viral infections [115, 116]. Several PRRs are involved in the sensing of IAV and are discussed in the following sections.

1.5.3.1 Toll-like receptors (TLRs)

TLRs are transmembrane proteins harboring a ligand-binding domain at the N – and a cytoplasmic signaling domain at the C – terminus [117]. TLR3 has been shown to localize to endosomes [118], where it detects dsRNA and subsequently induces the production of type I interferons and NF-κB-dependent transcription [119]. In agreement with the fact that no dsRNA should be exposed on endosomal incoming IAV particles it has been shown that TLR3 activation in dendritic cells (DCs) depends on phagocytosis of infected cells [120] that have been hypothesized to contain RNA structures able to induce TLR3 signaling [121]. In contrast, TLR7, another endosomally localized TLR, has been found to directly respond to IAV by sensing ssRNA upon infection of plasmacytoid DCs (pDCs). Subsequent immune signaling leads to type I IFN and inflammatory cytokine production [122, 123]. The authors hypothesize that endosomal proteases might lead to a certain degree of IAV degradation, thereby exposing its ssRNA genome [122].

1.5.3.2 Retinoic acid-inducible gene I (RIG-I)

Studies performed in RIG-I deficient mouse fibroblasts and DCs established this cytosolic RNA helicase as an important mediator of type I IFN signaling upon RNA virus infection [124]. More precisely, RIG-I has been shown to get activated by virus-specific 5'-mono and -triphosphate ssRNA [125-127]. However, also dsRNA and polyU sequences have been shown to trigger RIG-I-mediated signaling [128-130]. ATP is recruited to RIG-I upon binding of viral RNA, facilitating a conformational change liberating RIG-I's caspase-recruitment domains (CARDs) [115, 131, 132]. CARDs subsequently interact with mitochondrial antiviral signaling (MAVS) adaptor proteins, resulting in the recruitment of a myriad of signaling molecules leading to NF-κB-, IRF3-, and IRF7-dependent transcription of antiviral genes [128, 133].

The importance of RIG-I in the antiviral immune response against IAV has been corroborated by the finding that IAV evolved measures to counteract its action: NS1 has been shown to bind to RIG-I, thereby inhibiting its activation [125].

1.5.3.3 NOD-LIKE RECEPTOR FAMILY PYRIN DOMAIN CONTAINING 3 (NLRP3)

Nucleotide-binding oligomerization domain-like receptors (NOD-like receptors or NLRs) are cytosolic PRRs expressed in immune as well as epithelial cells. They harbor a variable effector domain in their N-terminus and leucine-rich repeats (LRRs) in their C-terminus that are responsible for ligand binding [134]. Stimulation of NLRs induces the formation of the so-called "inflammasome": the oligomerization of NLRs and their association with adaptor proteins and pro-caspases. The subsequent activation of caspases promotes the maturation of the proinflammatory cytokines pro-IL-1β and pro-IL-18 into their mature forms that can then be secreted [135].

NLRP3 is an NLR harboring a pyrin domain in its effector domain [136]. Upon IAV infection, this pyrin domain interacts with the pyrin domain of its adaptor protein, the inflammasome is assembled and pro-inflammatory cytokines are secreted [137]. Two components of IAV have been observed to induce NLRP3 activation: ssRNA [138] and PB1-F2 [139]. Furthermore, M2 ion channel activity in IAV-infected cells has been shown to trigger NLRP3 activation, possibly through proton imbalance in the cytoplasm [140]. *Nlrp3* knockout mice have been shown to be compromised in their immune response upon IAV infection, which was associated with an increase in mortality, highlighting NLRP3's relevance *in vivo* [141].

Although countless *in vitro* and *in vivo* studies established the importance of the different PRRs in sensing IAV in order to mount an antiviral immune response, the individual contribution of and potential redundancies between different PRRs are not resolved entirely and have been described to be cell type-dependent [124].

1.5.4 SELECTED ISGS WITH ACTIVITY AGAINST IAV

1.5.4.1 MYXOVIRUS RESISTANCE PROTEIN (MX)

The observation that mice of a particular strain survived IAV challenges found to be lethal in other strains led to the discovery of Myxovirus resistance protein 1 (Mx1) [142]. Mx1 is expressed in wild mice but absent from most laboratory mouse strains due to deletions and nonsense mutations in the Mx1 locus [143, 144].

Mx proteins are dynamin-like GTPases induced by type I and type III IFN [145]. In mice, Mx1 has been identified as one of the most effective ISGs combating IAV infections. Further studies described the

presence of Mx proteins in almost all vertebrate species, where they exert diverse antiviral functions against a broad range of RNA as well as DNA viruses [146].

Human cells express two types of Mx proteins: MxA present in the cytoplasm [147] and MxB localized to the cytoplasmic side of nuclear pores [148, 149]. Only MxA has been found to restrict IAV infection and will therefore be discussed in further detail [150-152]. Essentially two models have been described explaining the mechanism of MxA's antiviral action. Based on crystal structures, one model suggests the assembly of MxA into oligomeric rings around incoming vRNPs, thereby leading to their disintegration [153]. However, this model is challenged by the fact that MxA had previously been observed to block IAV at a step after primary transcription [152]. The second model proposes an interaction of MxA dimers with *de novo* produced NP in the cytoplasm that restricts viral replication [154]. In agreement with both models, several studies identified the viral NP protein as determinant for MxA sensitivity, hence NP mutants evading MxA restriction have been described [155, 156].

1.5.4.2 PROTEIN KINASE R (PKR)

PKR is a constitutively expressed but IFN-inducible serine/threonine kinase. Upon binding to dsRNA, 5'-triphosphate ss-dsRNA (dsRNA with a single-stranded tail) or IAV vRNPs (most likely its pan-handle structure) [157, 158] PKR gets activated through autophosphorylation [159]. Activated PKR phosphorylates eukaryotic translation initiation factor 2α (EIF2α), thereby preventing translation initiation [160, 161]. As viruses depend on their host cell's translation machinery, this strongly reduces viral replication [157]. In addition, activated PKR phosphorylates the inhibitor of NF-κB, thereby enabling NF-κB-dependent transcription of antiviral genes such as IFN-β [162]. PKR knockout mice showed increased susceptibility to IAV infection, establishing PKR as an important antiviral factor *in vivo* [163]. The fact that IAV evolved measures to counteract the activity of PKR further corroborates its *in vivo* relevance: NS1 has been shown to bind to PKR, thereby inhibiting its activation [164].

1.5.4.3 2',5'-OLIGOADENYLATE SYNTHETASE (OAS)/RNASEL

The 2',5'-oligoadenylate synthetase (OAS)/RNAseL system has been shown to lead to the degradation of cytoplasmic RNAs. Upon activation by dsRNA (or ssRNA forming a stem structure), OAS polymerizes ATP to 2'-5' adenosine oligomers that activate the endoribonuclease RNAseL which cleaves cytoplasmic RNA [165, 166]. IAV has been shown to avert endonuclease restriction of its RNA by inhibiting OAS activation through the action of NS1. By binding to dsRNA, NS1 potentially sequesters cytoplasmic RNA that could otherwise activate OAS [167].

1.5.4.4 CHOLESTEROL-25-HYDROXYLASE (CH25H)

CH25H, upregulated in macrophages and DCs upon IFN stimulation or TLR activation [168, 169], catalyzes the oxidation of cholesterol to 25-hydroxycholesterol (25HC) [170]. 25HC has been shown to inhibit a wide variety of enveloped viruses, such as IAV, HIV, VSV and HSV at the step of viral fusion [171, 172]. Increased 25HC concentrations seem to perturb cellular cholesterol homeostasis and lead to membrane modifications. Although the nature of these modifications has not been resolved completely, changes in membrane expansion, curvature or fluidity have been suggested and it was hypothesized that those perturbations of the host cell membrane interfered with the fusion process [171]. Interestingly, in addition to its direct antiviral role 25HC has also been shown to amplify inflammatory signals by increasing transcription of inflammatory cytokines. Intriguingly, deletion of the CH25H locus in mice was shown to be protective against IAV challenges lethal in wild type (wt) mice, most likely due to a decrease in inflammatory pathology [173].

1.5.4.5 INTERFERON-INDUCED TRANSMEMBRANE PROTEINS (IFITMS)

The first description of IFITMs dates back to the early 1980ies when they were identified as IFN-stimulated genes in neuroblastoma cells [174]. Subsequent studies reported their upregulation in response to type I and type II IFNs [175]. However, for many years their antiviral potential remained undiscovered and their role was assigned to germ cell specification [176], transduction of anti-proliferative and cell adhesion signals [177, 178] and immune cell signaling [179-181]. Two studies published in the late 1990ies and the early 2000s for the first time linked IFITMs to antiviral activity. IFITM1 was described to partially inhibit VSV [182] and IFITM3 was shown to impede hepatitis C virus RNA replication [183]. However, it was not until 2009 that the broad and potent antiviral potential of IFITM proteins was discovered in an siRNA screen and their antiviral activity against IAV, West Nile Virus and Dengue Virus demonstrated in tissue culture experiments [184]. Studies comparing IAV growth and pathology in IFITM3 wt vs. knockout mice observed accelerated disease progression, increased mortality and higher viral burdens in the absence of IFITM3 [185, 186]. Interestingly, IFITM3 knockout mice and mice having the entire IFITM locus deleted showed the same disease phenotype, suggesting that in mice protection against IAV is solely mediated by IFITM3 [185]. Further adding to the *in vivo* relevance of IFITM3, genome-wide association studies in humans hospitalized with a severe course of IAV infection during the swine flu pandemic in 2009 identified a single nucleotide polymorphism (SNP) in IFITM3 that leads to the generation of a splice acceptor site resulting in a truncated form of IFITM3 that lacks its first 21 amino acids (IFITM3 NΔ21). This shortened form of IFITM3 has been found less efficient in IAV restriction [186]. Authors analyzing different patient cohorts confirmed the association of this particular SNP in IFITM3 and the increased risk of a) acquiring IAV and b) suffering from a severe course of infection [187]. However, the

decrease in virus restriction capacity of IFITM3 NΔ21 could not be confirmed in another study that observed similar anti-IAV activities for IFITM3 and IFITM3 NΔ21 [188]. Nevertheless, many studies confirmed the importance of IFITMs, mostly IFITM3, as antiviral factors and demonstrated the IFITM-mediated restriction of a vast variety of viruses, such as HIV [189, 190], VSV [191], Zika virus [192]), Ebola virus [193], and Rift Valley Fever virus [194].

IFITMs can be categorized into three subfamilies: immunity-related IFITMs (IFITM1-3 in humans), IFITM5 and IFITM10 [195]. Only immunity-related IFITMs have been shown to be induced by IFN [174, 175]. The presence of various immunity-related IFITMs next to each other on the same chromosome in most vertebrate species suggests that they arose through gene duplication. Together with the fact that they have been shown to be under positive selection and to protect against a variety of different viruses suggests that they are involved in the co-evolution of viruses and their hosts [195]. IFITM5 is exclusively restricted to bone cells, mostly osteoblasts, where it is involved in bone mineralization and maturation [196]. So far, no role could be assigned to IFITM10 but positive selection and gene duplication events in aquatic vertebrates suggests that IFITM10 might play a role in the adaptation to the aquatic environment [195].

IFITM proteins belong to the family of dispanins that comprises proteins harboring two transmembrane domains. Due to the presence of dispanins in several different phyla of bacteria one might speculate that they were acquired by eukaryotes through horizontal transmission [197]. IFITM proteins all follow the same architecture: a conserved CD225 middle domain is flanked by a variable N – and C – terminus, while the two transmembrane domains are located in the CD225 domain and at the transition between CD225 domain and C-terminus [195]. The transmembrane topology of IFITM proteins has been a matter of debate though. While some studies reported the accessibility of the N – and C – terminus by antibodies in unpermeabilized cells [179, 184, 191, 198] (Fig. 4a), others convincingly showed that the N-terminus is ubiquitylated [199] as well as phosphorylated [200], implying its accessibility by cytoplasmic enzymes (Fig. 5b/c). Introduction of a prenylation motif into the IFITM C-terminus allowed for its prenylation in the cytoplasm, proposing its cytoplasmic localization [199] (Fig. 5b). This study was challenged by another that reported the retention of IFITM3 in the ER, when an ER retention motif was added to the C-terminus [201] (Fig. 5a/b). The partial consensus of all these studies seems to be a type II transmembrane topology of IFITM proteins, as seen in Fig. 5c [202]. Nevertheless, the study describing a type II transmembrane topology for IFITM3 also reported that a minor fraction of IFITM3 had its N-terminus facing the ER lumen, suggesting that IFITMs could adopt different membrane topologies, thereby reconciling conflicting literature [201, 202].

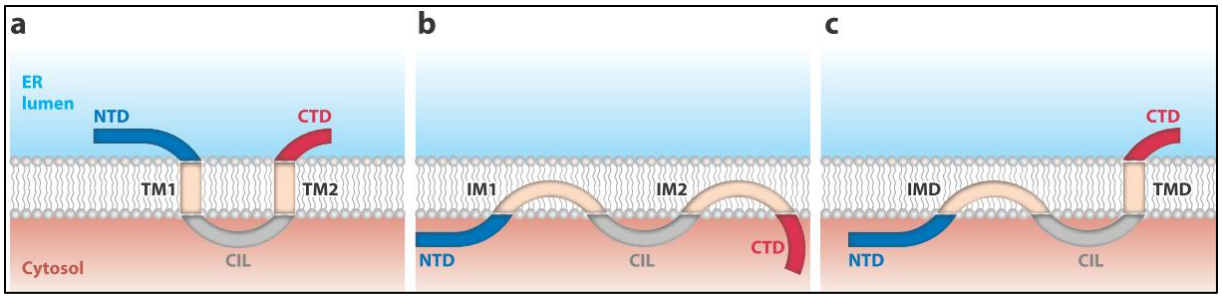

Figure 5: IFITM protein membrane topology. (a) Predicted type III membrane topology with N – and C – termini facing the lumen of the ER. **(b)** Predicted intramembrane topology with the N – as well as the C – terminus facing the cytoplasm. **(c)** Predicted type II membrane topology with a cytoplasmic N – and a luminal C – terminus. Abbreviations: NTD, N-terminal domain; CTD, C-terminal domain; CIL, conserved intracellular loop; TM, transmembrane domain; IM, intramembrane domain [202]

Subcellular localization of immunity-related IFITMs varies according to cell type. However, IFITM2 and IFITM3 proteins have mainly been observed to localize to late endosomes and lysosomes in human and murine cells [185, 190, 193, 194, 203]. More precisely, IFITM3 has been shown to be expressed in alveolar type II pneumocytes in mice where it localizes to late endosomes and lysosomes. However, in murine ciliated respiratory epithelial cells, IFITM3 has been detected at the apical membrane [185]. Similarly, in activated murine CD8 T cells IFITM3 partly co-localized with the T cell receptor, while also early endosomal and lysosomal localization was observed [204]. IFITM1 shows a subcellular localization distinct from IFITM2 and IFITM3 [194] and has been found mainly at the plasma membrane, although some studies also observed partial IFITM1 localization to late endosomal/lysosomal compartments [202].

IFITMs are subject to several post-translational modifications. They harbor three conserved cysteine residues shown to be S-palmitoylated, and this is associated with increased membrane affinity and antiviral activity [199, 205]. Furthermore, IFITM3 has been shown to be poly-ubiquitylated at several lysine residues by the cellular ubiquitin ligase NEDD4, which accelerates its turnover and negatively regulates its antiviral activity [199, 206]. Intriguingly, the IFN effector ISG15 has been reported to inhibit NEDD4 [207], suggesting that while IFITM3 is rapidly degraded in a non-infected cell to avoid cytotoxicity, it is upregulated and protected from degradation in an infected cell [206]. In addition, mono-methylation of a specific lysine residue in IFITM3 was reported to decrease its antiviral activity, but the underlying mechanism thereof remains to be discovered [208]. Interestingly, a recent study connected the IFITM3 SNP associated with an increased risk of acquiring and suffering from a severe course of IAV infection [186, 187] to a cellular phenotype. While IFITM3 resides primarily in late endosomes and lysosomes, IFITM3ΔN21 was shown to localize to the cell periphery [200]. Later, the same authors identified an N-terminal endocytosis motif in IFITM3 that is lacking in IFITM3ΔN21, which is responsible for the endosomal localization of IFITM3 [209]. Interestingly, phosphorylation of

a Tyrosine residue in this endocytosis motif has been shown to abrogate endosomal localization of IFITM3 [200]. Collectively, these studies indicate that post-translational modifications govern the subcellular localization and antiviral activity of IFITM proteins.

Although the antiviral potential of IFITM proteins has been clearly established, their mechanism of antiviral action is still under debate. It was reported early on that IAV particles still bind to and are taken up in IFITM3-expressing cells, but their vRNPs are retained in the cytosol and do not reach the nucleus. Indeed, IAV seems to get trapped in late endosomes or lysosomes in IFITM3-expressing cells [203]. The exact step at which IFITMs block viral infection was then narrowed down to fusion by several studies. For fusion proteins activated at a low pH, lowering pH at 4 °C (cold arrested state) leads to so-called hemifusion (only the outer leaflets of two membranes mix). Fusion pore formation only takes place upon an increase in temperature (at neutral pH) or upon addition of chlorpromazine (CPZ). Intriguingly, while control cells displaying either the Jaagsiekte sheep retrovirus (JSRV) envelope glycoprotein (Env) or IAV HA on their surface proceeded to fusion upon raising the temperature or adding CPZ, IFITM1-expressing cells did not. This indicates that in IFITM1-expressing cells hemifusion might either not have occurred, or that IFITM1 inhibits the progression from hemifusion to fusion. Similarly, cell-cell fusion of HIV-1 Env- or IAV HA-expressing cells was reduced upon expression of IFITM1, 2 or 3 [198]. Further studies examining lipid mixing and fusion pore formation between labeled IAV particles and the endosomal membrane observed that lipid mixing occurred in the presence or absence of IFITM3, while fusion pore formation was inhibited when IFITM3 was present [210]. Potentially explaining the inhibitory activity of IFITMs on membrane fusion, two independent studies provided convincing evidence that the presence of IFITMs in a membrane decreases its fluidity [198, 211]. The first study made use of Laurdan, a hydrophobic fluorescent probe that shows differential emission depending on the polarity of its environment. Laurdan is used to report on the amount of water permeating a membrane, which serves as correlate of lipid packing [212]. Membranes of cells expressing IFITM1, 2 or 3 were shown to be more ordered compared to control cells [198]. The second study employed fluorescence recovery after photobleaching (FRAP) to study membrane fluidity in control cells or cells expressing IFITM1. The delayed return of fluorescence in IFITM1-expressing cells compared to control cells indicated a decrease in membrane fluidity upon presence of IFITM1 in cellular membranes [211]. In support of this notion, the antifungal compound amphotericinB known to increase membrane fluidity has been reported to abrogate IFITM3-mediated inhibition of IAV [211]. Similarly, some studies hypothesized that IFITMs might confer positive curvature to membranes which would also hamper the fusion process [198, 211, 213], especially if IFITMs formed multimers, as reported by one study [213]. However, while one report showed the abrogation of the IFITM-mediated block on fusion by the

addition of oleic acid (OA) which induces negative membrane curvature [198], no effect of OA addition could be observed in another [211]. Yeast two-hybrid studies looking for cellular interaction partners of IFITMs discovered that IFITM1, 2 and 3 can interact with the vesicle-membrane protein-associated protein A (VAPA), thereby disturbing its association with oxysterol-binding protein (OSBP). VAPA-OSBP is involved in the regulation of cholesterol homeostasis and disruption of this interaction by IFITM3 was hypothesized to be the cause for the late-endosomal accumulation of cholesterol in IFITM-expressing cells [214]. An increase in cholesterol decreases membrane fluidity, matching previous observations that the presence of IFITMs in membranes increases their lipid order [198, 211]. Accordingly, overexpression of VAPA alleviated the inhibition IFITM3 exerted on IAV [211, 214]. However, although the intracellular accumulation of cholesterol upon overexpression of IFITM1 or IFITM3 was independently observed [211, 214], several studies challenged the hypothesis of cholesterol being the determinant of IFITM-mediated restriction of viral entry. These studies did not observe any influence on IFITM-mediated viral restriction upon modulation of cellular cholesterol levels [210, 211].

Recently, IFITMs have also been appreciated for their functions during late stages of viral infection, in addition to their role in inhibiting incoming viruses. Two studies reported the incorporation of IFITMs into budding HIV-1 virions which was found to be associated with a decrease in virion fusion capacity [215, 216]. The authors of both studies speculated that an increase in positive membrane curvature and a decrease in membrane fluidity upon IFITM incorporation into the viral membrane would negatively affect fusion of viral and host cell membranes, comparable to what has been hypothesized for IFITMs residing in target cell membranes. They also observed a dose-dependency between the amount of IFITM incorporated and the reduction in virion entry capacity [215, 216]. In contrast, other investigators while also reporting IFITM incorporation into HIV-1 virions could not confirm such dose-dependent effects. Rather, they observed a direct interaction between IFITM2 or 3 and Env. This interaction resulted in an impairment of Env processing and incorporation, leading to the production of virions with a decreased entry capacity [217].

Although we gained a deep understanding on how IFITM expression levels and localization are regulated and inhibit viral entry, several key questions remain unanswered. For example, it needs to be elucidated why some viruses are inhibited by IFITMs while others are not. For many viruses it has been shown that they are specifically inhibited by IFITMs localized to their fusion site, as IAV for example is blocked by IFITM3 localized to late endosomes. In contrast, the arenavirus Machupo virus that follows the same cellular entry route as IAV (clathrin-mediated endocytosis followed by pH-

induced fusion in late endosomes) is not affected by IFITM3 [184, 218, 219]. This cannot be explained by the current models for the antiviral mechanism of IFITM proteins.

1.6 AIMS OF THE PHD THESIS

IFITM proteins have been described as potent antiviral factors inhibiting the entry of a variety of different viruses, such as IAV and HIV. While human and mouse IFITMs have been studied in great detail, very little was known about IFITM proteins and their activity in other species at the time this PhD project was started. Since IAV is a zoonotic virus we aimed to address whether hosts other than humans, such as birds or pigs, are also protected from infection by IFITM proteins. Thus, the first part of this PhD project was dedicated to

the characterization of swine IFITM proteins in terms of localization, IFN-inducibility and antiviral potential against IAV.

In the second part of this PhD thesis we aimed to elucidate the antiviral mechanism of action of IFITM proteins in more detail. In particular we investigated

the contribution of IFITM proteins to the cellular antiviral defense during late stages of the IAV life cycle.

Chapter 2

Swine Interferon-Inducible Transmembrane Proteins Potently Inhibit Influenza A Virus Replication

Caroline Lanz,[a,b] Emilio Yángüez,[a] Dario Andenmatten,[a] Silke Stertz[a]

[a]Institute of Medical Virology, University of Zurich, Winterthurerstrasse 190, 8057 Zurich, Switzerland

[b]Life Sciences Zurich Graduate School, ETH and University of Zurich, 8057 Zurich, Switzerland

CL contributed to this study as follows: Experiments for figures 2,3 and 4 D&E were designed and performed by CL and CL wrote the manuscript.

JVI Journals.ASM.org

Swine Interferon-Inducible Transmembrane Proteins Potently Inhibit Influenza A Virus Replication

Caroline Lanz,[a,b] Emilio Yángüez,[a] Dario Andenmatten,[a] Silke Stertz[a]

Institute of Medical Virology, University of Zurich, Zurich, Switzerland[a]; Life Sciences Zurich Graduate School, ETH and University of Zurich, Zurich, Switzerland[b]

Human interferon-inducible transmembrane proteins (IFITMs) were identified as restriction factors of influenza A virus (IAV). Given the important role of pigs in the zoonotic cycle of IAV, we cloned swine IFITMs (swIFITMs) and found two IFITM1-like proteins, one homologue of IFITM2, and a homologue of IFITM3. We show that swIFITM2 and swIFITM3 localize to endosomes and display potent antiviral activities. Knockdown of swIFITMs strongly reduced virus inhibition by interferon, establishing the swIFITMs as potent restriction factors in porcine cells.

The *i*nter*f*eron-*i*nducible *t*rans*m*embrane proteins (IFITMs) were identified as potent inhibitors of different viruses, including influenza A virus (IAV), West Nile virus, severe acute respiratory syndrome (SARS) coronavirus, and others (1–5). In particular, human and mouse IFITM3 have been studied with regard to their antiviral potential but also their mechanisms of viral restriction. *ifitm3* knockout mice showed accelerated disease progression and higher morbidity and mortality upon IAV infection than wild-type mice (6). Moreover, it was found that humans with a single nucleotide polymorphism in the *ifitm3* gene have a significantly higher risk for a severe course of IAV infection (6, 7). The antiviral mechanism of the IFITMs is not yet fully understood, but it has become clear that viral fusion is targeted by these proteins (8–11). While we have a good understanding of the antiviral potential of human and mouse IFITMs, much less is known about the activities of IFITMs in other species. Given the important role of pigs in the zoonotic cycle of IAV, we aimed to elucidate the antiviral potential of swine IFITMs (swIFITMs).

We cloned swIFITMs from cDNA obtained from interferon (IFN)-stimulated pig cells according to sequences deposited in the NCBI database. We were able to amplify the porcine homologues of human IFITM1, IFITM2, and IFITM3. For IFITM1, two porcine homologues that differ in their N and C termini, named swIFITM1a and -1b, were found. Swine IFITM5 could not be amplified out of cDNA and was thus synthesized. The amino acid alignment of the IFITMs from humans, pigs, and chickens shows that the IFITMs display certain features that are conserved across all three species, such as the two transmembrane domains, the palmitoylation sites at positions 73 and 74, or the ubiquitination sites at positions 85, 90, and 106 (Fig. 1A) (12–14). Moreover, swine and human IFITM2 and IFITM3 share an N-terminal extension of about 20 amino acids that contains the endocytosis motif YEML, which the IFITM1s of both species lack (Fig. 1A) (15, 16). This alignment suggests that the swine IFITMs may have antiviral properties similar to those of their human counterparts.

The induction of human IFITM1 to -3 upon IFN stimulation or virus infection is well established (1, 17). While Miller et al. showed that in pig swIFITMs are induced in tracheobronchial lymph nodes upon infection (18), a direct induction of swIFITMs upon IFN treatment has not been established to date. We thus tested the inducibility of swIFITMs upon IFN stimulation or IAV infection in porcine cell lines. We stimulated porcine NpTr, PK-15, or NSK cells with universal IFN (1,000 U/ml) for 24 h or infected them with A/WSN/33 (WSN) (multiplicity of infection [MOI], 0.01) for 24 h or 48 h (19). Reverse transcription-quantitative PCR (RT-qPCR) with specific primers for the individual swIFITMs (primer sequences are available upon request) revealed a pronounced upregulation of swIFITM1a, swIFITM1b, swIFITM2, and swIFITM3 upon IFN stimulation or infection in NSK as well as PK-15 cells (Fig. 1B and C). In contrast, swIFITM transcripts were induced less than 3-fold in NpTr cells (Fig. 1D). Moreover, when we treated NpTr cells with strong inducers of the IFN response, such as IAV lacking NS1, poly(I·C), or a preparation of Sendai virus that contains large amounts of defective interfering particles, we detected only low levels of swIFITM induction (Fig. 1E). This was not limited to swIFITMs; also swine MX1 and swine OAS, both known to be upregulated by IFN, displayed only low levels of induction. This suggests that the NpTr cells are not able to mount a strong IFN response. Despite these differences in the levels of induction of the swIFITMs, all three cell lines were permissive for robust replication of IAV (Fig. 1F). Expression of swIFITM5 could not be detected in any of the cell lines (data not shown). These results suggest that like their human counterparts, swIFITM1 to -3 constitute a first line of defense against viral infections.

Next, we analyzed the subcellular localization of the swIFITMs. We transiently transfected human A549, swine NpTr, or swine NSK cells with constructs encoding Flag-tagged human or swine IFITMs. IFITMs were stained using an antibody against the Flag tag, while late endosomes were marked using an antibody recognizing lysobisphosphatidic acid (LBPA) (20). Confocal microscopy revealed that the subcellular localization of porcine IFITMs is similar to that of their human homologues, with swIFITM1a and -1b localizing predominantly to the plasma membrane but

Received 5 September 2014 **Accepted** 9 October 2014

Accepted manuscript posted online 15 October 2014

Citation Lanz C, Yángüez E, Andenmatten D, Stertz S. 2015. Swine interferon-inducible transmembrane proteins potently inhibit influenza A virus replication. J Virol 89:863–869. doi:10.1128/JVI.02516-14.

Editor: T. S. Dermody

Address correspondence to Silke Stertz, stertz.silke@virology.uzh.ch.

doi:10.1128/JVI.02516-14

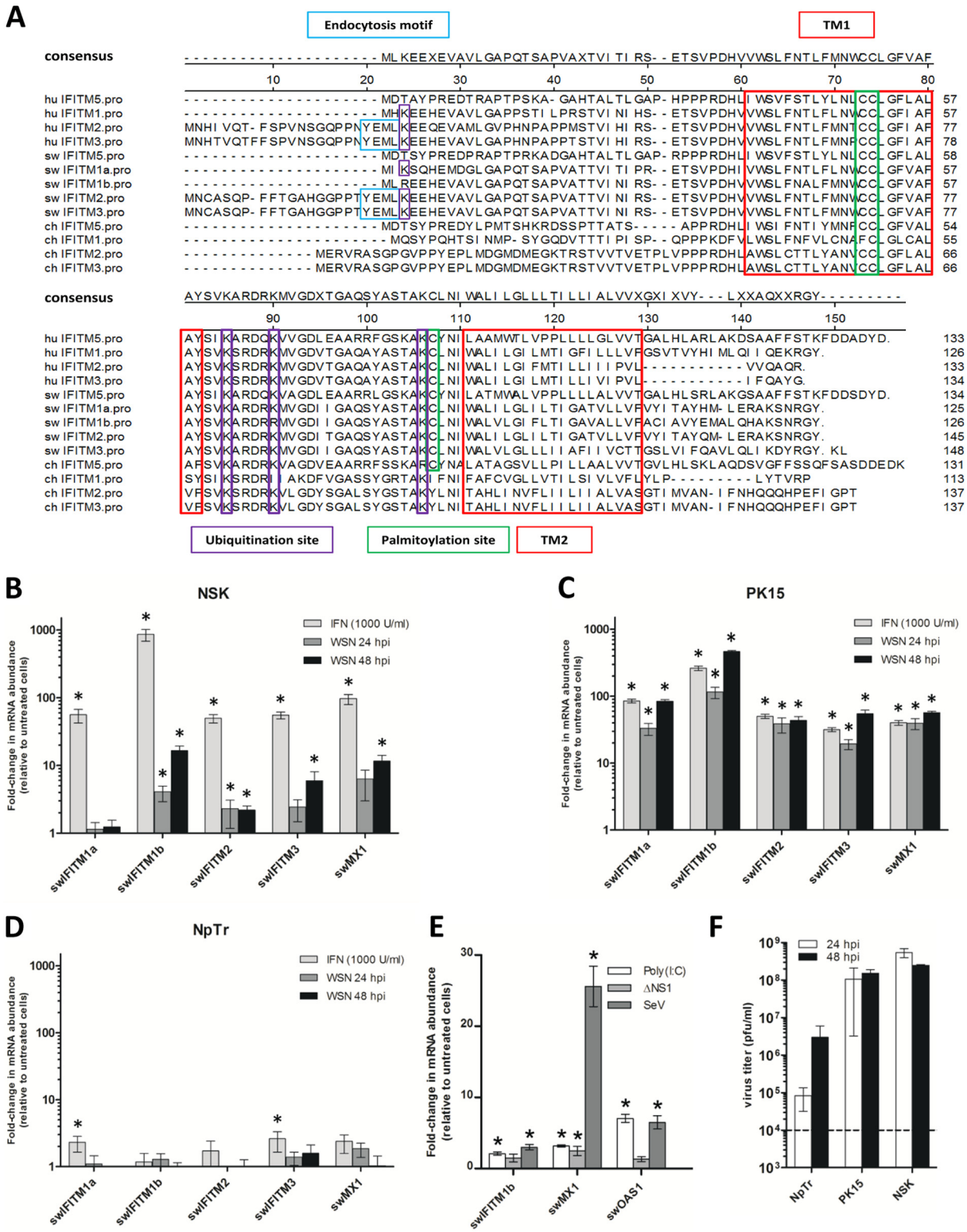

FIG 1 Amino acid alignment of human, swine, and chicken IFITMs and induction of swine IFITMs upon IFN stimulation or virus infection. (A) Amino acid alignment of human, swine, and chicken IFITM1, IFITM2, IFITM3, and IFITM5. Functional motifs and domains are highlighted with colored boxes. Abbreviations: hu, human; sw, swine; ch, chicken; TM, transmembrane domain. (B to D) Induction of swIFITM expression by IFN or IAV infection. NSK (B), PK15 (C), or NpTr (D) porcine cells were infected with A/WSN/33 at an MOI of 0.01 or treated with universal IFN (1,000 U/ml) for 24 h. At the indicated times posttreatment, total mRNA was extracted and used to perform RT-qPCR using specific oligonucleotides for the different swIFITMs or swMX1 as a positive control. Fold changes were calculated according to the Pfaffl method (24) using swine GAPDH (glyceraldehyde-3-phosphate dehydrogenase) mRNA as a reference. A representative experiment from two biological replicates, each performed in triplicate, is shown, with error bars representing the 95% confidence interval. Statistical significance between results for IFN-treated or IAV-infected cells and control untreated cells was assessed by an unpaired two-tailed Student *t* test

with swIFITM2 and -3 accumulating in late endosomes. This is illustrated by their colocalization with the late endosomal marker LBPA in representative images (Fig. 2A) and the quantification of colocalization from 8 to 12 cells per construct and cell line (Fig. 2B). Of note, human and swine IFITM2 displayed the highest degrees of colocalization with LBPA. The observed localization for the human IFITMs is in agreement with that found in previous reports for overexpressed but also for endogenous human IFITMs, validating our approach (8). Moreover, the endosomal localization of human and swine IFITM2 and -3 confirms the importance of the endocytosis motif in the N terminus for pronounced localization to endosomes (15, 16). When we analyzed the localization of the swIFITMs during IAV infection, we did not detect changes in their intracellular distribution from that in uninfected cells (Fig. 2C).

To evaluate the antiviral potential of swIFITMs, we performed an IAV reporter assay with cells transiently transfected with the different swIFITMs. The reporter plasmid encodes luciferase in complementary reverse orientation flanked by IAV noncoding regions, preceded by a human or swine pPolI promoter for use in human or porcine cells, respectively. This assay provides the advantage that only reporter activity from transfected cells is measured, enabling us to assess the impact of the different IFITMs on IAV in a transient-transfection system. The construct for human cells has been used before (21), and for porcine cells, we adapted a construct described previously by introducing three mutations at positions 3, 5, and 8 in the promoter region (22, 23). After transfection with the reporter plasmid plus the IFITM-encoding plasmid indicated in the figures, we used IAV A/WSN/33 to infect HEK293-T cells at an MOI of 0.1 and NpTr cells at an MOI of 1 and measured luciferase production 24 h postinfection (p.i.). We observed that swIFITMs show a dose-dependent restriction of IAV in HEK293-T cells, with swIFITM2 and -3 being the most antivirally active and their activities being comparable to that of human IFITM3 (huIFITM3) (Fig. 3A). However, it should also be noted that swIFITM2, swIFITM3, and huIFITM3 were expressed to higher levels than the other IFITMs, which is in line with the dose dependency of restriction. We then confirmed the antiviral activities of swIFITMs in porcine cells, with swIFITM2 showing the most potent restriction of IAV (Fig. 3B). These data from the transient-transfection assay suggest that the swIFITMs possess antiviral activities.

In order to corroborate these findings, we generated stable cell lines overexpressing the different swIFITMs in the background of the porcine NpTr and NSK cells by lentiviral transduction. Cells were subcloned until more than 99% of cells were positive for expression. To test the antiviral activities of overexpressed swIFITMs, we infected the cell lines with either the human strain A/Hong Kong/68 (MOI, 1) or the swine isolate A/swine/Zurich/25/06 (MOI, 1). At 48 h p.i., supernatants were harvested and viral titers determined by plaque assay. Expression of the swIFITMs reduced titers of IAV in the NpTr cell lines; swIFITM2 was the most potent, with reducing titers of around 1,000-fold (Fig. 3C and D). It should be noted that we were not able to generate stable NpTr cell lines expressing high levels of swIFITM3 and -5 (Fig. 3E), which might contribute to the reduced potency of swIFITM3 compared to that of swIFITM2. In the NSK cell lines, we also observed potent inhibition of IAV replication upon expression of the different swIFITMs, except for swIFITM1b (Fig. 3F and G). Again, swIFITM2 displayed the most potent antiviral activity. As in the NpTr cells, we were not able to generate cell lines expressing high levels of swIFITM3 or swIFITM5. These data suggest that high expression levels of these two swIFITMs are not well tolerated in porcine cells. The differences in expression levels make a direct comparison of the antiviral activities difficult since we observed in the transient-transfection assay of 293T cells that higher expression levels lead to better inhibition of IAV. However, when we compared swIFITM2 to swIFTIM1a or -1b, expression levels were similar, but swIFITM2 was the most active. Moreover, swIFITM3, despite being expressed at much lower levels than swIFITM1a or -1b, had comparable activity. We therefore suggest that swIFITM2 and swIFITM3, which localize predominantly to late endosomes, display the strongest antiviral potential.

Since the assays described above were performed with overexpressed swIFITMs, we next assessed whether endogenous swIFITMs also reduce viral replication. To this aim, porcine NSK cells were transfected with two different small interfering RNAs (siRNAs) targeting swIFITMs (siIFITM1, siIFITM2), a positive-control siRNA against the viral nucleoprotein (NP), or a negative-control nontargeting siRNA. At 36 h posttransfection, cells were either mock treated or treated with universal type I IFN (1,000 U/ml). At 12 h posttreatment, cells were infected with IAV A/WSN/33 (MOI, 0.0001), supernatants were harvested at 24 h p.i., and virus titers were determined by plaque assay. In the absence of IFN, knockdown of swIFITM had no effect on virus titers (Fig. 4A, gray bars). However, in IFN-treated cells, viral titers were increased by 10-fold when swIFITMs were downregulated (Fig. 4A, black bars). To confirm that knockdown by siRNA was successful, we measured mRNA levels for the different swIFITMs and swMX1 in parallel samples and found that both siRNAs designed to target all IFN-induced swIFITMs potently downregulated their expression but that swMX1 as a control IFN-stimulated gene was not affected (Fig. 4B and C). Knockdown of swIFITMs by the two different siRNAs was further confirmed at the level of protein. Since detection of endogenous porcine swIFITMs was unsuccessful using available antibodies for human IFITMs, we tested the siRNAs in the NSK cell lines overexpressing swIFITMs and confirmed knockdown (Fig. 4D). Downregulation of viral NP levels by the NP-specific siRNA was also confirmed by Western blotting (Fig. 4E). These data show that swIFITMs constitute an important part of the IFN response against IAV in porcine cells and confirm our results obtained with overexpression of swIFITMs.

In summary, we show that swIFITM1 to -3 are upregulated by type I IFN and IAV infection in porcine PK-15 and NSK cells.

(*, $P < 0.05$). (E) NpTr cells were transfected with poly(I·C) or infected with A/PR/8/34ΔNS1 (ΔNS1) or Sendai virus (SeV) for 24 h. Total mRNA was extracted and used to perform RT-qPCR with specific oligonucleotides. Fold changes were calculated according to the Pfaffl method using swGAPDH mRNA as a reference. The results of a representative experiment are shown, with error bars representing the 95% confidence intervals. Statistical significance between poly(I·C)-treated or infected cells and control untreated cells was assessed by an unpaired two-tailed Student *t* test (*, $P < 0.05$). (F) IAV replication in porcine cell lines. NSK, PK-15, and NpTr cells were infected with A/WSN/33 as described for panels B to D, and viral titers in the supernatant at 24/48 h p.i. were determined by plaque assay. The dashed line indicates the limit of detection.

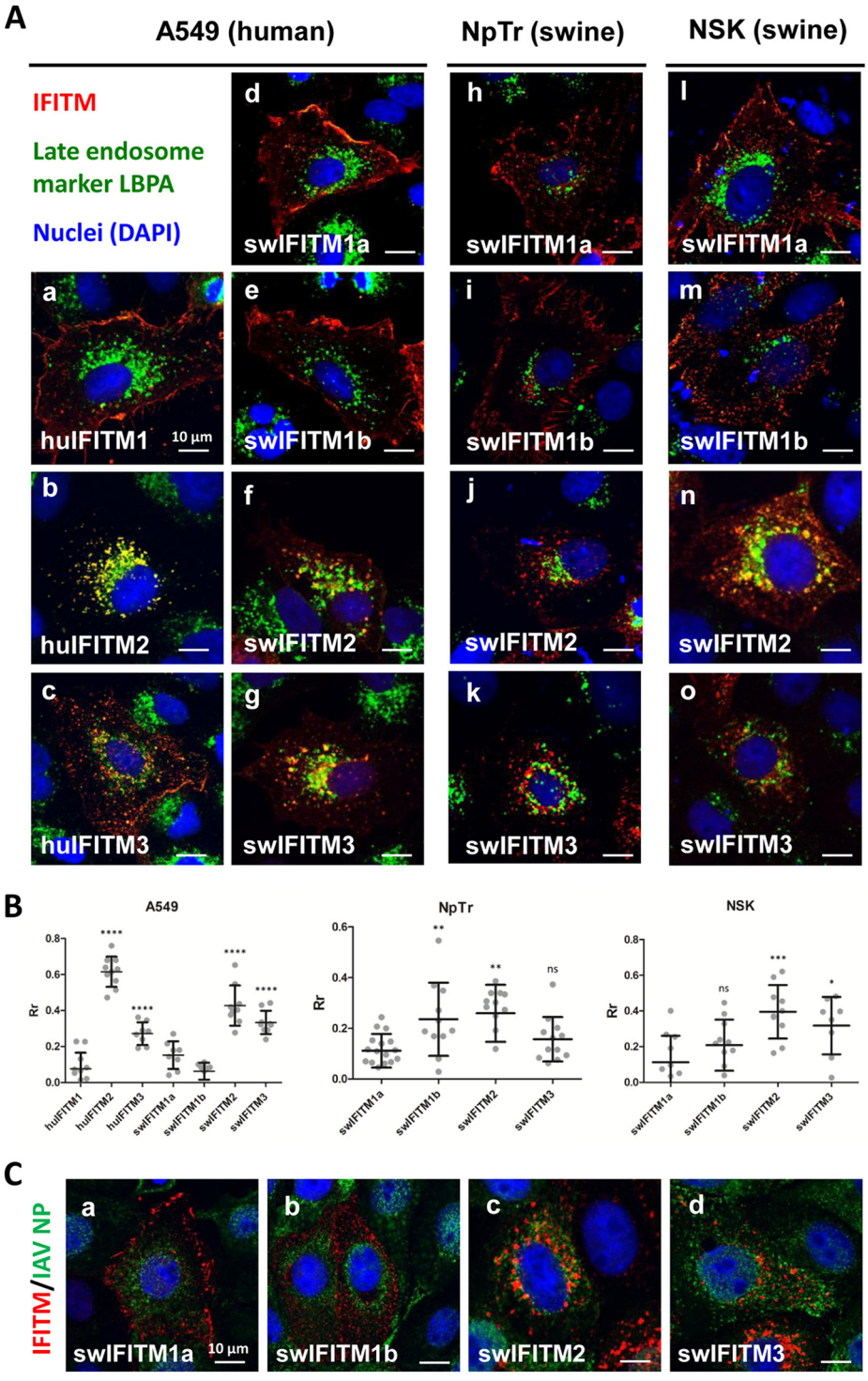

FIG 2 Localization of human and swine IFITMs in human and porcine cells. (A) Representative confocal images of human A549 cells (a to g), porcine NpTr cells (h to k), or porcine NSK cells (l to o) transfected with Flag-tagged human or porcine IFITM-encoding constructs are shown. IFITMs were stained using an antibody against the Flag epitope (red) late endosomes using an antibody against the late endosomal marker LBPA (green), and cell nuclei were marked using DAPI (4′,6-diamidino-2-phenylindole) (blue). Cells were imaged using a 63× objective and a magnification of ×3 (scale bar = 10 μm). (B) Colocalization of IFITMs with the late endosome marker LBPA was quantified. Horizontal bars represent the mean of the Pearson's correlation coefficient (Rr) calculated for 8 to 12 cells using ImageJ, with error bars marking the 95% confidence interval. Statistical significance of increased colocalization for the indicated IFITM construct compared to that of huIFITM1 or swIFITM1a, respectively, was assessed by an unpaired two-tailed Student *t* test (*, $P < 0.05$; **, $P < 0.01$; ***, $P < 0.001$; ****, $P < 0.0001$). (C) Representative confocal images of NSK cells transfected with Flag-tagged porcine IFITM-encoding constructs and infected with A/WSN/33 at an MOI of 5 are shown. IFITMs were stained using an antibody against the Flag epitope (red), infection was controlled using an antibody against IAV NP (green), and cell nuclei were marked using DAPI (blue). Cells were imaged using a 63× objective and a magnification of ×3 (scale bar = 10 μm).

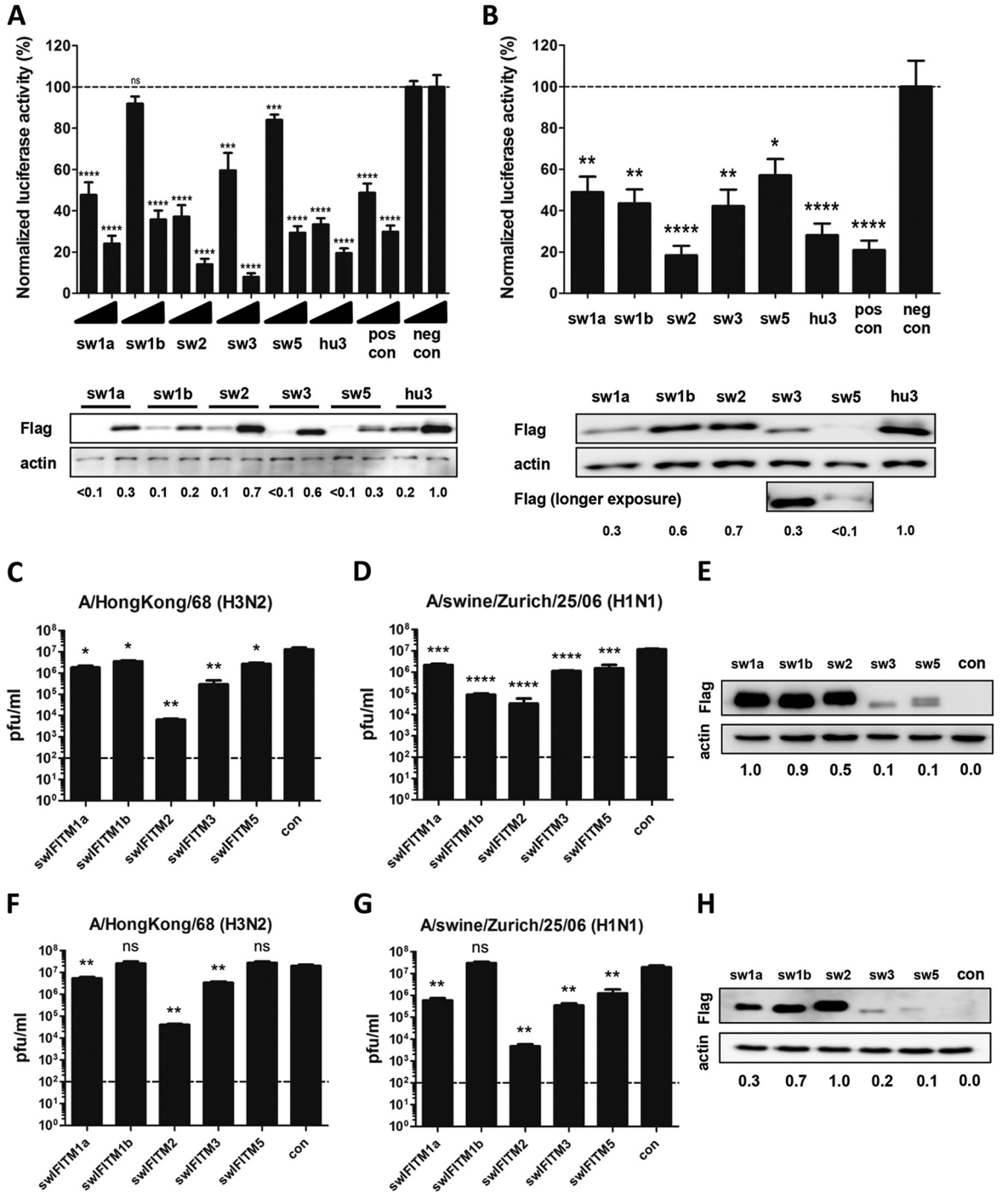

FIG 3 Expression of swIFITMs potently inhibits IAV. (A and B) Transient-transfection assays. HEK293-T (A) and NpTr (B) cells were transfected with an IAV-dependent firefly luciferase reporter construct and increasing amounts of plasmids encoding Flag-tagged swine IFITMs. At 24 h posttransfection, cells were infected with A/WSN/33 at an MOI of 0.1 (A) or 1 (B). At 24 h p.i., cells were lysed and firefly luciferase activity was measured. Data were normalized to luciferase activity in cells transfected with an inactive Mx1 mutant (neg con), while murine Mx1 and human IFITM3 served as positive controls (pos con). Mean values from three biological replicates, each performed in triplicate, are shown, with error bars representing standard deviations. Statistical significance between cells transfected with swIFITMs and cells expressing the negative control was assessed by an unpaired two-tailed Student *t* test (*, $P < 0.05$; **, $P < 0.01$; ***, $P < 0.001$; ****, $P < 0.0001$). Expression levels of swine IFITMs were confirmed by Western blotting and quantified using Multi Gauge software; expression levels in relation to human IFITM3 expression are given below the Western blots. (C to H) Stable cell lines expressing swIFITMs. NpTr (C, D) or NSK (F, G) cells stably overexpressing Flag-tagged swIFITMs were infected with A/Hong Kong/68 (MOI, 1) (C, F) or A/swine/Zurich/25/06 (MOI, 1) (D, G). At 48 h p.i., supernatants were harvested and virus titers determined via plaque assay on MDCK cells. Mean values from three replicates are shown, with error bars representing standard deviations. Statistical significance between titers from cells expressing swIFITMs and cells transduced with the empty vector (con) was assessed by an unpaired two-tailed Student *t* test (*, $P < 0.05$; **, $P < 0.01$; ***, $P < 0.001$; ****, $P < 0.0001$). The dashed lines indicate the limit of detection. Expression levels of swIFITMs were confirmed by Western blotting and quantified by Multi Gauge software, and expression levels relative to the strongest band are given below the Western blots (E, H).

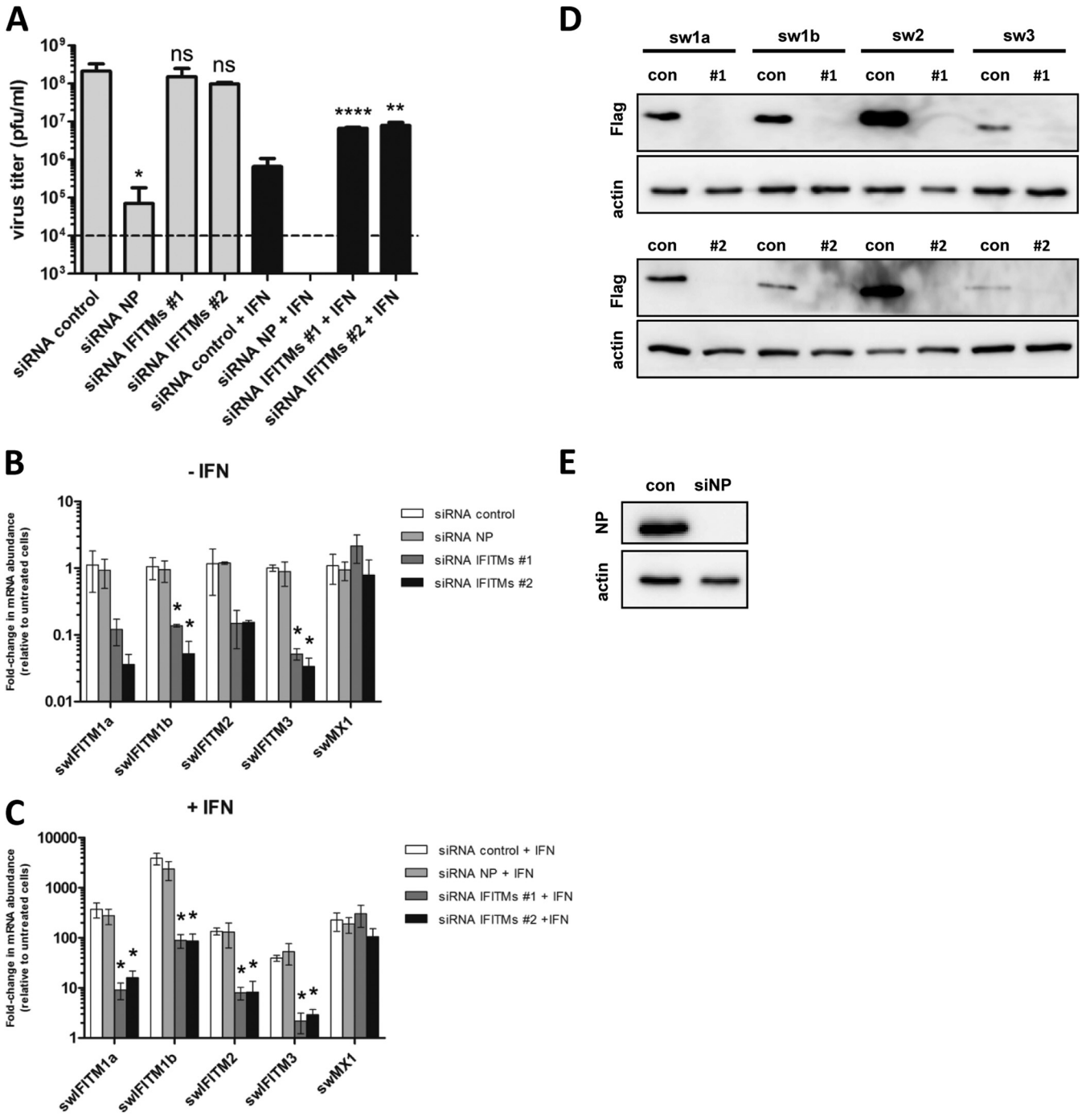

FIG 4 Endogenous swIFITMs contribute to the antiviral activity of IFN in porcine cells. (A) NSK cells were transfected with two siRNAs targeting swIFITMs (#1 and #2) or the viral nucleoprotein (NP) or with a nontargeting control siRNA. At 36 h posttransfection, cells were either left untreated or treated with universal type I IFN (1,000 U/ml). At 12 h posttreatment, cells were infected with A/WSN/33 (MOI, 0.0001) and supernatants were harvested at 24 h p.i. Viral titers were determined by plaque assay. Mean values with standard deviations from three replicates are shown. The dashed line indicates the limit of detection. (B, C) A parallel set of samples was siRNA transfected and mock or interferon treated as described above. At 48 h posttransfection, cells were harvested and mRNA levels of the different swIFITMs and swMX1 were determined by RT-qPCR. Fold changes were calculated according to the Pfaffl method using swGAPDH mRNA as a reference. Mean values with the 95% confidence interval from three replicates are shown. Statistical significance between NP- or swIFITM-silenced cells and cells transfected with the nontargeting siRNA was assessed by an unpaired two-tailed Student *t* test (*, $P < 0.05$). (D) Stable NSK cells expressing swIFITMs were transfected with either an siRNA targeting swIFITMs or a nontargeting control siRNA (con). At 48 h posttransfection, cells were lysed and the amount of Flag-tagged swIFITMs was assessed by Western blotting. Results for two different swIFITM-specific siRNAs (#1 and #2) are shown. (E) NSK cells were transfected with either an siRNA targeting IAV NP or a nontargeting control siRNA (con). At 36 h posttransfection, cells were treated with universal type I IFN (1,000 U/ml), and 12 h posttreatment, cells were infected with A/WSN/33 (MOI, 0.0001) as described for panel A. At 24 h p.i., cells were lysed and NP levels assessed by Western blotting.

While swIFITM1a and -1b displayed prominent plasma membrane localization, swIFITM2 and -3 were found to colocalize with a marker for late endosomes. Overexpression of swIFITMs resulted in reduced influenza virus reporter activity and reduced viral titers. Although different expression levels of the swIFITMs make a direct comparison of the antiviral potencies difficult, the data suggest that swIFITM2 and swIFITM3 display the strongest antiviral activities. Importantly, we also show that endogenous swIFITMs constitute a large part of the antiviral activity of IFN in porcine cells. In future studies, it will be interesting to characterize the IFITMs from different swine breeds for their antiviral potential and thereby help to select pig breeds with increased resistance to IAV infections.

ACKNOWLEDGMENTS

This work was supported by grants from the Swiss National Science Foundation (31003A_135278) and the Novartis Research Foundation to S.S.

We thank Georg Kochs (University Hospital Freiburg, Germany) and Monika Engels (University of Zurich, Switzerland) for providing porcine cell lines and swine influenza viruses and Wendy Barclay (Imperial College London, United Kingdom) for the influenza virus reporter construct for porcine cells. Imaging was performed with support from the Center for Microscopy and Image Analysis, University of Zurich.

REFERENCES

1. **Brass AL, Huang IC, Benita Y, John SP, Krishnan MN, Feeley EM, Ryan BJ, Weyer JL, van der Weyden L, Fikrig E, Adams DJ, Xavier RJ, Farzan M, Elledge SJ.** 2009. The IFITM proteins mediate cellular resistance to influenza A H1N1 virus, West Nile virus, and dengue virus. Cell **139:**1243–1254. http://dx.doi.org/10.1016/j.cell.2009.12.017.
2. **Mudhasani R, Tran JP, Retterer C, Radoshitzky SR, Kota KP, Altamura LA, Smith JM, Packard BZ, Kuhn JH, Costantino J, Garrison AR, Schmaljohn CS, Huang IC, Farzan M, Bavari S.** 2013. IFITM-2 and IFITM-3 but not IFITM-1 restrict Rift Valley fever virus. J Virol **87:**8451–8464. http://dx.doi.org/10.1128/JVI.03382-12.
3. **Huang IC, Bailey CC, Weyer JL, Radoshitzky SR, Becker MM, Chiang JJ, Brass AL, Ahmed AA, Chi X, Dong L, Longobardi LE, Boltz D, Kuhn J H, Elledge SJ, Bavari S, Denison MR, Choe H, Farzan M.** 2011. Distinct patterns of IFITM-mediated restriction of filoviruses, SARS coronavirus, and influenza A virus. PLoS Pathog **7:**e1001258. http://dx.doi.org/10.1371/journal.ppat.1001258.
4. **Anafu AA, Bowen CH, Chin CR, Brass AL, Holm GH.** 2013. Interferon-inducible transmembrane protein 3 (IFITM3) restricts reovirus cell entry. J Biol Chem **288:**17261–17271. http://dx.doi.org/10.1074/jbc.M112.438515.
5. **Lu J, Pan Q, Rong L, He W, Liu SL, Liang C.** 2011. The IFITM proteins inhibit HIV-1 infection. J Virol **85:**2126–2137. http://dx.doi.org/10.1128/JVI.01531-10.
6. **Everitt AR, Clare S, Pertel T, John SP, Wash RS, Smith SE, Chin CR, Feeley EM, Sims JS, Adams DJ, Wise HM, Kane L, Goulding D, Digard P, Anttila V, Baillie JK, Walsh TS, Hume DA, Palotie A, Xue Y, Colonna V, Tyler-Smith C, Dunning J, Gordon SB, Smyth RL, Openshaw PJ, Dougan G, Brass AL, Kellam P.** 2012. IFITM3 restricts the morbidity and mortality associated with influenza. Nature **484:**519–523. http://dx.doi.org/10.1038/nature10921.
7. **Zhang YH, Zhao Y, Li N, Peng YC, Giannoulatou E, Jin RH, Yan HP, Wu H, Liu JH, Liu N, Wang DY, Shu YL, Ho LP, Kellam P, McMichael A, Dong T.** 2013. Interferon-induced transmembrane protein-3 genetic variant rs12252-C is associated with severe influenza in Chinese individuals. Nat Commun **4:**1418. http://dx.doi.org/10.1038/ncomms2433.
8. **Feeley EM, Sims JS, John SP, Chin CR, Pertel T, Chen LM, Gaiha GD, Ryan BJ, Donis RO, Elledge SJ, Brass AL.** 2011. IFITM3 inhibits influenza A virus infection by preventing cytosolic entry. PLoS Pathog **7:**e1002337. http://dx.doi.org/10.1371/journal.ppat.1002337.
9. **Li K, Markosyan RM, Zheng YM, Golfetto O, Bungart B, Li M, Ding S, He Y, Liang C, Lee JC, Gratton E, Cohen FS, Liu SL.** 2013. IFITM proteins restrict viral membrane hemifusion. PLoS Pathog **9:**e1003124. http://dx.doi.org/10.1371/journal.ppat.1003124.
10. **Desai TM, Marin M, Chin CR, Savidis G, Brass AL, Melikyan GB.** 2014. IFITM3 restricts influenza A virus entry by blocking the formation of fusion pores following virus-endosome hemifusion. PLoS Pathog **10:**e1004048. http://dx.doi.org/10.1371/journal.ppat.1004048.
11. **Amini-Bavil-Olyaee S, Choi YJ, Lee JH, Shi M, Huang IC, Farzan M, Jung JU.** 2013. The antiviral effector IFITM3 disrupts intracellular cholesterol homeostasis to block viral entry. Cell Host Microbe **13:**452–464. http://dx.doi.org/10.1016/j.chom.2013.03.006.
12. **Yount JS, Moltedo B, Yang YY, Charron G, Moran TM, Lopez CB, Hang HC.** 2010. Palmitoylome profiling reveals S-palmitoylation-dependent antiviral activity of IFITM3. Nat Chem Biol **6:**610–614. http://dx.doi.org/10.1038/nchembio.405.
13. **John SP, Chin CR, Perreira JM, Feeley EM, Aker AM, Savidis G, Smith SE, Elia AE, Everitt AR, Vora M, Pertel T, Elledge SJ, Kellam P, Brass AL.** 2013. The CD225 domain of IFITM3 is required for both IFITM protein association and inhibition of influenza A virus and dengue virus replication. J Virol **87:**7837–7852. http://dx.doi.org/10.1128/JVI.00481-13.
14. **Yount JS, Karssemeijer RA, Hang HC.** 2012. S-palmitoylation and ubiquitination differentially regulate interferon-induced transmembrane protein 3 (IFITM3)-mediated resistance to influenza virus. J Biol Chem **287:**19631–19641. http://dx.doi.org/10.1074/jbc.M112.362095.
15. **Chesarino NM, McMichael TM, Hach JC, Yount JS.** 2014. Phosphorylation of the antiviral protein IFITM3 dually regulates its endocytosis and ubiquitination. J Biol Chem **289:**11986–11992. http://dx.doi.org/10.1074/jbc.M114.557694.
16. **Jia R, Xu F, Qian J, Yao Y, Miao C, Zheng YM, Liu SL, Guo F, Geng Y, Qiao W, Liang C.** 2014. Identification of an endocytic signal essential for the antiviral action of IFITM3. Cell Microbiol **16:**1080–1093. http://dx.doi.org/10.1111/cmi.12262.
17. **Friedman RL, Manly SP, McMahon M, Kerr IM, Stark GR.** 1984. Transcriptional and posttranscriptional regulation of interferon-induced gene expression in human cells. Cell **38:**745–755. http://dx.doi.org/10.1016/0092-8674(84)90270-8.
18. **Miller LC, Jiang Z, Sang Y, Harhay GP, Lager KM.** 2014. Evolutionary characterization of pig interferon-inducible transmembrane gene family and member expression dynamics in tracheobronchial lymph nodes of pigs infected with swine respiratory disease viruses. Vet Immunol Immunopathol **159:**180–191. http://dx.doi.org/10.1016/j.vetimm.2014.02.015.
19. **Ferrari M, Scalvini A, Losio MN, Corradi A, Soncini M, Bignotti E, Milanesi E, Ajmone-Marsan P, Barlati S, Bellotti D, Tonelli M.** 2003. Establishment and characterization of two new pig cell lines for use in virological diagnostic laboratories. J Virol Methods **107:**205–212. http://dx.doi.org/10.1016/S0166-0934(02)00236-7.
20. **Sun E, He J, Zhuang X.** 2013. Dissecting the role of COPI complexes on influenza virus infection. J Virol **87:**2673–2685. http://dx.doi.org/10.1128/JVI.02277-12.
21. **Hoffmann HH, Palese P, Shaw ML.** 2008. Modulation of influenza virus replication by alteration of sodium ion transport and protein kinase C activity. Antiviral Res **80:**124–134. http://dx.doi.org/10.1016/j.antiviral.2008.05.008.
22. **Moncorge O, Long JS, Cauldwell AV, Zhou H, Lycett SJ, Barclay WS.** 2013. Investigation of influenza virus polymerase activity in pig cells. J Virol **87:**384–394. http://dx.doi.org/10.1128/JVI.01633-12.
23. **Neumann G, Hobom G.** 1995. Mutational analysis of influenza virus promoter elements *in vivo*. J Gen Virol **76:**1709–1717. http://dx.doi.org/10.1099/0022-1317-76-7-1709.
24. **Pfaffl MW.** 2001. A new mathematical model for relative quantification in real-time RT–PCR. Nucleic Acids Res **29:**e45.

JVI Journals.ASM.org

AUTHOR CORRECTION

Correction for Lanz et al., Swine Interferon-Inducible Transmembrane Proteins Potently Inhibit Influenza A Virus Replication

Caroline Lanz,[a,b] Emilio Yángüez,[a] Dario Andenmatten,[a] Silke Stertz[a]

Institute of Medical Virology, University of Zurich, Zurich, Switzerland[a]; Life Sciences Zurich Graduate School, ETH and University of Zurich, Zurich, Switzerland[b]

Volume 89, no. 1, p. 863–869, 2015. Page 864, Fig. 1A: The alignment of IFITM proteins shown in Fig. 1A contained an incorrect sequence for chicken IFITM2. This has been corrected in Fig. 1A below.

This does not affect the original data, data interpretation, or conclusions of this study.

Citation Lanz C, Yángüez E, Andenmatten D, Stertz S. 2015. Correction for Lanz et al., Swine interferon-inducible transmembrane proteins potently inhibit influenza a virus replication. J Virol 89:2988. doi:10.1128/JVI.03533-14.

doi:10.1128/JVI.03533-14

Chapter 3

Incorporation of IFITM3 into influenza A virus particles leads to increased sensitivity to antibody-mediated virus neutralization

Caroline Lanz,[a,b] Eva E. Müller,[a,b] Benjamin G.Hale[a] and Silke Stertz[a]

[a]Institute of Medical Virology, University of Zurich, Winterthurerstrasse 190, 8057 Zurich, Switzerland

[b]Life Sciences Zurich Graduate School, ETH and University of Zurich, 8057 Zurich, Switzerland

CL contributed to this study as follows: Experiments for figures 1-5 and supplemental figure 1 were designed by CL. CL performed experiments for figures 1, 2, 3 A&B, 4, 5 and S1. Experiments for figure 1 C-F were performed together with Eva E. Müller.

Incorporation of IFITM3 into influenza A virus particles leads to increased sensitivity to antibody-mediated virus neutralization

Caroline Lanz[a, b], Eva E. Müller [a, b], Benjamin G. Hale [a] and Silke Stertz[a*]

[a] Institute of Medical Virology, University of Zurich, Winterthurerstrasse 190, 8057 Zurich, Switzerland

[b] Life Sciences Zurich Graduate School, ETH and University of Zürich, 8057 Zurich, Switzerland

* Corresponding author: Silke Stertz, Ph.D.
E-mail: stertz.silke@virology.uzh.ch
Phone: +41 44 634 2899

Abstract

Interferon-inducible transmembrane proteins (IFITMs) are potent antiviral factors that inhibit a variety of different viruses, such as influenza A virus (IAV), HIV and West Nile virus, at the step of viral entry. Recently, IFITMs have been reported to be incorporated into HIV virions upon budding, thereby decreasing virion infectivity. Here we provide evidence that IFITM3 also incorporates into IAV VLPs and IAV virions. IAV VLPs were compromised in their infectivity when produced in IFITM3-expressing cells and this effect was alleviated in a dose-dependent manner by increasing HA concentrations in producer cells. In contrast, IAV virions were not negatively affected in their infectivity upon presence of IFITM3 in producer cells, however, they showed increased neutralization sensitivity to HA-directed antibodies, potentially compromising them in an *in vivo* situation. In summary, we establish a role for IFITM3 in late stages of the IAV life cycle.

Introduction

Interferon-inducible transmembrane proteins (IFITMs) have been described as potent antiviral factors blocking the entry step of many different viruses, such as influenza A virus (IAV), HIV, West Nile virus, Dengue virus, Zika virus, VSV and others [1-8]. Although basally expressed, IFITMs 1, 2 and 3 are highly upregulated upon stimulation of cells with type I or type II interferon (IFN) [1, 9, 10]. Importantly, IFITM3 has been shown to constitute a major part of the interferon response against IAV in human cells [1].

Nevertheless, how exactly IFITMs inhibit viral infections is still under debate. Current literature agrees that cellular membranes show increased positive curvature and decreased membrane fluidity upon incorporation of IFITMs, offering a convincing explanation to why IFITMs block the fusion between cellular and viral membranes [11-13]. In addition to their biophysical properties, IFITMs also rely on an appropriate subcellular localization to exert their antiviral function. The presence of an N-terminal endocytosis motif in IFITM2 and 3 responsible for endo-lysosomal targeting of those proteins has been proven necessary for antiviral activity [3, 14, 15]. In addition, post-translational palmitoylation of conserved cysteine residues was found to be required for the clustering of IFITM3 in membranes, which in turn is a prerequisite for antiviral activity [16]

While the inhibitory effect on viral entry exerted by IFITMs residing in target cells has been studied in great detail, knowledge on the consequences of IFITM presence in virus-producing cells is still accumulating. Compton [17] and Tartour [18] and colleagues were the first to show that IFITM proteins get incorporated into budding HIV-1 virions, which they find to be associated with a decrease in virion entry capacity. Consequently, knockdown of endogenous IFITMs increased the infectivity [18] and the cell-to-cell spread [17] of HIV-1 virions. Both authors favour the hypothesis of biophysical properties (positive membrane curvature, decreased membrane fluidity) imposed on the viral membrane through IFITM incorporation to explain the reduction in virion infectivity. Intriguingly, in recent studies performed by Yu and colleagues [19] incorporation of IFITMs into HIV-1 virions was also demonstrated but the authors did not observe a correlation between the amount of IFITM incorporated and the reduction in virion entry capacity. They observed that IFITM2 and 3 can interact with Env, the envelope glycoprotein of HIV-1, impair its processing and decrease its incorporation into newly produced virions, thereby leading to a decrease in virion infectivity.

Knowing that IAV is strongly inhibited by IFITMs at the entry step [1, 3, 4, 12, 20-22], we wondered whether similar to the situation in HIV-1, IFITMs also target later stages of the IAV life cycle. To address this question we assessed the infectivity of HIV virus-like particles (VLPs) pseudotyped with IAV HA and NA and IAV VLPs that were produced in the presence or absence of IFITM3 and found a significant decrease in VLP infectivity when IFITM3 was present in producer cells. We present experimental evidence that IFITM3 acts on the IAV envelope glycoprotein HA in producer cells by

demonstrating that IFITM3-induced negative effects on VLP infectivity are alleviated in a dose-dependent manner by increasing HA concentrations. In contrast, when comparing IAV grown on IFITM3-overexpressing cells versus control cells infectivity remained unaffected by the presence of IFITM3. However, we observed an increase in neutralization sensitivity of virus grown in the presence of IFITM3, which we hypothesize to be detrimental for the virus in an *in vivo* situation. Therefore, our study establishes a role for IFITM3 in late stages of IAV infection.

Materials and Methods

Cells

HEK293-T, A549, TZM-bl and MDCKII cells were maintained in Dulbecco's Modified Eagle Medium (DMEM) supplemented with 10% fetal calf serum (FCS; Thermo Fisher Scienific) and penicillin-streptomycin (100 U/mL; Thermo Fisher Scientific). IFITM3 was amplified from cDNA extracted from IFN-α-stimulated A549 cells using the following primers: 5'-gacagaattcatggactacaaagacgatgacg-ataaaaatcacactgtccaaa-3' (forward) and 5'-gacactcgagctatccataggcctggaa-3' (reverse). After restriction by EcoRI and XhoI, the IFITM3 PCR product was ligated into the pLVX-IRES-Puromycin vector plasmid (Clontech) to yield pLVX-IFITM3. A549 and TZM-bl cells stably overexpressing IFITM3 were generated by lentiviral transduction with particles harboring pLVX-IFITM3. IFITM3-expressing cells were subcloned and cultured in the presence of 1 μg/mL puromycin (Thermo Fisher Scientific).

HIV-based virus-like particle production, purification and infection

HIV-VLPs pseudotyped with either the HIV-1 JRFL, IAV A/WSN/33 or VSV envelope glycoproteins were generated by transfecting HEK293-T cells with pNLLuc-AM [23], envelope expression – and Flag-IFITM3 expression plasmids (or the empty vector pCAGGS for the production of VLPs in the absence of IFITM3) at the ratio of 9 : 1.5 : 1. Polyethyleneimine (PEI; Sigma-Aldrich) was used as transfection reagent (2 μg PEI/μg DNA). VLPs were harvested 72 hours post-transfection and their concentration was determined by an in-house p24 ELISA. A549 or TZM-bl cells seeded into 96-well plates were infected with VLPs at an equivalent of 3 ng p24/well for 90 minutes in the presence of DEAE-dextran (150 μg/mL; Sigma-Aldrich), before the inoculum was removed and replaced by DMEM supplemented with 10% FCS and penicillin-streptomycin (100 U/mL). VLP infectivity was measured 48 hours post-infection by quantifying firefly luciferase activity using the ONE-Glo Luciferase Assay System (Promega) according to the manufacturer's protocol. For analysis of VLPs by Western Blot VLPs were purified as follows: After an initial centrifugation at 1500 x g for 5 minutes to remove cellular debris, VLP-containing supernatant was filtered through a 0.45 μm filter. To achieve a more stringent removal of cellular debris, supernatant was ultracentrifuged at 10'000 rpm at 4 °C for 20 minutes, before ultracentrifugation of VLPs through a 20% (w/v) sucrose cushion in NTE buffer (100mM NaCl, 10 mM Tris-HCl pH7.5, 1mM EDTA pH8) at 25'000 rpm for 90 minutes. Supernatant was then decanted and the VLP pellet dissolved in Optimem at 4 °C O/N (Gibco).

IAV-based virus like particle (BlaM1 VLP) production, normalization and infection

VLPs harboring β-lactamase-M1 (BlaM1) fusion proteins were produced essentially as described by Tscherne & Garcìa-Sastre [24]. Briefly, HEK293-T cells seeded into poly-L-lysine-coated (Sigma-Aldrich) 6-well plates were transfected in Optimem (Gibco) with 2.5 µg BlaM1, 500 ng pCAGGS-WSN-HA, 1.125 µg pCAGGS-WSN-NA, 250 ng pCAGGS-WSN-M2 and 300 ng pCAGGS-IFITM3/pCAGGS-eV per well using ViaFect (Promega) as transfection reagent (2.5 µl ViaFect/µg DNA). Medium was exchanged 8 hours post-transfection. VLPs were harvested 72 hours after transfection and treated with 6 µg/mL TPCK-trypsin (Sigma-Aldrich) for efficient HA cleavage. For infection of MDCKII cells BlaM1 VLP input was normalized by Western Blotting for BlaM1 using the mouse monoclonal anti-IAV M1 (HB-64, American Type Culture Center) antibody. Four hours post-infection cells were harvested by trypsinization and incubated with the fluorigenic substrate CCF2-AM (ThermoFisher Scientific). CCF2-AM taken up into the cells is cleaved into CCF2 by cellular esterases and is thereby trapped inside the cell. CCF2 is cleaved by β-lactamase brought in by the infecting VLPs, thereby shifting its emission wavelength from 520 nm to 447 nm when excited at 409 nm. Cells were analysed on a FACSVerse System (BD) and dead cells excluded by a live/dead staining (LIVE/DEAD Fixable Near-IR Dead Cell Stain Kit, ThermoFisher Scientific).

Influenza A virus infections

All cells were washed with PBS prior to infection. IAV A/WSN/33 was diluted to an MOI of 0.1 or 1 in PBS supplemented with 2 mM Mg^{2+}, 1 mM Ca^{2+}, 0.3% BSA and 1% penicillin-streptomycin (infection PBS; PBSi). Infection was performed at 37 °C for 1 hour. Thereafter, virus inoculum was removed and cells washed with PBS, before DMEM containing 20 mM HEPES, 0.3 % BSA and 1% penicillin-streptomycin (post-infection DMEM; p.i.DMEM) was added to the cells. Virus was grown in the presence of 1 µg/mL TPCK trypsin (Sigma-Aldrich) for 48 hours.

To normalize viral input in subsequent infectivity assays, qPCR on the viral M segment was performed. Viral RNA was extracted using the QIAamp Viral RNA Kit (Qiagen) and cDNA synthesized by the SuperScript III Reverse Transcriptase (ThermoFisher Scientific) using random primers (Promega). qPCR was performed using EvaGreen Master Mix for qPCR (Biotium) with the following primers: 5'-GCAGCAGAGGCCATGGATATTG-3' (forward) and 5'-TTTGCTGCAATGACGAGAGGATC-3' (reverse). Virus grown on control or IFITM3-expressing A549 cells was prediluted according to qPCR results for all infectivity assays.

Virus infectivity was measured in an IAV reporter assay described by Hoffmann and colleagues [25]. Briefly, HEK293-T cells seeded into 96-well plates were transfected with 20 ng/well of an IAV reporter plasmid encoding firefly luciferase in complementary reverse orientation, flanked by IAV non-coding regions, thus mimicking an IAV segment. 24 h post-transfection, cells were infected with A/WSN/33

at an MOI of 0.3. 24 h post-infection luciferase activity was measured using the ONE-Glo luciferase assay substrate (Promega) according to manufacturer's protocols.

To assess IFITM incorporation into IAV by Western Blotting virus was purified as described for HIV VLPs and subjected to Western Blotting as described below.

Western Blotting

To prepare cell extracts, cells were lysed in 1X Laemmli buffer (62.5 mM Tris-HCl, pH 6.8, 10% glycerol, 2% SDS, 100 mM dithiothreitol, 0.02% bromophenol blue). Viruses and VLPs were mixed with 5X Laemmli buffer to obtain 1X Laemmli buffer lysates. Samples were run on SDS-PAGE gels and blotted onto nitrocellulose membranes (Hybond ECL, GE healthcare). All stainings were performed in tris-buffered saline mixed with 0.5 % Tween-20 (Sigma-Aldrich) and 3 % powdered milk. The following antibodies were used: mouse monoclonal anti-Flag (clone M2, Sigma-Aldrich), rabbit polyclonal anti-IFITM3 (Proteintech), mouse monoclonal anti-β-actin (Santa Cruz Biotechnology), mouse monoclonal anti-HIV-1 p24 (ab9071, abcam), mouse monoclonal anti-IAV M1 (HB-64, American Type Culture Center), rabbit polyclonal anti-NP (a kind gift of A. Nieto), mouse monoclonal anti-A/WSN/33 HA (clone H15-B9-22 [26], Wistar) and rabbit polyclonal anti-A/WSN/33 (a kind gift of B. Hale). Secondary antibody staining was performed using near-infrared fluorescent secondary antibodies (Li-Cor) and images were acquired on an Odissey Fc imaging system. Western Blot signal intensities were quantified using the Image Studio™ software (Li-Cor).

Transmission Electron Microscopy of immunogold-labeled viral particles

Viral particles were purified as described above. Carbon-coated nickel grids were glow-discharged before purified viral particle solution was applied. Samples were fixed with 4% paraformaldehyde in 0.1 M HEPES for 7 min. After one short wash in PBS, samples were permeabilized with 0.5% Triton-X-100 in PBS for 1 min and washed again three times in PBS. Free aldehydes were quenched with 0.15 % glycine in PBS. To prevent unspecific antibody binding samples were blocked in 1% bovine serum albumin (BSA, Merck) in PBS. Primary antibody staining was performed using rabbit polyclonal anti-IFITM3 antibody (Proteintech) diluted in 1% BSA in PBS. Samples were washed three times in 1% BSA in PBS, before secondary antibody staining was performed using a goat anti-mouse IgG Gold antibody (Sigma-Aldrich) at on optical density of 0.15. After secondary antibody staining, samples were washed in PBS and fixed in 4% paraformaldehyde in 0.1M HEPES, before being negatively stained with 1% uranyl acetate and imaged in a Philips CM100 transmission electron microscope operated at 100 kV.

Results

IFITM3 present in VLP-producing cells restricts the entry capacity of HIV VLPs pseudotyped with IAV HA/NA and HIV envelopes

While several papers elucidated the role of IFITM3 incorporation into HIV particles and its negative effect on virion infectivity [17-19], nothing is known about similar mechanisms occuring in the IAV life cycle. First, we employed a virus-like particle (VLP) system based on HIV to address whether the presence of IFITM3 in VLP producer cells also leads to a reduction in entry capacity of VLPs pseudotyped with IAV HA/NA, similar to what has been described for VLPs pseudotyped with HIV Env. We transfected HEK293-T cells with pNL-LucAM, a plasmid encoding the HIV strain NL4-3 genome but having its envelope gene replaced by a luciferase gene, together with plasmids encoding either the HIV-1 JRFL, IAV A/WSN/33 or VSV envelope genes (or the empty vector plasmid pCAGGS for the no envelope control) in the presence or absence of Flag-IFITM3 (Fig. 1A). VLPs produced under these conditions were purified and analysed for IFITM3 incorporation by Western Blotting for the Flag epitope (Fig. 1B). All VLPs exhibited a strong Flag signal, suggesting that IFITM3 was incorporated into VLPs and that incorporation occurred envelope-independently, as previously described by Compton and colleagues [17]. VLPs produced in the absence of IFITM3 were subsequently tested for their infectivity in A549 human lung epithelial cells (Fig. 1C) or HeLa TZM cells (Fig. 1D) engineered to express the HIV-1 receptors CD4 and CCR5. While A549 cells could be infected with IAV HA/NA – as well as VSV-G - pseudotyped VLPs, TZM cells could be infected with VLPs pseudotyped with HIV – as well as VSV envelopes. We then compared the infectivity of VLPs produced in the presence of IFITM3 with VLPs produced in the absence of IFITM3. Interestingly, VLPs pseudotyped with IAV HA/NA or HIV-1 Env were restricted in their infectivity when produced in cells expressing IFITM3, while VSV-G pseudotyped VLPs did not seem to be affected in their infectivity by the presence of IFITM3 in producer cells (Fig. 1E&F).

IFITM3 blocks VLP infectivity at the level of the producer cell as well as the target cell for IAV and HIV-1 but not for VSV in an HIV-based VLP system

Next, we were interested to see whether we can see differential effects of IFITM3 presence in producer and target cells in the context of IAV, HIV-1 and VSV VLP infection. To this end we generated A549 and HeLa TZM cells stably overexpressing IFITM3 that were subsequently infected with VLPs produced in the presence or in the absence of IFITM3.

In accordance with previous studies we observed a significant reduction in IAV VLP entry into A549 cells upon IFITM3 expression in those cells (Fig. 2A). Interestingly, this reduction is comparable to the decrease in VLP infectivity we see upon presence of IFITM3 in VLP producer cells. Similar results were obtained for HIV-1 VLPs infecting TZM cells (Fig. 2B). VSV VLPs were significantly inhibited in their

infectivity when IFITM3 was expressed in target cells, while presence of IFITM3 in VLP producer cells did not negatively affect their infectivity (Fig. 2C).

IFITM3 in VLP-producing cells restricts the entry capacity of IAV VLPs

In a next step we aimed to see whether the observed decrease in VLP infectivity could be reproduced in an IAV-based VLP system. To this end we made use of a β-lactamase-M1 VLP assay described by Tscherne and Garcìa-Sastre [24]. Briefly, HEK293-T cells were transfected with plasmids encoding a β-lactamase-M1 fusion protein, IAV HA, NA and M2 (in the presence or in the absence of IFITM3) to produce IAV VLPs. The entry efficiency of these VLPs can be assessed by loading of infected target cells with CCF2, a fluorigenic substrate that shifts in emission upon cleavage by β-lactamase carried into the cell by the infecting VLP (Fig. 3A). When we then tested those VLPs for their infectivity in MDCKII cells we observed a marked reduction in entry efficiency for VLPs produced in the presence of IFITM3. The left panel of Fig. 3B shows one representative experiment, while the right panel summarizes the results of three independently performed experiments.

To check whether IFITM3 also incorporates into IAV VLPs, VLPs produced in the absence or in the presence of IFITM3 were purified and subjected to Western Blot analysis. A distinct Flag-IFITM3 band could be detected in VLPs produced in IFITM3-expressing cells, suggesting that similar to HIV VLPs, IFITM3 also incorporates into IAV VLPs (Fig. 3C). Interestingly, we observed a decrease in VLP HA signal upon presence of IFITM3 in VLP producer cells (Fig. 3C). This decrease in envelope glycoproteins was also detected in HIV VLPs pseudotyped with HIV Env or IAV HA/NA (Suppl. Fig. 1). We thus conclude that IFITM3 can also be incorporated into IAV-based VLPs and that the presence of IFITM3 in IAV VLP producer cells leads to an entry deficiency of those VLPs, possibly through a reduction in HA abundance on the VLP's surface.

HA but not NA outcompetes IFITM3 in VLP producing cells

Given that IFITM3 reduced the abundance of HA in IAV VLPs we wondered whether IFITM3 already decreased the amount of HA present in producer cells. To this end, 293-T cells were co-transfected with increasing amounts of a Flag-IFITM3 encoding plasmid and a constant amount of a plasmid coding for HA. However, Western Blot analysis revealed that total HA levels were only marginally reduced upon an increase in IFITM3 expression (Fig. 4A). Next, we tested whether IAV HA or NA could outcompete the negative effect of IFITM3 on VLP infectivity when present in producer cells. To this end, IAV VLPs were produced in 293-T cells transfected with a constant amount of IFITM3 or the empty vector pCAGGS as negative control in the presence of increasing amounts of HA or NA. Western Blot analysis of these VLPs confirmed that transfecting increasing amounts of HA led to increased amounts of HA present in the VLPs. Furthermore, we could confirm our previous

observation that IFITM3 reduced the amount of HA incorporated into VLPs. Interestingly, in the presence of IFITM3, the increase in HA incorporation was paralleled by a decrease in IFITM3 incorporation (Fig. 4B). We then normalized the input amount of VLPs via Western Blot for BlaM1 and infected MDCKII cells. Intriguingly, while the negative effect of IFITM3 on VLP infectivity was alleviated in a dose-dependent manner by an increase in HA, increasing the amount of NA did not affect VLP infectivity (Fig. 4C).

IFITM3 incorporates into wild type IAV and increases its neutralization sensitivity

Our experiments described so far showed that IFITM3 present in producer cells negatively affected infectivity of HIV- and IAV-based VLPs pseudotyped with IAV glycoproteins. To address whether this was also true for IAV virions we infected A549 cells stably overexpressing IFITM3 with a high MOI of A/WSN/33 for 72 hours. When purifying and analysing viral supernatants via Western Blot we observed an enrichment of IFITM3 in supernatants from infected cells compared to mock-infected cells, suggesting that IFITM3 incorporated into viral particles (Fig. 5A). To corroborate our finding on IFITM3 incorporation into IAV, viral supernatants were subjected to transmission electron microscopy, where incorporation of IFITM3 into IAV virions was confirmed (Fig. 5B). Furthermore, HA levels were found to be reduced in virus cultured on IFITM3-overexpressing cells compared to virus grown on control cells (Fig. 5A), similar to what has been observed for HIV and IAV VLPs (Suppl. Fig. 1, Fig. 3C, Fig. 4C). To compare the infectivity of virus grown on IFITM3-overexpressing vs. control cells we performed a luciferase IAV mini-genome reporter assay or plaque assays using qPCR-normalized viral inputs. In contrast to the results obtained with VLPs, IAV grown on IFITM3-overexpressing cells was not reduced in its infectivity compared to virus cultured on control cells (Fig. 5C). In an attempt to explain these conflicting results and remembering that sensitivity to IFITM3 depended on the levels of HA present in VLP producer cells (Fig. 4C) we analysed producer cell lysates from IAV, HIV VLP and IAV VLP samples (Fig. 5D). Interestingly, ratios between IFITM3 and HA signal intensities varied between the different samples, with HIV and IAV VLPs showing higher IFITM3:HA ratios than IAV, correlating with their respective IFITM3 sensitivities.

Finally, our observation that IFITM3 decreased the amount of HA incorporated into virions (Fig. 5A) would predict that virus grown on IFITM3-expressing cells would be more susceptible to neutralization by HA-directed antibodies than virus grown on control cells. To test this, viral supernatants from either control or IFITM3-expressing cells normalized by qRT-PCR were pre-incubated with a dilution series of a monoclonal anti-A/WSN/33 HA antibody, before being used to infect MDCKII cells. Indeed, when treated with the same amount of anti-HA antibody, virus grown in the absence of IFITM3 was more infectious than virus grown in the presence of IFITM3, as depicted in Fig. 5E.

In summary, we show that IAV VLPs are decreased in their infectivity upon IFITM3 presence in VLP producer cells and that sensitivity to IFITM3 is alleviated in a dose-dependent manner by an increase in producer cells' HA but not NA concentration. Furthermore, we observed a reduction in HA incorporation into IAV as well as IAV VLPs when IFITM3 was expressed in producer cells, which was corroborated by the finding that IAV cultured on IFITM3-expressing cells showed increased HA-neutralization sensitivity. Together these findings suggest a role for IFITM3 in late stages of the IAV life cycle.

Discussion

IFITM proteins are potent interferon-induced antiviral factors blocking IAV as well as many other viruses at the step of viral entry [1-5, 7]. Intriguingly, recent studies [17], [18] [19] established an additional antiviral function of IFITMs exerted against HIV-1 much later in the viral life cycle. Compton [17] and Tartour [18] and colleagues reported the incorporation of IFITMs into nascent virions, which they found to be associated with a decrease in virus infectivity. Although not ruling out a potential effect of IFITMs on the envelope glycoprotein (Env), the authors hypothesized that the biophysical properties imposed on membranes through IFITM incorporation (positive curvature, decreased membrane fluidity), account for the decrease in virion fusogenicity. In contrast, Yu [19] and colleagues observed an interaction between IFITM3 and Env that led to the impairment of Env processing and incorporation. Interestingly, although they also reported IFITM incorporation into budding virions, they saw no correlation between the amount of IFITM incorporation and decrease in fusion capacity.

Here, we show that HIV-based VLPs pseudotyped with IAV HA and NA, HIV-1 Env or VSV-G incorporated IFITM3 (Fig. 1B). Of note, IFITM3 was also detected in no Env VLP controls, confirming that IFITM3 incorporation occurs Env-independently, as has been shown previously [17]. In agreement with current literature [17-19] we observed a reduction in entry capacity of VLPs pseudotyped with HIV-1 Env upon presence of IFITM3 in producer cells. Intriguingly, the same was found to hold true for VLPs displaying IAV HA and NA. We did not observe a negative effect on the entry capacity of VSV-G pseudotyped VLPs upon presence of IFITM3 in VLP producer cells, disagreeing with findings published earlier [17, 18]. This might be explained by differences in VSV-G to IFITM3 ratios in VLP producer cells between the different studies. Furthermore, we observed that IFITM3 blocked VLP infectivity at the level of the producer as well as the target cell for HIV Env and IAV HA/NA, but not VSV-G pseudotyped VLPs. We therefore suggest that for certain viral envelopes, IFITM3 in producer cells contributes to IFITM3's antiviral activity to a similar extent as IFITM3 expressed in target cells. While VLPs pseudotyped with VSV-G were not inhibited by IFITM3 expressed in producer cells (Fig. 1E-F & Fig. 2C), IFITM3 in target cells potently blocked VSV-G VLP infection, in line with previous observations that VSV was inhibited by IFITMs [7].

We also report IFITM3 incorporation into β-lactamse-M1 (BlaM1) IAV VLPs and show that the presence of IFITM3 in producer cells significantly decreased the entry capacity of those VLPs (Fig. 3B). We therefore conclude that IFITM incorporation into VLPs is not specific to the HIV-based, but also true for an IAV-based VLP system. Interestingly, we observed a reduction in IAV VLP HA upon presence of IFITM3 in VLP producer cells (Fig. 3C) which could negatively affect and thus explain the reduction in VLP infectivity. Since IFITM3 was not found to reduce cellular HA levels (Fig. 4A) we hypothesize that the reduction in VLP HA is either brought about by competition between IFITM3

and HA in cellular membranes or by a direct interaction between IFITM3 and HA that negatively regulates HA incorporation. We then determined whether an increase in HA in VLP producer cells would outcompete IFITM3. By testing the entry efficiency of BlaM1 VLPs produced in the presence of increasing amounts of HA or NA we show that HA indeed is targeted either directly or indirectly by IFITM3, since increasing amounts of HA titrated out the negative effect of IFITM3 on VLP infectivity in a dose-dependent manner, while increasing the amount of NA did not have any consequences on VLP infectivity (Fig. 4C). Interestingly, we again observed a decrease in HA signal in VLPs produced in IFITM3-expressing cells compared to VLPs produced in control cells. At the same time, an increase in HA incorporation was paralleled by a decrease in VLP-associated IFITM3 (Fig. 4B), suggesting that HA and IFITM3 might indeed compete for incorporation into cellular membranes.

When analyzing supernatants from either mock-treated or IAV-infected IFITM3-expressing cells we observed an enrichment of IFITM3 in the supernatant of infected cells (Fig. 5A), suggesting that IFITM3 was incorporated into nascent virions. However, as it had been observed previously [19, 27], we also detected a significant amount of IFITM3 in the supernatant of uninfected cells (Fig. 5A), most likely stemming from IFITM3-containing exosomes that potentially confound our conclusions. To clarify whether or not IFITM3 incorporates into IAV we subjected our samples to transmission electron microscopy and could indeed demonstrate that IFITM3 was present in the membrane of IAV cultured on IFITM3-expressing cells (Fig. 5B). Furthermore, we detected a decrease in the HA_0 : M1 ratio in IAV grown on IFITM3-overexpressing cells compared to virus grown on control cells (Fig. 5A), reminiscent of the reduction in HA upon presence of IFITM3 in HIV and IAV VLP producer cells (Fig. 3C, 4C, S1) and similar to observations described for HIV-1 [19]. Surprisingly, neither IFITM3 incorporation, nor a reduction in HA, negatively affected IAV infectivity, as assessed by plaque assay or a luciferase reporter mini-genome assay (Fig. 5C). One might speculate that the IFITM3:HA ratio in producer cells might be decisive in whether or not IFITM3 negatively imprints on virus/VLP infectivity (Fig. 5D). In fact, IFITM3:HA ratios in producer cells determined for the experiments reported in this study correlated with the negative effect IFITM3 exerted on virus/VLP infectivity. Although we did not observe a negative effect on IAV infectivity upon IFITM3 presence in infected cells, we wondered whether the observed reduction in HA might render the virus more neutralization-sensitive. By incubating virus grown on either control or IFITM3-overexpressing cells (normalized by qRT-PCR) with different dilutions of an HA-directed antibody prior to infection, we could indeed show that IAV cultured on IFITM3-overexpressing cells was more neutralization-sensitive. It is tempting to speculate that this would compromise a virus in an *in vivo* situation.

Sensing an invading virus or stimulated by IFN, a cell expresses a broad variety of interferon-stimulated genes (ISGs) that act as antiviral factors [28]. IFITM3 has been described as one of the most potent ISGs in human cells and mice. Brass and colleagues [1] demonstrated that IFITM3

constitutes approx. 50 % of the IFN-α and –γ response in cultured human cells and Bailey and colleagues [22] reported faster disease progression, higher viral loads and a higher mortality in mice lacking the *ifitm3* locus. While the role of IFITM3 in blocking the entry step of various viruses has been extensively studied [1, 2, 4-8, 11, 20, 29], the notion that IFITM3 also acts on later stages of the viral life cycle and incorporates into budding virions [17-19] is rather new. However, other ISGs have been reported to be packaged into viruses before. A prime example is APOBEC3G, a cytidine deaminase that damages the viral genome through hypermutation by inducing G to A mutations in the viral cDNA [30-32]. In the constant arms race between virus and host, HIV-1 evolved countermeasures to antagonize APOBEC3G-mediated restriction. Its accessory protein Vif has been found to promote proteasomal degradation of APOBEC3G, as well as its exclusion from budding virions [33]. In contrast to Vif, no viral antagonist counteracting IFITM has been discovered to date. While two studies [19, 34] reported the emergence of HIV strains partly refractory to IFITM-mediated inhibition, resistance was attributed to truncations in Vpu and mutations in Env in both cases. Interestingly, a recent publication identified the HIV V3 loop as determinant for IFITM3 susceptibility in the context of IFITM incorporation [35]. This is in line with previous observations that HIV susceptibility to IFITMs is modulated by co-receptor usage [36], which is known to be steered by the V3 loop [37].

We found no direct correlation between IFITM incorporation and reduction in viral/VLP infectivity but rather suggest that the interplay between IFITMs and envelope glycoproteins determines virus/VLP sensitivity to IFITM incorporation. For IAV it is tempting to speculate that on an evolutionary scale, IFITMs might drive the virus towards higher levels of HA incorporation. Further studies will be needed to elucidate whether other viruses have evolved different strategies to circumvent IFITM restriction.

In summary, we show that IAV is targeted by IFITM3 not only at the step of viral entry but also at late stages of infection. By blocking viruses at different steps of their life cycle IFITM3 broadens its antiviral potential and likely impedes the development of viral resistances.

Acknowledgements

Imaging was performed with equipment and support of the Center for Microscopy and Image Analysis, University of Zurich.

References

1. Brass, A.L., et al., *The IFITM proteins mediate cellular resistance to influenza A H1N1 virus, West Nile virus, and dengue virus.* Cell, 2009. **139**(7): p. 1243-54.
2. Savidis, G., et al., *The IFITMs Inhibit Zika Virus Replication.* Cell Rep, 2016. **15**(11): p. 2323-30.
3. Everitt, A.R., et al., *IFITM3 restricts the morbidity and mortality associated with influenza.* Nature, 2012. **484**(7395): p. 519-23.
4. Huang, I.C., et al., *Distinct patterns of IFITM-mediated restriction of filoviruses, SARS coronavirus, and influenza A virus.* PLoS Pathog, 2011. **7**(1): p. e1001258.
5. Lu, J., et al., *The IFITM proteins inhibit HIV-1 infection.* J Virol, 2011. **85**(5): p. 2126-37.
6. Mudhasani, R., et al., *IFITM-2 and IFITM-3 but not IFITM-1 restrict Rift Valley fever virus.* J Virol, 2013. **87**(15): p. 8451-64.
7. Weidner, J.M., et al., *Interferon-induced cell membrane proteins, IFITM3 and tetherin, inhibit vesicular stomatitis virus infection via distinct mechanisms.* J Virol, 2010. **84**(24): p. 12646-57.
8. Weston, S., et al., *Alphavirus Restriction by IFITM Proteins.* Traffic, 2016. **17**(9): p. 997-1013.
9. Friedman, R.L., et al., *Transcriptional and posttranscriptional regulation of interferon-induced gene expression in human cells.* Cell, 1984. **38**(3): p. 745-55.
10. Reid, L.E., et al., *A single DNA response element can confer inducibility by both alpha- and gamma-interferons.* Proc Natl Acad Sci U S A, 1989. **86**(3): p. 840-4.
11. Li, K., et al., *IFITM proteins restrict viral membrane hemifusion.* PLoS Pathog, 2013. **9**(1): p. e1003124.
12. Lin, T.Y., et al., *Amphotericin B increases influenza A virus infection by preventing IFITM3-mediated restriction.* Cell Rep, 2013. **5**(4): p. 895-908.
13. Yount, J.S., R.A. Karssemeijer, and H.C. Hang, *S-palmitoylation and ubiquitination differentially regulate interferon-induced transmembrane protein 3 (IFITM3)-mediated resistance to influenza virus.* J Biol Chem, 2012. **287**(23): p. 19631-41.
14. Jia, R., et al., *The N-terminal region of IFITM3 modulates its antiviral activity by regulating IFITM3 cellular localization.* J Virol, 2012. **86**(24): p. 13697-707.
15. Jia, R., et al., *Identification of an endocytic signal essential for the antiviral action of IFITM3.* Cell Microbiol, 2014. **16**(7): p. 1080-93.
16. Yount, J.S., et al., *Palmitoylome profiling reveals S-palmitoylation-dependent antiviral activity of IFITM3.* Nat Chem Biol, 2010. **6**(8): p. 610-4.
17. Compton, A.A., et al., *IFITM proteins incorporated into HIV-1 virions impair viral fusion and spread.* Cell Host Microbe, 2014. **16**(6): p. 736-47.
18. Tartour, K., et al., *IFITM proteins are incorporated onto HIV-1 virion particles and negatively imprint their infectivity.* Retrovirology, 2014. **11**: p. 103.
19. Yu, J., et al., *IFITM Proteins Restrict HIV-1 Infection by Antagonizing the Envelope Glycoprotein.* Cell Rep, 2015. **13**(1): p. 145-56.
20. Desai, T.M., et al., *IFITM3 restricts influenza A virus entry by blocking the formation of fusion pores following virus-endosome hemifusion.* PLoS Pathog, 2014. **10**(4): p. e1004048.
21. John, S.P., et al., *The CD225 domain of IFITM3 is required for both IFITM protein association and inhibition of influenza A virus and dengue virus replication.* J Virol, 2013. **87**(14): p. 7837-52.
22. Bailey, C.C., et al., *Ifitm3 limits the severity of acute influenza in mice.* PLoS Pathog, 2012. **8**(9): p. e1002909.
23. Pugach, P., et al., *HIV-1 clones resistant to a small molecule CCR5 inhibitor use the inhibitor-bound form of CCR5 for entry.* Virology, 2007. **361**(1): p. 212-28.
24. Tscherne, D.M. and A. Garcia-Sastre, *An enzymatic assay for detection of viral entry.* Curr Protoc Cell Biol, 2011. **Chapter 26**: p. Unit 26 12.
25. Hoffmann, H.H., P. Palese, and M.L. Shaw, *Modulation of influenza virus replication by alteration of sodium ion transport and protein kinase C activity.* Antiviral Res, 2008. **80**(2): p. 124-34.

26. Nohinek, B., W. Gerhard, and I.T. Schulze, *Characterization of host cell binding variants of influenza virus by monoclonal antibodies.* Virology, 1985. **143**(2): p. 651-6.
27. Zhu, X., et al., *IFITM3-containing exosome as a novel mediator for anti-viral response in dengue virus infection.* Cell Microbiol, 2015. **17**(1): p. 105-18.
28. Schneider, W.M., M.D. Chevillotte, and C.M. Rice, *Interferon-stimulated genes: a complex web of host defenses.* Annu Rev Immunol, 2014. **32**: p. 513-45.
29. Feeley, E.M., et al., *IFITM3 inhibits influenza A virus infection by preventing cytosolic entry.* PLoS Pathog, 2011. **7**(10): p. e1002337.
30. Bishop, K.N., et al., *APOBEC-mediated editing of viral RNA.* Science, 2004. **305**(5684): p. 645.
31. Mangeat, B., et al., *Broad antiretroviral defence by human APOBEC3G through lethal editing of nascent reverse transcripts.* Nature, 2003. **424**(6944): p. 99-103.
32. Sheehy, A.M., et al., *Isolation of a human gene that inhibits HIV-1 infection and is suppressed by the viral Vif protein.* Nature, 2002. **418**(6898): p. 646-50.
33. Sheehy, A.M., N.C. Gaddis, and M.H. Malim, *The antiretroviral enzyme APOBEC3G is degraded by the proteasome in response to HIV-1 Vif.* Nat Med, 2003. **9**(11): p. 1404-7.
34. Ding, S., et al., *HIV-1 mutates to evade IFITM1 restriction.* Virology, 2014. **454-455**: p. 11-24.
35. Wang, Y., et al., *The V3-loop of HIV-1 Env determines viral susceptibility to IFITM3 impairment of viral infectivity.* J Virol, 2017.
36. Foster, T.L., et al., *Resistance of Transmitted Founder HIV-1 to IFITM-Mediated Restriction.* Cell Host Microbe, 2016. **20**(4): p. 429-442.
37. Pollakis, G., et al., *N-linked glycosylation of the HIV type-1 gp120 envelope glycoprotein as a major determinant of CCR5 and CXCR4 coreceptor utilization.* J Biol Chem, 2001. **276**(16): p. 13433-41.
38. Science, B.I.o.C.a.M. *FRET based gene reporter system - CCF2 mode of action*. [cited 2017 February 1st]; Available from: http://www.icms.qmul.ac.uk/flowcytometry/uses/fret/diagrams/CFF2.jpg.

Figure legends

Figure 1: IFITM3 present in VLP-producing cells restricts the entry capacity of HIV VLPs pseudotyped with IAV and HIV envelopes. A) Schematic depiction of HIV VLP generation. 293-T cells were co-transfected with pNL-LucAM (NL4-3 genome having the envelope gene replaced by the firefly luciferase gene), plasmids encoding the HIV JRFL, IAV A/WSN/33 or VSV envelope gene and either Flag-IFITM3 or the empty vector pCAGGS. VLPs were harvested 72 h post-transfection. **B)** VLPs described in A) were purified and concentrated by ultracentrifugation through a 20% sucrose cushion, normalized via p24 ELISA and analyzed by Western Blot. Membrane was probed with anti-Flag and anti-p24 antibodies. **C)** Fold luciferase activity (compared to the empty vector control) in A549 cells infected for 48h with VLPs produced in the absence of IFITM3. **D)** Fold luciferase activity (compared to the empty vector control) in TZM cells infected for 48h with VLPs produced in the absence of IFITM3. **E)** % infectivity (compared to infectivity of VLPs produced in the absence of IFITM3) of VLPs pseudotyped with IAV or VSV envelopes in the presence or absence of IFITM3 in A549 cells. **F)** % infectivity (compared to infectivity of VLPs produced in the absence of IFITM3) of VLPs pseudotyped with HIV or VSV envelopes in the presence or absence of IFITM3 in TZM cells. **C-F)** Mean values from three biological replicates, each performed in triplicate, are shown, with error bars representing standard deviations. **E-F)** Statistical significance was assessed by a paired two-tailed Student *t* test (**, P<0.01; ****, P<0.0001).

Figure 2: IFITM3 blocks VLP infectivity at the level of the producer cell as well as the target cell for IAV and HIV-1 but not for VSV in an HIV-based VLP system. A-C) % infectivity of HIV VLPs pseudotyped with IAV A/WSN/33 HA and NA **(A)**, HIV JRFL Env **(B)** or VSV-G **(C)** produced in the presence or absence of IFITM3. VLPs pseudotyped with IAV Envs were used to infect A549 cells **(A)**, while VLPs harboring HIV-1 or VSV Envs were used to infect TZM cells **(B-C)** that were either IFITM3-negative (-IFITM3) or IFITM3-positive (+IFITM3). Data were normalized to infectivity in control cells infected with VLPs produced in the absence of IFITM3. Mean values from three biological replicates, each performed in triplicate, are shown, with error bars representing standard deviations. Statistical significance was assessed by a paired two-tailed Student *t* test (*, P<0.05; **, P<0.01), comparing the infectivity in the different conditions to infectivity of VLPs produced in the absence of IFITMs infecting IFITM3-negative cells.

Figure 3: IFITM3 in VLP-producing cells restricts the entry capacity of IAV VLPs. A) Schematic depiction of the β-lactamase-M1 (BlaM1) VLP assay. VLPs harboring a β-lactamase-M1 fusion protein and displaying A/WSN/33 HA and NA at their surface are used to infect target cells. Upon cellular entry, β-lactamase is released into the cytoplasm and cleaves the fluorigenic substrate CCF2 which

shifts in emission upon cleavage (modified from [38]). **B)** BlaM1 VLPs produced in the presence (+IFITM3) or absence (-IFITM3) of IFITM3 normalized via Western Blot were used to infect MDCKII cells. VLP entry-positive (harboring cleaved CCF2) and -negative (harboring uncleaved CCF2) cells were assessed by FACS. Left: Depiction of density plots of one representative experiment. The percentage of entry-positive cells is indicated. Right: Infectivity of +IFITM3 VLPs normalized to –IFITM3 VLPs. Bars represent the mean of three biological replicates, with the error bar representing standard deviation. Statistical significance was assessed by a paired two-tailed Student *t* test (**, P<0.01), comparing the infectivity of +IFITM3 VLPs to the infectivity of –IFITM3 VLPs. **C)** VLPs described in B) were purified and concentrated by ultracentrifugation through a 20% sucrose cushion before being analyzed by Western Blot. Membrane was stained using a polyclonal antibody against A/WSN/33 proteins and an antibody against IFITM3. Expression levels of HA_2 normalized to BlaM1 levels are given below the HA_2 WB.

Figure 4: HA but not NA outcompetes IFITM3 in VLP producing cells. A) 293-T cells were co-transfected with pCAGGS-HA and increasing amounts of pCAGGS-Flag-IFITM3. Whole cell lysates were analyzed by Western Blot and membrane was stained for HA, Flag and actin. Expression levels of HA_0 in relation to the strongest band are given below the HA_0 WB. The asterisk marks the condition used for the production of VLPs with the lowest amount of HA in B). **B)** VLPs produced in the presence or absence of IFITM3 and increasing amounts of HA were analyzed by Western Blot. Membrane was stained using a polyclonal antibody against A/WSN/33 proteins and a Flag antibody. HA_2 and IFITM3 band intensities were normalized to BlaM1. Expression levels of HA_2 and IFITM3 in relation to the strongest band are given below the respective WBs. **C)** BlaM1 VLPs produced in IFITM3-positive (+I3) or IFITM3-negative (-I3) cells in the presence of increasing amounts of HA (left) or NA (right) were used to infect MDCKII cells. For each condition, bars representing the percentage of entry-positive cells from +I3 VLP infection normalized to entry-positive cells from –I3 VLP infection are shown.

Figure 5: IFITM3 incorporates into wt IAV and increases its neutralization sensitivity. A) A549 control or IFITM3-overexpressing cells were infected with A/WSN/33 at MOI 1 for 72h. Supernatants were purified and concentrated by ultracentrifugation through a 20% sucrose cushion before being lysed and analyzed by Western Blot. Membrane was probed for HA, M1 and IFITM3. HA_0 band intensities were normalized to M1 and the expression level of HA_0 in relation to the stronger band is given below the respective WB. **B)** Virus described in A) was purified and concentrated by ultracentrifugation through a 20% sucrose cushion. For Immuno-EM studies virus was fixed and immunogold labeled using a polyclonal anti-IFITM3 antibody. Scale bar: 100 nm **C)** Left: Virus

described in A) was normalized via RT-qPCR and its infectious titer determined via plaque assay on MDCK cells. Right: 293-T cells were transfected with a reporter plasmid encoding firefly luciferase in complementary reverse orientation flanked by IAV noncoding regions, thus mimicking a viral genome segment. Cells were subsequently infected with virus described in A) that was normalized via RT-qPCR. Luciferase signal was measured 48h p.i. **D)** IFITM3-positive (+I3) and -negative (-I3) virus, HIV VLP and IAV VLP producer cells were lysed and analyzed by Western Blot. Membrane was stained using a polyclonal antibody against A/WSN/33 proteins and antibodies against Flag and GAPDH. Flag-IFITM3 : HA ratios for each condition are given below the Western Blot. **E)** Virus described in A) was normalized via RT-qPCR and incubated with different dilutions of a monoclonal anti-A/WSN/33 HA antibody before being used for infecting MDCKII cells. Cells were fixed 4h p.i. and infectivity was assessed by microscopy-based quantification of NP-positive cells.

Supplemental Figure 1: HIV VLPs pseudotyped with HIV or IAV Envs show decreased glycoprotein levels when produced in IFITM3-overexpressing cells. A) VLPs described in Fig. 1B) were analyzed by Western Blot. Membrane was stained using antibodies against p24, Flag, HIV Env, VSV-G and A/WSN/33 proteins. The panel on the left depicts one representative Western Blot, while the right panel shows the quantification of normalized Env signal intensities from Western Blots performed using three independent VLP batches. Statistical significance was assessed by a paired two-tailed Student *t* test (*, $p<0.05$).

Fig. 1

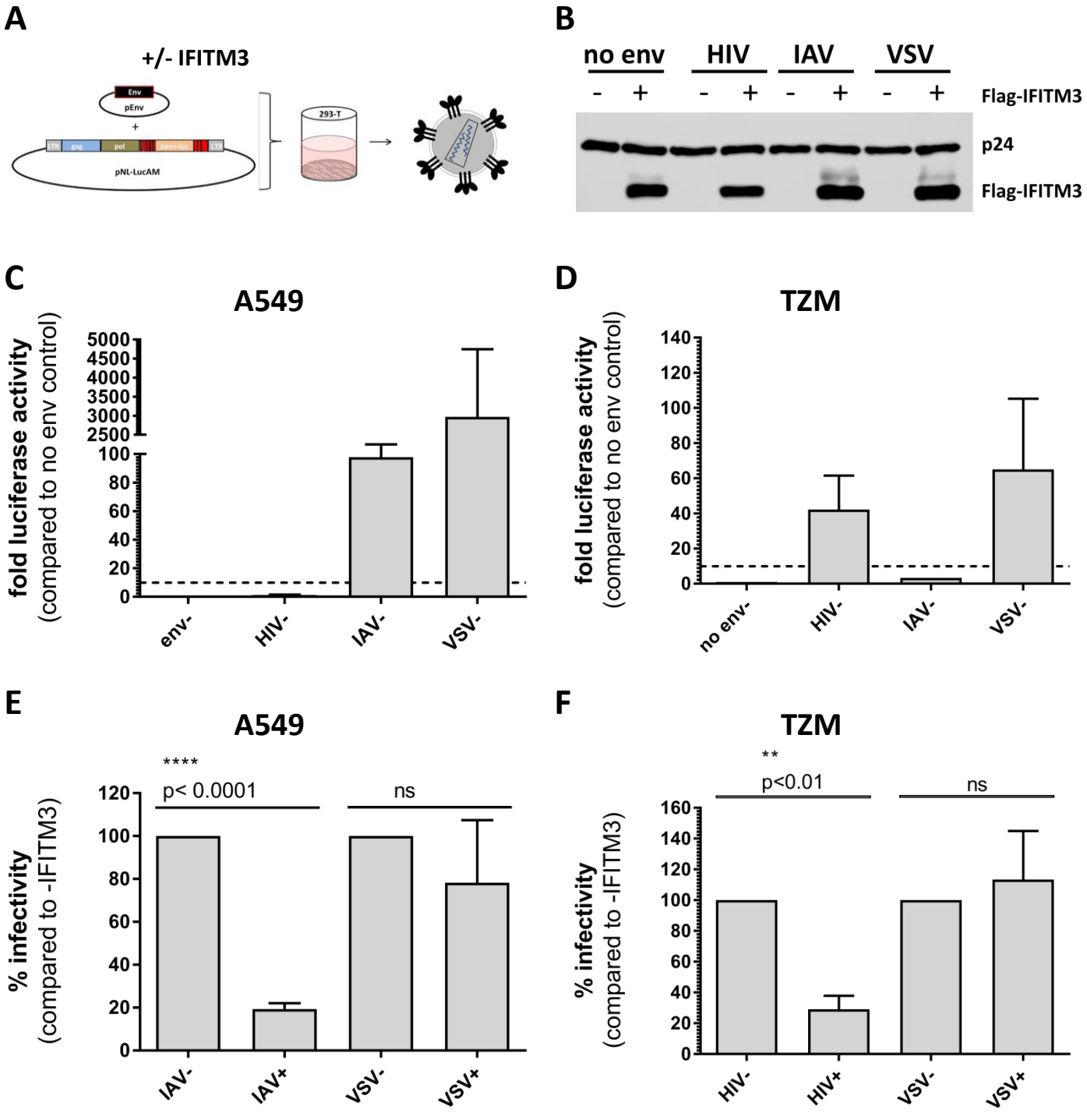
A
+/- IFITM3
Env
pEnv
+
pNL-LucAM
293-T
B
no env
HIV
IAV
VSV
- + - + - + - +
Flag-IFITM3
p24
Flag-IFITM3
C
A549
fold luciferase activity
(compared to no env control)
5000
4500
4000
3500
3000
2500
100
80
60
40
20
0
env-
HIV-
IAV-
VSV-
D
TZM
fold luciferase activity
(compared to no env control)
140
120
100
80
60
40
20
0
no env-
HIV-
IAV-
VSV-
E
A549
****
p< 0.0001
ns
% infectivity
(compared to -IFITM3)
120
100
80
60
40
20
0
IAV-
IAV+
VSV-
VSV+
F
TZM
**
p<0.01
ns
% infectivity
(compared to -IFITM3)
160
140
120
100
80
60
40
20
0
HIV-
HIV+
VSV-
VSV+

Fig. 2

A

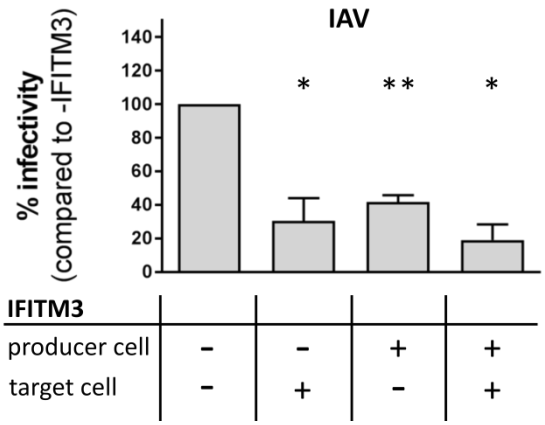
IAV
% infectivity (compared to -IFITM3)
140
120
100
80
60
40
20
0
* ** *
IFITM3
producer cell - - + +
target cell - + - +

B

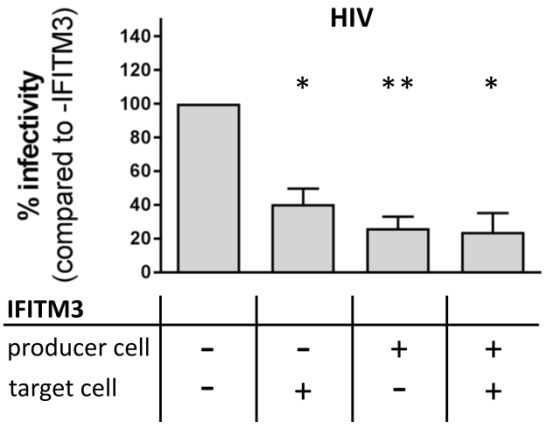
HIV
% infectivity (compared to -IFITM3)
140
120
100
80
60
40
20
0
* ** *
IFITM3
producer cell - - + +
target cell - + - +

C

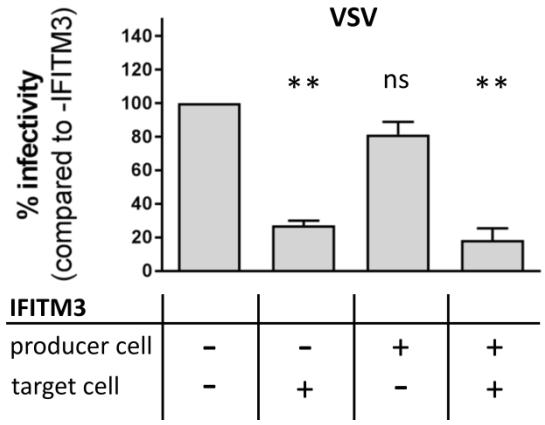
VSV
% infectivity (compared to -IFITM3)
140
120
100
80
60
40
20
0
** ns **
IFITM3
producer cell - - + +
target cell - + - +

Fig. 3

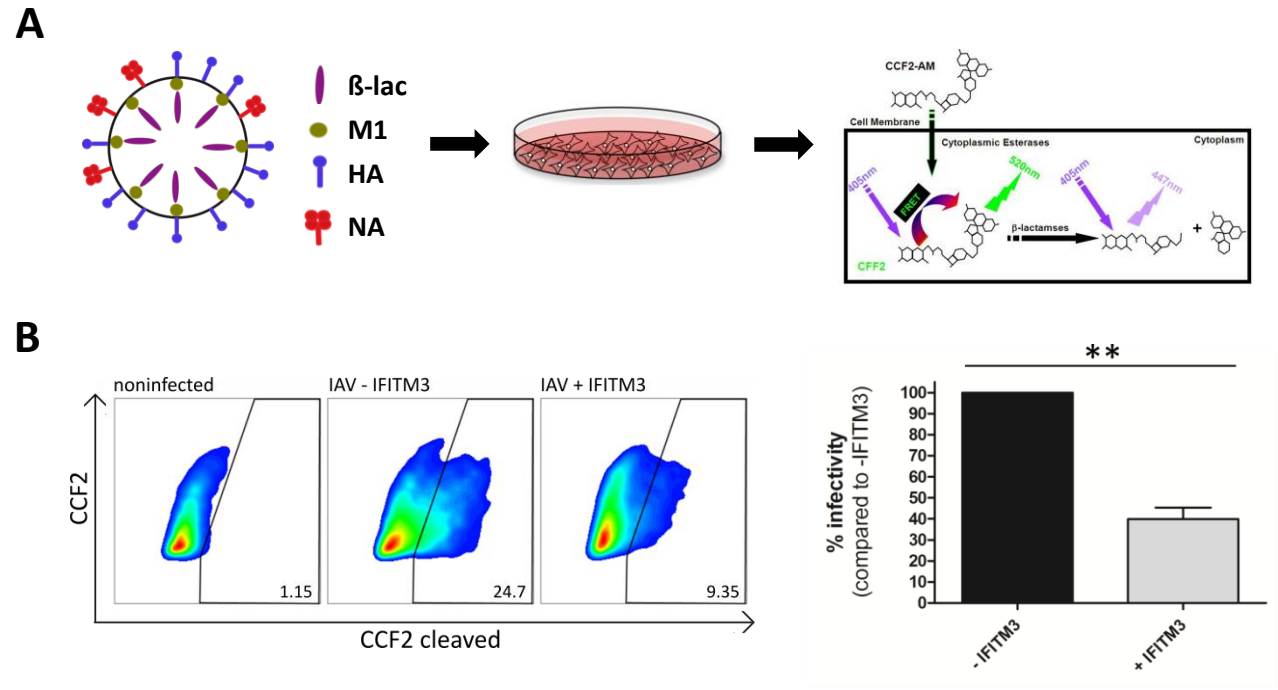
A
ß-lac
M1
HA
NA
CCF2-AM
Cell Membrane
Cytoplasmic Esterases
Cytoplasm
405nm
FRET
520nm
405nm
447nm
β-lactamses
CFF2
B
noninfected
IAV - IFITM3
IAV + IFITM3
CCF2
1.15
24.7
9.35
CCF2 cleaved
**
% infectivity
(compared to -IFITM3)
100
90
80
70
60
50
40
30
20
10
0
- IFITM3
+ IFITM3
C
- +
Flag-IFITM3
BlaM1
HA2
1.0 0.57
Flag-IFITM3

Fig. 4

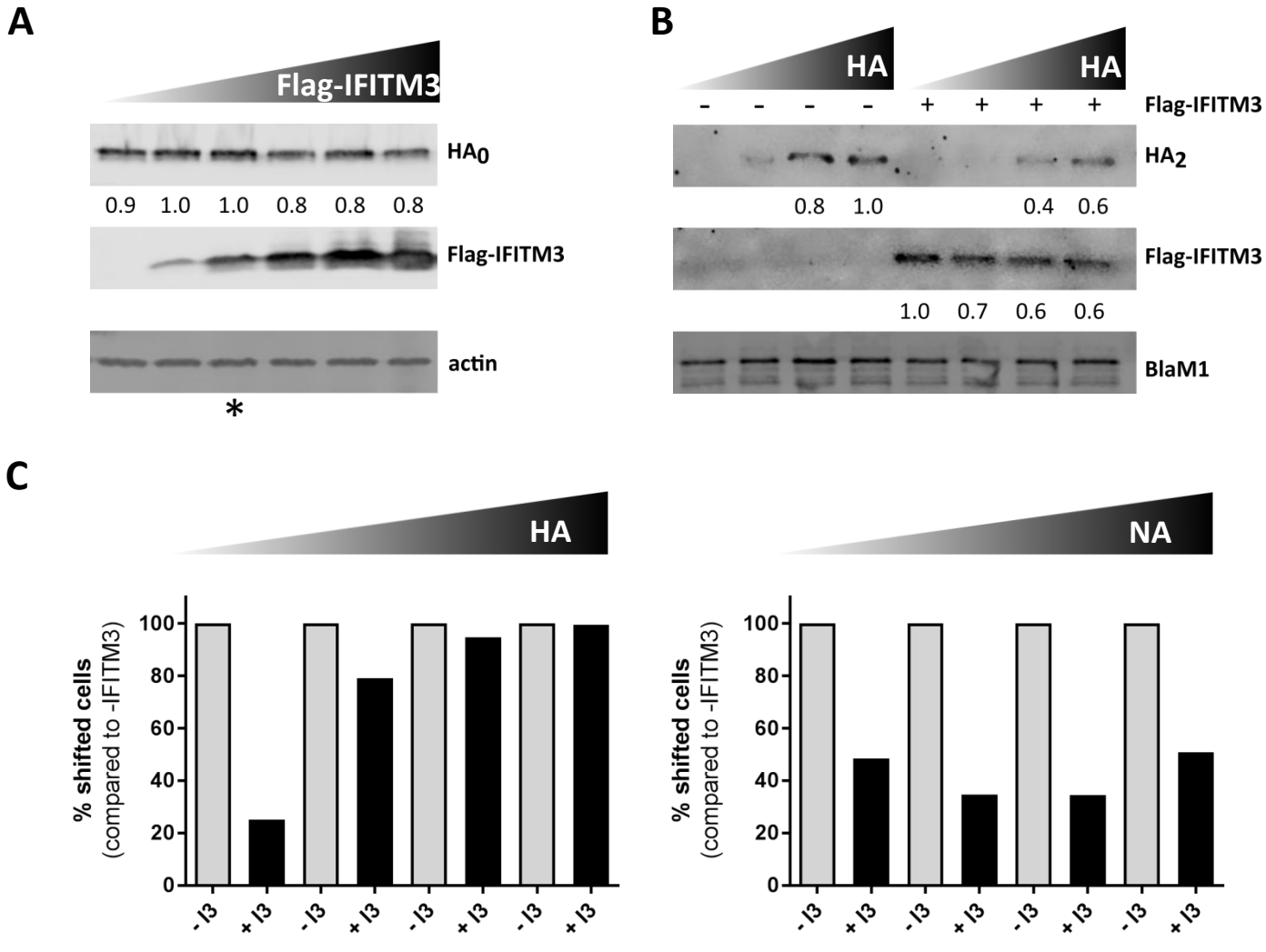
A
Flag-IFITM3
HA0
0.9 1.0 1.0 0.8 0.8 0.8
Flag-IFITM3
actin
*
B
HA
HA
- - - - + + + + Flag-IFITM3
HA2
0.8 1.0 0.4 0.6
Flag-IFITM3
1.0 0.7 0.6 0.6
BlaM1
C
HA
NA
% shifted cells
(compared to -IFITM3)
100
80
60
40
20
0
- I3
+ I3

Fig. 5

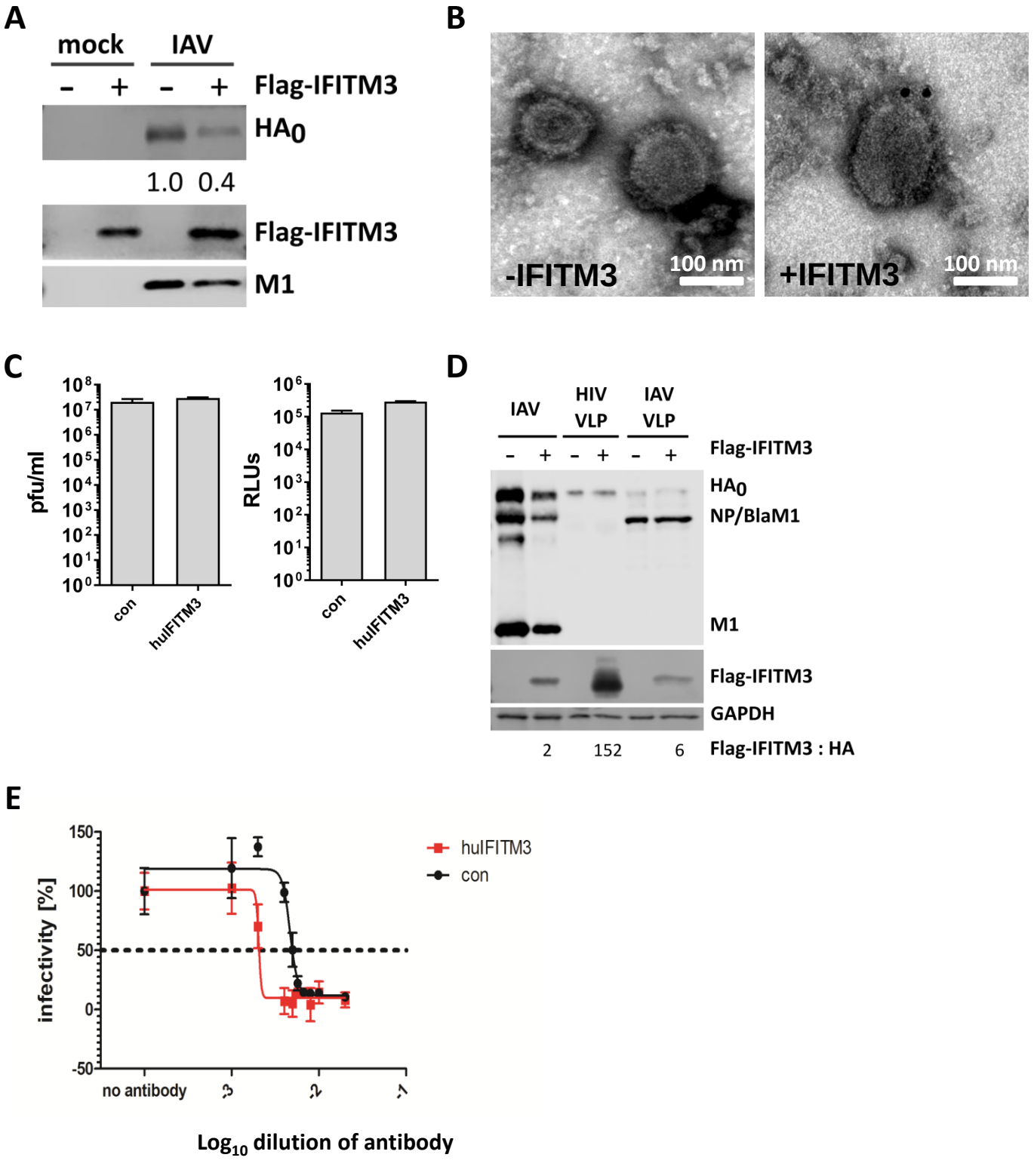
A
mock
IAV
- + - +
Flag-IFITM3
HA0
1.0 0.4
Flag-IFITM3
M1
B
-IFITM3
100 nm
+IFITM3
100 nm
C
pfu/ml
RLUs
con
hulFITM3
con
hulFITM3
D
IAV
HIV VLP
IAV VLP
- + - + - +
Flag-IFITM3
HA0
NP/BlaM1
M1
Flag-IFITM3
GAPDH
2 152 6
Flag-IFITM3 : HA
E
infectivity [%]
150
100
50
0
-50
no antibody
hulFITM3
con
Log10 dilution of antibody

Supp. Fig. 1

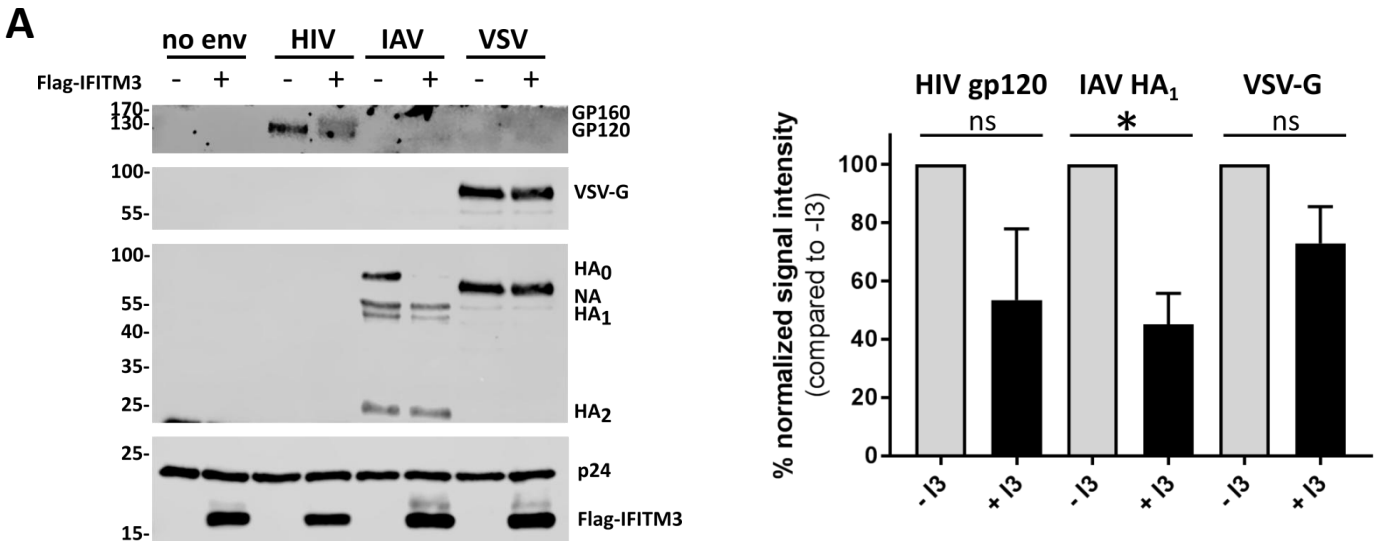
A
no env
HIV
IAV
VSV
Flag-IFITM3
- + - + - + - +
170-
130-
GP160
GP120
100-
55-
VSV-G
100-
55-
40-
35-
25-
HA0
NA
HA1
HA2
25-
p24
15-
Flag-IFITM3
HIV gp120
IAV HA1
VSV-G
ns
*
ns
% normalized signal intensity
(compared to -I3)
100
80
60
40
20
0
- I3
+ I3
- I3
+ I3
- I3
+ I3

Chapter 4

DISCUSSION

4.1 IFITM PROTEINS ARE POTENT INHIBITORS OF VIRAL ENTRY

Immunity-related IFITMs (IFITM1-3 in humans) are interferon-stimulated genes (ISGs) that inhibit a broad variety of different viruses from entering their target cells [202]. It is likely that the multiple IFITM gene duplication events that occurred in various species [195, 197] allowed for the functional diversification of these proteins from their roles in germ cell homing and maturation [220-222] to functions in antiviral immunity. Among immunity-related IFITMs, further gene duplications enabled the evolution of an array of IFITM proteins differing in their motifs responsible for subcellular localization, thereby facilitating their distribution to the different sites within a cell where viral fusion occurs [223]. Although IFITM proteins have been shown to increase positive membrane curvature [198, 211, 213] and to decrease membrane fluidity [198, 211] which was shown to interfere with the viral fusion process, the precise mechanism of IFITM's antiviral activity has not been resolved to date. While IFITMs have been reported to inhibit the entry of a variety of enveloped viruses, such as HIV [189, 190], VSV [191], IAV [184, 186] and Zika virus [192] and of one non-enveloped virus (reovirus) [224], several viruses have been shown to be refractory to IFITM-mediated restriction or to even profit from their activity. Human cytomegalovirus (HCMV) assembly takes place at the vAC, a perinuclear structure induced by the virus that has been shown to require IFITMs for their correct formation, possibly through the IFITM-mediated cholesterol accumulation in late endosomes/lysosomes [214, 225]. In contrast to HCMV that was shown to require IFITMs for virion assembly, human coronavirus OC43 (HCoV-OC43), a virus that enters host cells via endocytosis and whose envelope protein undergoes pH-dependent activation, was reported to benefit from IFITMs upon entry. While IFITMs did not influence envelope protein activation, the authors suggested IFITM's influence on membrane rigidity was required for the enhancement of HCoV-OC43 entry, since IFITM mutants unable to homo – or heterodimerize failed to enhance viral entry, a phenotype copied by the addition of amphotericin B to the cells [226], a compound that has been reported to increase membrane fluidity [214]. However, considering that IFITMs are also involved in cellular signaling processes [178, 180, 227] and that the IFITM's C-terminus was found to be critical for HCoV-OC443 entry enhancement [226], one might also speculate that HCoV-OC43 interacts with the IFITM C-terminus (which according to the most current membrane topology models is assumed to be accessible by virus binding to the cell surface [202]) to induce a signaling cascade that ultimately facilitates the process of viral fusion.

Furthermore, IFITMs have been reported to be ineffective in inhibiting certain viruses even though they do enter cells via endocytosis and require a low pH for envelope-mediated entry, such as human papillomavirus, adenovirus, cytomegalovirus [228] and arenaviruses [184]. Further studies on IFITM's antiviral mechanism might provide insight into potential strategies employed by these viruses to circumvent IFITM-mediated restriction, as for example the usage of alternative entry pathways to bypass IFITM-rich cellular compartments.

4.2 IDENTIFICATION OF SWINE INTERFERON-INDUCIBLE TRANSMEMBRANE PROTEINS AS POTENT INHIBITORS OF INFLUENZA A VIRUS REPLICATION

Due to the presence of α2,3 – as well as α2,6-linked sialic acid residues in the porcine trachea, pigs can be simultaneously infected with IAV strains from avian and human origin. They are thus hypothesized to play an important role in zoonotic transmission of IAV by facilitating genetic reassortment between IAV strains of different origin [88]. Wondering whether similar to humans [186] and mice [185] pigs are also protected from IAV infection by IFITM proteins we cloned the porcine homologues of human IFITM1-3 from IFN-stimulated porcine cells. IFITM proteins have been described to be very conserved in terms of protein motifs [197] and indeed, swIFITM protein sequences were very similar to their human counterparts, with the respective endocytosis motifs, transmembrane domains, intracellular loops, ubiquitination and palmitoylation sites highly conserved (Chapter 2, Fig. 1A). Interestingly, pigs were found to express two homologues of IFITM1, named swIFITM1a and swIFITM1b. All porcine IFITM homologues were found to be induced upon IAV infection or stimulation with universal IFN in porcine newborn swine kidney (NSK) and porcine kidney 15 (PK15) cells, except for swIFITM1a, which in NSK cells was only induced upon IFN-stimulation (Chapter 2, Fig. 1B-C). These observations matched results published in a previous study that reported the upregulation of swIFITMs in tracheobronchial lymph nodes in pigs infected with IAV [229]. Newborn pig trachea (NPTr) cells were found to be unresponsive to IFN-stimulation (Chapter 2, Fig. 1D). Like their human homologues, swIFITM2 and 3 localized to late endosomes and lysosomes and swIFITM1a was found predominantly at the plasma membrane in human as well as porcine cells. Intriguingly, while swIFITM1b localized almost exclusively to the plasma membrane in human A549 cells, some degree of colocalization with late endosomal/lysosomal markers was observed in porcine cells (Chapter 2, Fig.2). SwIFITM1a and 1b differ only slightly in their N – and C – termini. However, it was shown for human IFITM1 that the C-terminus regulates part of its anti-HIV-1 activity by modulating subcellular localization [230]. Since this has not been linked to a sequence motif so far, it might be interesting to swap the C-termini of swIFITM1a and swIFITM1b to check whether

differences in their localization and antiviral potential are solely attributable to their C-termini. Furthermore, testing the inhibitory potential of swIFITM1a and swIFITM1b against retroviruses and comparing them to human IFITM1 may provide additional insights into motifs or residues required for viral restriction.

While IFITM1's antiviral activity is steered by the protein's C-terminus, human IFITM3 harbors an N-terminal endocytosis motif responsible for its localization to late endosomes/ lysosomes [29], which has been shown to be required for anti IAV activity. Interestingly, N-terminal deletion mutants localize predominantly to the plasma membrane where they efficiently inhibit HIV-1. Compton and colleagues [223] showed in primates that IFITM3 underwent recurrent duplications (marmosets harbor as many as 25 copies of IFITM3), thereby allowing for the introduction of various mutations that have been shown to affect protein turn over and localization and ultimately antiviral potential against different viruses. Along those lines, it might be interesting to test porcine viruses and compare their sensitivities to swIFITM1a versus swIFITM1b.

In our study, we already assessed the antiviral potential of the different swIFITMs in human as well as porcine cells in an IAV mini-genome reporter assay [231] and a dose-dependent restriction capacity was observed for all swIFITMs tested, with swIFITM2 and 3 being the most antivirally active IFITMs, comparable to huIFITM3 which was used as positive control (Chapter 2, Fig. 3A-B). With the exception of swIFITM1b and swIFITM5 expressed in NSK cells, swIFITMs overexpressed in porcine NSK and NPTr cells significantly reduced IAV replication. In contrast to human or mouse Mx proteins that are highly active against avian IAV but lost their antiviral potential against human IAV strains [232], no differential sensitivity to swIFITMs was detected when comparing IAV strains of human and porcine origin (Chapter 2, Fig. 3C-H). Later, this observation was extended to avian IAV strains (Master thesis Eva Müller, unpublished data). This is in line with the hypothesis that IFITMs block fusion between the viral and the host cell membrane [198, 210] by decreasing membrane fluidity and increasing positive membrane curvature [198, 211, 213], which makes the occurrence of resistances rather unlikely, since all IAV strains, independent of their origin, eventually need to fuse with host cell membranes. Altering their HA to increase their optimal fusion pH might enable IAVs to fuse in an early endosome, thereby (partly) evading IFITM3. However, such viruses would likely suffer from decreased environmental stability [233, 234]. In contrast, Mx targets the viral NP protein that evades antiviral restriction by undergoing adaptive mutations [156].

Interestingly, the cell type-specific restriction capacity observed for swIFITM1b correlated with its subcellular localization. swIFITM1b showed higher co-localization with late endosomes/lysosomes in NPTr cells compared to NSK cells (Chapter 2, Fig. 2A-B), suggesting that in NPTr cells swIFITM1b was present at the site of IAV fusion, thereby increasing its antiviral capacity. However, this interpretation fails to explain why swIFITM1a which is expressed predominantly at the plasma membrane still

restricted IAV growth in both porcine cell lines. It is possible that in addition to blocking the fusion between viral and host cell membranes, IFITMs expressed at the plasma membrane also decrease endocytosis, which would result in a reduction in viral infection. To my knowledge, this has never been tested. Furthermore, since IFITMs have been reported to decrease membrane fluidity [198, 211], they might interfere with receptor tyrosine kinase (RTK) signaling in lipid rafts induced upon binding of IAV to the cell, which has been hypothesized to be required for IAV uptake [54].

Due to variations in IFITM expression levels in the different overexpressing cell lines (Chapter 2, Fig. 3E&H) it was difficult to assess the individual potency of each swIFITM, especially since IFITMs have been shown to act in a dose-dependent manner (Chaper 2, Fig. 3A). However, the fact that swIFITM3 levels were considerably lower than swIFITM1a levels, yet both IFITMs showed comparable inhibition of IAV, we hypothesized that a combination between IFITM localization and abundance determines its antiviral potential.

Finally, we determined the contribution of endogenous swIFITMs to the antiviral IFN response in porcine NSK cells. While the simultaneous knockdown of all swIFITMs had no impact on IAV titers in the absence of IFN, stimulation of cells with IFN prior to infection resulted in a 10fold increase in viral titers in swIFITM knockdown cells compared to control cells, highlighting the importance of swIFITMs in the antiviral activity of IFN in porcine cells (Chapter 2, Fig. 4).

In summary, we established swIFITM proteins as potent viral restriction factors that constitute a significant part of the anti-IAV activity of IFN in porcine cells, a finding corroborated by the fact that swIFITM proteins are highly upregulated in pigs infected with various swine respiratory disease viruses [229].

Although replicating in various species such as humans and pigs, aquatic birds are the main reservoir for IAV [1]. Low pathogenic avian IAVs (LPAI) replicate in the intestinal tract of aquatic but also gallinaceous birds causing no or only very mild disease symptoms [38]. However, upon acquiring mutations in the HA_0 cleavage site that facilitate the activation of HA by a much broader range of cellular proteases, viruses become highly pathogenic and are no longer restricted to the intestines, but also replicate in the lungs of infected animals, before ultimately spreading systemically if not contained by the host [235]. While chickens rapidly succumb to the infection with highly pathogenic avian influenza (HPAI) viruses, ducks efficiently control viral replication [236]. Smith et al [237] compared host responses mounted in ducks and chickens upon IAV infection and found that in ducks IFITM1, 2 and 3 were upregulated in lungs as well as intestines upon infection with a HPAI virus, while IFITM induction was negligible in chickens. These findings were corroborated by a study conducted by Blyth and colleagues [238] that showed a pronounced upregulation of IFITM proteins in lungs of ducks infected with a HPAI virus. Duck IFITM3 was subsequently reported to restrict the replication of LPAI viruses of avian as well as mammalian origin. Interestingly, no anti-IAV activity was

observed for duck IFITM1, which harbored an extensive N-terminal insertion. It might be interesting to test whether duck IFITM1 evolved to counteract other pathogens infecting ducks. Although chicken IFITMs were not found to be upregulated by IAV infection *in vivo* [237], possibly due to the lack of RIG-I (a sensor of viral RNA) in chicken cells [239], chicken IFITM3 was found to be induced upon IFNα-stimulation and to reduce IAV titers when overexpressed in chicken fibroblast cells [240]. In the future, in order to determine the *in vivo* relevance of IFITM proteins in chickens beyond IAV restriction, it might be worthwhile testing the IFITM induction upon challenge with pathogens that are recognized by the cell in the absence of RIG-I. In addition, to identify whether IFITM expression is decisive in controlling HPAI infection in ducks as compared to chickens it might be interesting to infect *ifitm3*$^{-/-}$ ducks with HPAI viruses.

Finally, considering the recent identification of bats as an alternative reservoir of IAV-like viruses [9, 10], one study reported the presence and antiviral activity of IFITM3 in *Myotis myotis*, a bat species known to be susceptible to infection with several highly pathogenic viruses [241].

Altogether, multiple studies assessing the antiviral potential of IFITM proteins present in species involved in zoonotic IAV transmission established these proteins as potent antiviral factors restricting IAV infection. IFITM proteins thus represent a major barrier that zoonotic as well as non-zoonotic IAVs have to overcome when infecting their hosts.

4.3 Assessing the role of IFITMs during late stages of the influenza A virus life cycle

In order to efficiently interfere with viral replication, different ISGs evolved to target presumably every step of the viral life cycle. While ISGs differ in their antiviral activity with some antiviral proteins showing only modest viral restriction capacity when expressed in isolation, their concerted upregulation enables the efficient elimination of invading pathogens [242, 243].

Several ISGs have been reported to be involved in late stages of the IAV life cycle, among them tetherin and viperin. Originally identified as antiviral factor inhibiting the release of retroviral particles [244], tetherin has later been shown to target a broad variety of enveloped viruses comprising filoviruses, rhabdoviruses, herpesviruses and arenaviruses [245]. Tetherin harbors an N-terminal cytosolic domain followed by a transmembrane and an extracellular coiled-coiled domain. A glycophosphatidylinositol (GPI) moiety is attached to its C-terminus, anchoring the protein to membranes, similar to its transmembrane domain [246]. Tetherin occurs as disulfide-linked dimers [247]. By incorporation of its transmembrane domain into virions while its GPI anchor remains inserted into the host cell membrane (or vice versa) tetherin can tether newly budded virions to the

cellular surface, thereby blocking their release. Alternatively, since tetherin comes in dimers, one tetherin molecule might also have both, transmembrane domain and GPI anchor, embedded in a virion's membrane, tethering the virion to the cellular surface by interacting with another tetherin molecule that is anchored to the host cell membrane [246]. Tetherin is antagonized by Vpu, an HIV-1 accessory protein that induces tetherin surface downregulation, degradation and deplacement from nascent virions [244, 245]. To what extent tetherin affects the release of IAV virions remains a matter of debate. Initial studies showed that NA-dependent budding of IAV VLPs was enhanced when tetherin was either knocked-down by siRNA treatment or counteracted by the expression of Vpu, suggesting that IAV was negatively affected by tetherin [248]. However, most further studies, although confirming negative effects on VLP budding, did not detect a tetherin-mediated inhibition of wt IAV [249, 250]. While some authors suggested IAV might encode a tetherin antagonist similar to Vpu [249], others showed that HIV-1/IAV co-infections could not relieve tetherin's block on HIV-1 [251], implicating that either IAV did not encode a tetherin antagonist, or the antagonist was not functional in the context of HIV-1 infection. Finally, one study suggested that tetherin-mediated IAV restriction was strain-dependent, showing that certain HAs could alleviate tetherin's negative effect on VLP budding [252]. The authors of this study thus hypothesized that strain-specific differences in HA and NA packaging on the virus' surface that have been described before [253] might contribute to differential tetherin sensitivity. Strains incorporating more HA and NA molecules might sterically impede tetherin incorporation, thereby evading its viral restriction. Interestingly, several studies reported the incorporation of tetherin into VLPs, but not into wt IAV [249, 250], so one might hypothesize that HA and NA packaging might be less dense in VLPs compared to wt virus, rendering VLPs more susceptible to tetherin-mediated restriction.

Viperin has been described to interfere with the life cycle of various viruses at different steps. Its interaction with the Dengue virus NS3 protein has been shown to inhibit viral replication [254], while its binding to farnesyl diphosphate synthase (FPPS), an enzyme catalyzing the formation of a precursor of cholesterol and thus important for the generation of lipid rafts, has been linked to HIV [255] as well as IAV [256] budding defects. While the viperin-mediated disruption of lipid rafts decreased the release of IAV particles *in vitro* [256], viperin-deficient mice showed neither an increase in viral loads nor pulmonary damage upon IAV infection [257].

While IFITMs residing in target cells have been established as potent antiviral factors inhibiting the entry of a whole variety of different viruses [184, 190-194], their roles during late stages of the viral replication cycle have been discovered only recently [215-217]. Compton [215] and Tartour [216] and colleagues observed that IFITM proteins were incorporated into nascent HIV virions, thereby decreasing virion fusogenicity in a dose-dependent manner. They hypothesized that biophysical properties of membranes harboring IFITM proteins (decreased fluidity, increased positive curvature)

are responsible for this effect. In contrast, while Yu and colleagues [217] also observed IFITM incorporation into HIV virions, they found no correlation between the amount of IFITM incorporated and the extent of the decrease in virus fusogenicity. However, they detected an interaction between IFITM proteins and Env, most distinct for IFITM2 and 3, that resulted in impaired Env processing and incorporation.

Given the strong negative effect IFITMs exert on IAV entry, we wondered whether IAV was also affected by the presence of IFITM proteins during late stages of its replication cycle. Indeed, we could show that IFITM3 was incorporated into IAV, IAV VLPs and HIV VLPs pseudotyped with IAV HA and NA (Chapter 3, Fig. 1B, 3C & 5A), and that this incorporation went along with a decrease in VLP envelope glycoprotein content. HIV VLP and IAV VLP entry capacity was found to be significantly reduced upon presence of IFITM3 in VLP producer cells (Chapter 3, Fig. 1E&F, 3B). In agreement with our observation that IFITM3 reduced VLP envelope levels, we could show for IAV VLPs that the negative effect IFITM3 exerted on VLP infectivity was alleviated in a dose-dependent manner when increasing amounts of HA were co-transfected into VLP producer cells. Whether IFITM3 interacts directly with HA similar to the interaction described for IFITM3 and HIV Env [217], or whether IFITM3 competes with HA for incorporation into cellular membranes remains to be discovered.

Surprisingly, in contrast to VLPs, wt IAV was not negatively affected in its entry capacity upon IFITM3 incorporation, although this was associated with a decrease in viral HA (Chapter 3, Fig. 5C). We provide experimental evidence that the IFITM3:HA ratio in virus producer cells might steer IFITM3 sensitivity during late stages of the viral life cycle (Chapter 3, Fig. 5D). However, although IFITM3 incorporation did not negatively impact on IAV infectivity, preliminary results suggest that the reduction in viral HA rendered the virus more neutralization-sensitive when incubated with an HA-directed antibody (Chapter 3, Fig. 5E), potentially compromising the virus in an *in vivo* situation.

Our study revealed interesting parallels between tetherin- and IFITM3- mediated restriction of VLPs versus wt virus. Both ISGs exerted negative effects on VLPs but not wt IAV. As mentioned above, this could be explained by HA/NA-mediated displacement of IFITM3 from VLP or viral membranes, which would be more efficient for wt virus, assuming that HA/NA packaging is more dense in wt IAV compared to VLPs. Alternatively, one might also hypothesize that IFITM3 incorporation into VLPs/virions increases the stoichiometry of entry (the number of HA trimers needed for viral fusion), since more energy might be required to induce fusion of a more rigid membrane that shows increased positive curvature. Again, hypothesizing that HA/NA-packaging is more dense in wt virus compared to VLPs, a wt IAV might more easily provide enough HA-trimers on its surface to successfully complete fusion, even in the presence of IFITM3. Future studies assessing HA/NA densities on wt IAV and VLPs will be needed to clarify this issue.

In summary, studies involving tetherin, viperin and IFITM3 establish lipid rafts as suitable sites to target late stages of the IAV life cycle. Tetherin and IFITM3 both localize to lipid rafts [202, 258]. While tetherin hampers viral particle release, IFITM3 negatively impacts virion infectivity. In contrast, viperin pursues a different strategy by disrupting lipid raft domains, thereby interfering with virus assembly and budding.

Overall, we established IFITM3 as antiviral factor that targets IAV during late stages of its life cycle and suggest the IFITM3-mediated viral restriction to be more intricate than previously appreciated. One might speculate that the increase in positive curvature and the decrease in fluidity of membranes upon IFITM3 incorporation might reduce virus infectivity under certain circumstances, but that the interplay with envelope glycoproteins and potentially other cellular and viral factors adds more levels of complexity we are only starting to resolve.

Chapter 5

Late stages of the influenza A virus replication cycle-a tight interplay between virus and host.

Marie O. Pohl,[a,b] Caroline Lanz[a,b] and Silke Stertz[a]

[a]Institute of Medical Virology, University of Zurich, Winterthurerstrasse 190, 8057 Zurich, Switzerland

[b]Life Sciences Zurich Graduate School, ETH and University of Zurich, 8057 Zurich, Switzerland

CL contributed to this study as follows: CL wrote the sections “Introduction” and “Incorporation of Cellular Proteins into Virions”.

Journal of General Virology (2016), **97**, 2058–2072 **DOI** 10.1099/jgv.0.000562

Review

Late stages of the influenza A virus replication cycle—a tight interplay between virus and host

Marie O. Pohl, Caroline Lanz and Silke Stertz

Institute of Medical Virology, University of Zurich, 8057 Zurich, Switzerland

Correspondence
Silke Stertz
stertz.silke@virology.uzh.ch

After successful infection and replication of its genome in the nucleus of the host cell, influenza A virus faces several challenges before newly assembled viral particles can bud off from the plasma membrane, giving rise to a new infectious virus. The viral ribonucleoprotein (vRNP) complexes need to exit from the nucleus and be transported to the virus assembly sites at the plasma membrane. Moreover, they need to be bundled to ensure the incorporation of precisely one of each of the eight viral genome segments into newly formed viral particles. Similarly, viral envelope glycoproteins and other viral structural proteins need to be targeted to virus assembly sites for viral particles to form and bud off from the plasma membrane. During all these steps influenza A virus heavily relies on a tight interplay with its host, exploiting host-cell proteins for its own purposes. In this review, we summarize current knowledge on late stages of the influenza virus replication cycle, focusing on the role of host-cell proteins involved in this process.

Introduction

Influenza A virus (IAV) is the causative agent of a febrile illness in humans, commonly referred to as 'the flu'. IAV causes seasonal epidemics and sporadic pandemics, imposing a huge burden on human health and economy.

IAV are enveloped viruses belonging to the family of *Orthomyxoviridae*, whose members are characterized by a single-stranded segmented RNA genome of negative polarity (Palese & Shaw, 2007). Unlike most other RNA viruses, orthomyxoviruses replicate in the nucleus of the infected cell (Cros & Palese, 2003). While nuclear replication confers several advantages, such as access to the cellular splicing machinery, the virus faces the challenge of overcoming the nuclear envelope. Due to its small genome size of 13.5 kb, IAV relies heavily on cellular factors to complete its life cycle. In this review we focus on late stages of infection and describe the interplay between the virus and its host in the process of vRNP nuclear export, transport of viral proteins to the assembly site, genome packaging, as well as budding and release of virions.

Transport of viral components to the assembly sites

vRNP transport

After successful transcription and replication of the viral genome the so-called viral ribonucleoprotein (vRNP) complexes that consist of the viral RNA (vRNA) which is encapsidated by the nucleoprotein (NP) and bound by the viral polymerase complex (Fig. 1) need to be exported from the nucleus and shuttled to the cell surface in order to be packaged into budding virions. For specific export, vRNPs need to be recognized in the nucleus and discriminated from other RNA species. Discrimination of cRNA and vRNA takes place in the nucleus and only vRNPs are exported into the cytoplasm (Tchatalbachev *et al.*, 2001). Likely, the viral polymerase adopts different conformations depending on whether it is associated with cRNA or vRNA, which might facilitate recognition of vRNPs as cargo for nuclear export (Tchatalbachev *et al.*, 2001; Gerber *et al.*, 2014). Furthermore, it has recently been suggested that vRNPs are not exported individually as proposed earlier (Chou *et al.*, 2013), but instead as complexes consisting of two or more genome segments (Lakdawala *et al.*, 2014). Nevertheless, export of fully assembled sets of vRNPs has not been observed yet. Export of newly assembled vRNPs takes place through the nuclear pore complexes (NPC), which is an active process, dependent on the help of cellular factors, so-called exportins (Pemberton *et al.*, 1998). Exportins recognize nuclear export sequences (NES) present in to-be-exported proteins and facilitate their transit through the NPC into the cytoplasm.

Studies indicate that the viral nuclear export protein(NEP) plays a critical role during vRNP export: viruses that lack NEP are not viable and interfering with the nuclear localization of NEP reduces viral growth (O'Neill *et al.*, 1998; Neumann *et al.*, 2000). Furthermore, microinjection of antibodies targeting NEP into IAV-infected cells specifically inhibits vRNP export (O'Neill *et al.*, 1998). The amino acid sequence of NEP is highly conserved between different influenza virus strains, especially with regard to the C-terminal α-helix (Paterson & Fodor, 2012). Within the C-

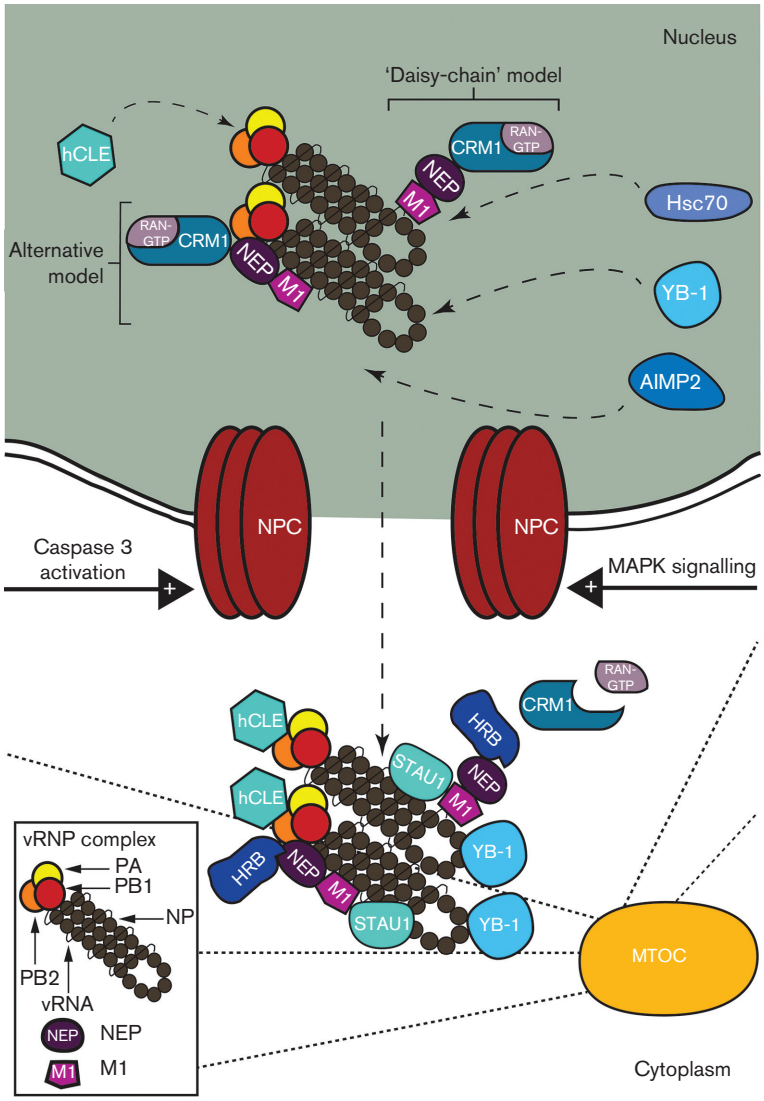

Fig. 1. vRNP export. vRNP export is primarily CRM1-dependent, occurs through the NPC, and is largely dependent on M1 and NEP. In this scenario, M1 and NEP connect the vRNP to the CRM1 export machinery according to the 'daisy-chain' or an alternative model. Other cellular factors such as YB-1, hCLE and Hsc70 also associate with the to-be-exported vRNP within the nucleus. vRNP export appears to be positively influenced by MAPK- and caspase signalling. AIMP2 promotes sumoylation of M1 which enhances vRNP export. In the cytoplasm, the vRNPs accumulate at the MTOC and associate with cellular factors such as HRB and STAU1. These factors, together with YB-1, facilitate the release from the CRM1 export machinery and mediate trafficking of vRNPs towards the cell surface.

terminal domain of NEP, the residue W78 has been identified to be important for the interaction with the nuclear localization signal (NLS) of matrix protein 1 (M1) (Akarsu *et al.*, 2003). M1 is known to be required for export and the NEP–M1 interaction appears to be critical for vRNP transport (Martin & Helenius, 1991; Akarsu *et al.*, 2003; Shimizu *et al.*, 2011). Introducing anti-M1 antibodies into IAV-infected cells prevents shuttling of M1 into the nucleus and leads to nuclear retention of NP (Martin & Helenius, 1991). Thus, both viral proteins, M1 and NEP, appear to play important roles during vRNP export. Their late synthesis during the viral life cycle, mediated by suboptimal splicing in case of NEP, may be a regulatory mechanism to time, and then promote transport of vRNPs from the nucleus to the budding zones (Chua *et al.*, 2013; Hutchinson & Fodor, 2013). In addition, vRNP export by NEP and M1 is also regulated by a switch in the post-translational modification pattern of M1: Early in infection M1 is ubiquitinated at lysine 242. M1 then becomes sumoylated at the same lysine during late stages, which seems to protect it from

proteasomal degradation and thereby leads to increased M1 levels and supports vRNP export (Wu *et al.*, 2011). NEP has also been identified to be sumoylated at late stages of infection (Domingues *et al.*, 2015), and interestingly, the switch in M1 modification from ubiquitination to sumoylation is promoted by the tumour suppressor AIMP2, which in turn binds NEP and is stabilized by its interaction with NEP (Gao *et al.*, 2015).

NEP contains two NES in its N-terminal domain and is known to interact with the cellular β-exportin chromosome maintenance region 1 (CRM1) (O'Neill *et al.*, 1998; Neumann *et al.*, 2000; Iwatsuki-Horimoto *et al.*, 2004; Huang *et al.*, 2013). Indeed, studies confirm that vRNP export is largely dependent on CRM1 and its cofactor Ran-GTP as blocking the CRM1-operated export pathway by leptomycin B largely abrogates vRNP export in IAV-infected cells (Fukuda *et al.*, 1997; Elton *et al.*, 2001; Ma *et al.*, 2001; Watanabe *et al.*, 2001). It has been proposed that M1 and NEP function as adaptors to bridge the association of a vRNP complex with the CRM1 export machinery: In this scenario, M1 associates with vRNPs through an interaction with NP or through binding directly to the vRNA (Elster *et al.*, 1997; Ye *et al.*, 1999; Baudin *et al.*, 2001; Noton *et al.*, 2007). In addition, M1 interacts with NEP (Yasuda *et al.*, 1993; Akarsu *et al.*, 2003; Shimizu *et al.*, 2011). NEP in turn is recognized by CRM1–Ran-GTP through its NES [however, binding of NEP to CRM1 in the absence of Ran-GTP occurs independently of the NES (Neumann *et al.*, 2000)], thereby enabling the CRM1-dependent transport of the vRNP export complex through the NPC (Fig. 1) (Paterson & Fodor, 2012). This model, referred to as the 'daisy-chain model', was recently challenged by a study which reported that the interaction between M1 and the vRNPs is dependent on the presence of NEP. Via its C-terminal domain, NEP interacts not only with M1 but also with the polymerase to provide an additional binding site and support the M1–vRNP association (Brunotte *et al.*, 2014). These data argue for an export complex in which the vRNP is bound by both M1 and NEP, and highlight again the requirement of NEP for CRM1-dependent export.

Of note, other studies suggest that other viral proteins play substantial roles in vRNP export. For example, inhibition of the CRM1 export machinery by leptomycin B caused perinuclear accumulation of NP, but did not affect the localization of NEP or M1 (Elton *et al.*, 2001). NP encodes three NES, one of which is recognized by CRM1 (Yu *et al.*, 2012), while the other two are CRM1-independent and might enable vRNP export independently of M1 and NEP. Also, M1 has previously been proposed as master regulator of vRNP export (Whittaker *et al.*, 1996) and was able to mediate vRNP export in the absence of NEP (Bui *et al.*, 2000). M1 also possesses an NES, which is not CRM1-specific. Mutations in this NES impair nuclear export of M1 and NP (Cao *et al.*, 2012). These data suggest that vRNP export is not entirely dependent on NEP and CRM1 and indicate that CRM1-independent transit routes exist.

Cellular factors have also been shown to influence vRNP export in IAV-infected cells (Fig. 1). For example, heat shock cognate 70 (Hsc70) binds to the C-terminal domain of M1 (Watanabe *et al.*, 2006) and, more weakly, to NEP with which it competes for binding to M1 (Watanabe *et al.*, 2014a). Due to its NES (Tsukahara & Maru, 2004), Hsc70 was suggested to promote CRM1-dependent nuclear export of M1-bound vRNPs (Watanabe *et al.*, 2008). Furthermore, Y-box-binding protein 1 (YB-1) was recently shown to associate with the vRNP export complex. vRNPs are bound in the nucleus by YB-1, where it accompanies the viral gene segments during their transport through the NPC (Kawaguchi *et al.*, 2012). YB-1 appears not to be involved in vRNP export directly but instead exerts its function in the cytoplasm where it plays an important role in the transport of vRNPs to the apical cell surface (Kawaguchi *et al.*, 2012). Another example is the mitogen-activated protein kinase (MAPK)-dependent signalling pathway, which stimulates NEP-dependent vRNP export (Pleschka *et al.*, 2001). Furthermore, inhibition of caspase 3 leads to retention of vRNPs in the nucleus and it was suggested that IAV-induced caspase 3 activation increases the diffusion capacity of the NPC, thereby promoting vRNP export (Wurzer *et al.*, 2003). Both, MAPK- and caspase 3-dependent pathways are activated during late phases of infection and appear to act independently to stimulate viral trafficking.

Following arrival in the cytoplasm, the vRNPs are transported to the cell surface for packaging into progeny virions. Even though diffusion of vRNPs towards the cell membrane has been reported (Babcock *et al.*, 2004; Amorim *et al.*, 2011), vRNP trafficking is generally believed to occur via Rab11- and microtubule-dependent vesicular transport (Bruce *et al.*, 2010; Eisfeld *et al.*, 2011a; Momose *et al.*, 2011). Once in the cytosol, vRNPs have been shown to associate with the microtubule organizing centre (MTOC) (Momose *et al.*, 2007; Amorim *et al.*, 2011; Kawaguchi *et al.*, 2012). Four cellular factors have been shown to be involved in these early steps of vRNP transport to the cell surface: the human immunodeficiency virus Rev-binding protein (HRB), Staufen 1 (STAU1), YB-1 and hCLE/C14orf166. HRB interacts with NEP after vRNP export in the perinuclear region late in infection (O'Neill *et al.*, 1998; Eisfeld *et al.*, 2011b). Due to its GTPase activating protein (GAP) domain, HRB was proposed to mediate release of vRNPs from the CRM1–Ran-GTP export complex after its transit through the NPC (Eisfeld *et al.*, 2011b). This has not been proven yet, but siRNA-mediated knockdown of HRB results in retention of vRNPs in the perinuclear region (Eisfeld *et al.*, 2011b). This indicates that HRB is required to promote apical shuttling of vRNPs in the cytoplasm. STAU1 is a cellular factor involved in mRNA transport, for example it has been implicated in transport of mRNAs to the site of their translation at the rough endoplasmic reticulum, and has been shown to bind to a number of viral proteins (e.g. NS1, NP and M1) as well as to viral mRNA and vRNA (Falcon *et al.*, 1999; Marion *et al.*, 1999; Shapira *et al.*, 2009; Watanabe *et al.*, 2014b). STAU1 co-localizes with vRNPs in the cytoplasm. Knockdown of STAU1 expression does not affect viral replication, but

reduces the amount of viral particles released from infected cells indicating a role for STAU1 in vRNP transport (de Lucas *et al.*, 2010). Furthermore, YB-1, which associates with vRNPs already in the nucleus, mediates the interaction of progeny vRNPs with microtubules (Kawaguchi *et al.*, 2012). Thus, YB-1 is required for vRNP accumulation at the MTOC and mediates, potentially in concert with HRB, the transfer of vRNPs to the endosomal vesicular trafficking system for subsequent transport to the plasma membrane. hCLE, a cellular transcription factor, associates with vRNPs in the nucleus where it promotes viral polymerase and Pol II activity (Huarte *et al.*, 2001; Rodriguez *et al.*, 2011). Recently, it was shown that hCLE interacts with vRNPs in the cytoplasm where it co-localizes with Rab11, PA and NP (Rodriguez-Frandsen *et al.*, 2016). Interestingly, hCLE appears to remain attached to vRNPs during further routing of the viral genome and is even incorporated into budding viral particles (Rodriguez-Frandsen *et al.*, 2016). However, the function of hCLE binding to vRNPs during vRNP transport and packaging remains to be determined.

The Rab11-dependent recycling endosomal pathway plays an important role in vRNP trafficking from the MTOC to the cell surface and virion assembly (Fig. 2) (Bruce *et al.*, 2010; Jo *et al.*, 2010; Amorim *et al.*, 2011; Eisfeld *et al.*, 2011a; Momose *et al.*, 2011; Avilov *et al.*, 2012b). Recycling endosomes transport endocytosed material from the plasma membrane to apical or perinuclear recycling endosomes and shuttle cargo back to the cell surface. Rab11 is a marker for recycling endosomes that mediates vesicle transport along cytoskeletal structures through interactions with downstream adaptor and effector proteins (Bruce *et al.*, 2012). Live-cell imaging using tagged vRNPs confirmed that exported vRNPs localize to Rab11-positive vesicles through a direct interaction of PB2 and active Rab11 (Amorim *et al.*, 2011; Avilov *et al.*, 2012b). Concordantly, knockdown of Rab11a abrogates apical vRNP localization in infected cells and leads to retention of the vRNPs in the perinuclear region (Eisfeld *et al.*, 2011a). In the presence of Rab11, transport occurs through intermittently directed movements of vRNPs, which are dependent on an intact microtubule network (Amorim *et al.*, 2011; Avilov *et al.*, 2012a). Indeed, destabilization of microtubules using nocodazole has been shown to disrupt vRNP accumulation at the MTOC as well as shuttling of vRNPs to the plasma membrane (Momose *et al.*, 2007; Amorim *et al.*, 2011; Eisfeld *et al.*, 2011a). Following transport, the vRNPs reside in patches adjacent to the plasma membrane (Eisfeld *et al.*, 2011a; Chou *et al.*, 2013; Hutchinson & Fodor, 2013). The genome segments then move to the budding zones for incorporation into virions. Interestingly, vRNPs appear to dissociate from Rab11 for insertion into the budzone (Eisfeld *et al.*, 2011a) and Rab11 has not been detected in progeny virions (Shaw *et al.*, 2008; Hutchinson *et al.*, 2014). However, mechanistically it is not clear how vRNPs are moved from Rab11-positive submembranous patches into the budding area on the apical plasma membrane.

Transport of viral envelope proteins

The structural proteins haemagglutinin (HA), neuraminidase (NA) and matrix protein 2 (M2) are synthesized and folded in the rough endoplasmic reticulum (ER) and then transported to the plasma membrane through the secretory pathway (Fig. 2) (Doms *et al.*, 1993). Both, HA and NA are glycosylated along their route through the ER and Golgi towards the apical cell surface (Deom & Schulze, 1985). HA is synthesized as a precursor, HA_0, which requires post-translational processing by proteases into HA_1 and HA_2 in order to gain fusion activity. Proteolytic cleavage of HA_0 takes place either in the trans-Golgi network (TGN) or at the cell surface. Cleavage is mediated by a variety of cellular proteases depending on the cell type as well as the type (mono- versus polybasic cleavage site) and sequence of the cleavage site present in HA [reviewed in (Bottcher-Friebertshauser *et al.*, 2013)]. Within the TGN, M2 is critical to ensure conformational stability of HA: Through its ion channel activity, M2 regulates the pH-balance between the cytoplasmic and trans-Golgi compartment which is important to prevent premature pH-induced changes in the HA conformation (Ciampor *et al.*, 1992; Grambas & Hay, 1992; Sakaguchi *et al.*, 1996). Indeed, the pH stability of HA and the activity of the ion function of M2 were found to be inversely correlated in a study by Grambas & Hay (1992).

HA and NA contain apical sorting signals in their transmembrane domains (TMDs) (Kundu *et al.*, 1996; Lin *et al.*, 1998; Barman & Nayak, 2000), targeting them for transport to the cell surface after synthesis in the ER. The coat protein I (COPI) complex, which is involved in vesicle transport of cargo between the Golgi and ER, was recently shown to be involved in apical targeting of the viral structural proteins HA, NA and M2 (Sun *et al.*, 2013). In addition, the Rho GTPase Cdc42 was suggested to promote apical transport of NA (Wang *et al.*, 2012). It is believed that both, HA and NA are associated to sphingolipid-, cholesterol-rich membrane patches (lipid raft microdomains) already during their transport through the TGN as well as after insertion into the apical membrane (Scheiffele *et al.*, 1997; Simons & Ikonen, 1997; Barman & Nayak, 2000). The TMD of the viral glycoproteins and their cytoplasmic tail (CT) were both shown to be required for lipid raft association (Barman & Nayak, 2000; Zhang *et al.*, 2000b; Chen *et al.*, 2005). Co-expression of HA and NA led to their accumulation in lipid rafts and accelerated their transport to the cell surface, which could indicate that clustering of lipid rafts contributes to HA and NA shuttling (Ohkura *et al.*, 2014). This is in line with previous studies that argue for a requirement of lipid rafts for apical targeting of HA and NA (Scheiffele *et al.*, 1997; Keller & Simons, 1998; Ohkura *et al.*, 2014). The dependency on lipid raft association for apical targeting might be virus strain-dependent, as other studies report only a weak delay of glycoprotein transport upon mutating the TMD or CT (Simpson & Lamb, 1992; Zhang *et al.*, 2000b; Takeda *et al.*, 2003).

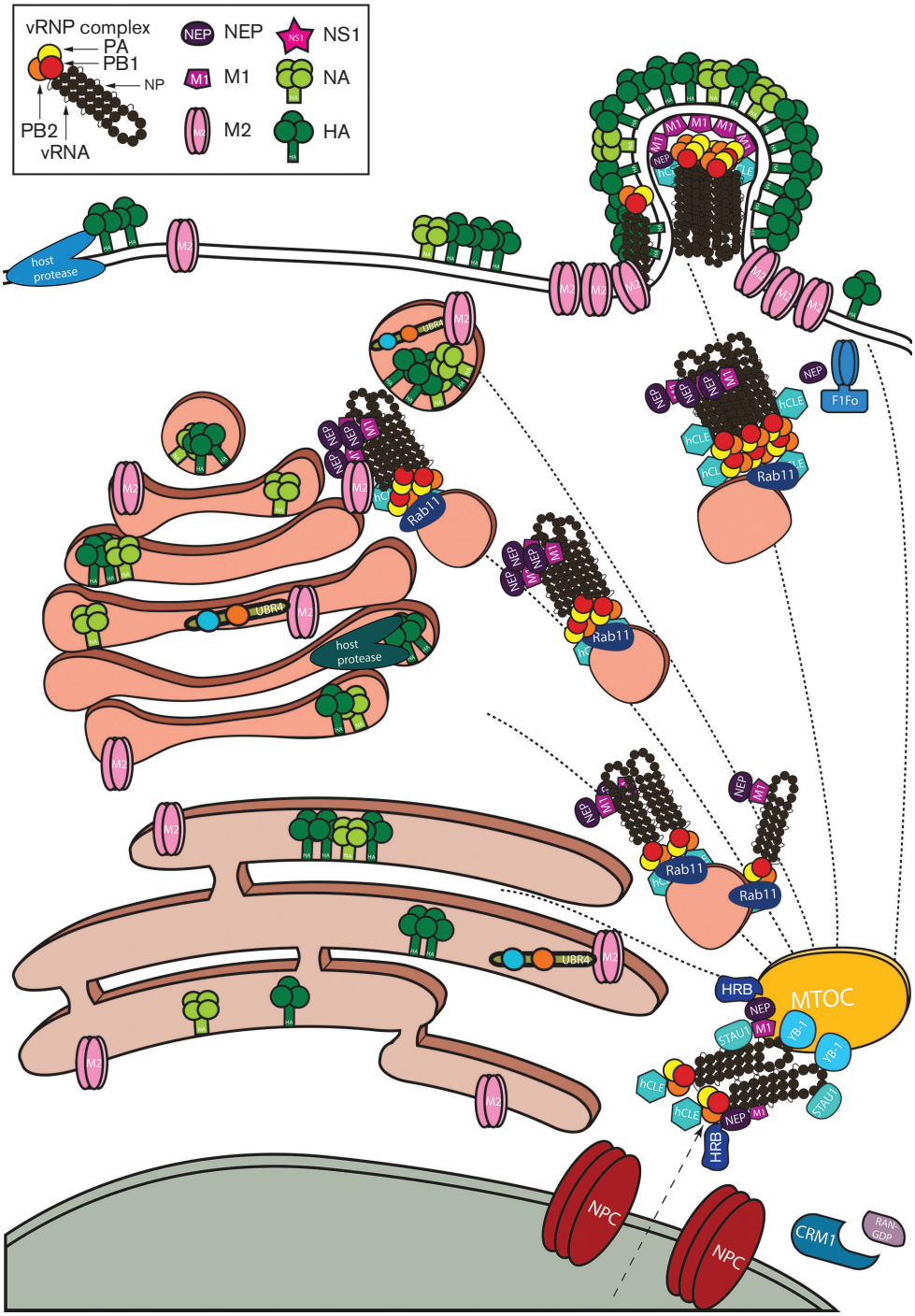

Fig. 2. Apical transport of viral components. vRNPs are transported in a microtubule-dependent manner on Rab11-positive recycling endosomes from the MTOC towards the cell surface. vRNPs associate with GTP-bound Rab11 through interactions with PB2. On these vesicles, vRNP sorting and bundling is believed to occur before complete genome sets are incoporated into budding virions. hCLE associates with vRNPs in the nucleus, remains attached to vRNPs during cytoplasmic trafficking and is incorporated into virions. Structural viral proteins, such as HA, NA and M2 are synthesized in the ER and are transported to the budding sites through the secretory pathway with the help of cellular factors such as UBR4. HA and NA are associated with lipid raft structures from which M2 is largely excluded. HA maturation is mediated through cleavage by several cellular proteases which are present in the trans-Golgi network, at the cell surface or the extracellular space. Other structural viral components (M1 and NEP) travel to the budding sites along with vRNPs or might be recruited by cellular factors such as the F1Fo-ATPase which binds to NEP.

M2 is excluded from these lipid raft microdomains (Leser & Lamb, 2005) and an apical sorting signal in M2 has not been identified. Nevertheless, in infected cells M2 is also targeted to the apical membrane in an actin-dependent manner where it clusters with HA (Hughey *et al.*, 1992; Thaa *et al.*, 2010). A recent study that combined a meta-analysis of genome-wide RNAi screens with a screen for interaction partners of the different viral proteins identified the ubiquitin ligase UBR4 (ubiquitin N-recognin domain-containing E3 ligase 4) as a required host factor for IAV and an interaction partner of M2 (Tripathi *et al.*, 2015). Interestingly, UBR4 positively influenced apical routing not only of M2 but also of the viral glycoproteins. Knockdown of UBR4 reduced M2 expression levels and viral particle production indicating that UBR4 might be required to protect M2 from degradation and to ensure delivery of viral components to the budding zones at the cell surface (Tripathi *et al.*, 2015).

Despite M2 being co-transported with HA and NA, Rab11 was also shown to be involved in apical delivery of M2 (Rossman *et al.*, 2010b). This could either indicate that the transport of M2 is at least partially mediated by the Rab11-dependent endosomal pathway or alternatively, Rab11 could affect M2 endocytosis and thereby impact the plasma membrane levels of M2.

Transport of M1 and NEP

M1 does not contain an apical localization signal. However, due to its ability to associate with lipids, vRNPs and the other structural viral proteins, M1 might be co-transported together with other viral components to the cell surface. In fact, transport of the viral gene segments and M2 through Rab11-containing vesicles might be linked by M1, which binds to both, M2 and vRNPs (Noton *et al.*, 2007; Chen *et al.*, 2008). It has been suggested that M1 stays attached to vRNPs after export, which on one hand prevents re-import of vRNPs into the nucleus (Martin & Helenius, 1991) and on the other hand promotes association of vRNPs with other viral components through interaction with M2 during vesicular shuttling and after apical delivery (Eisfeld *et al.*, 2015).

Even though the majority of NEP is localized in the nucleus and cytoplasm during late stages of the viral life cycle, small amounts of NEP have also been detected at the apical plasma membrane (Carrasco *et al.*, 2004; Gorai *et al.*, 2012). This is in line with earlier studies showing that NEP is incorporated into virions (Richardson & Akkina, 1991; Shaw *et al.*, 2008). It is not clear how NEP transport to the cell surface occurs, but NEP could piggy-back on vRNPs through its association with M1 (Yasuda *et al.*, 1993). In support of this model; NEP, M1 and NP were shown to co-localize at the apical plasma membrane (Carrasco *et al.*, 2004).

Genome assembly and packaging

It is currently believed that packaging of vRNPs into virus particles is a highly regulated process rather than a random one. In order to generate infectious virions, the distinct genome segments need to be sorted, bundled and inserted into budzones at the plasma membrane. Several studies suggest that sorting of vRNPs does not occur in the nucleus or during budding, but rather during cytoplasmic transport of the genome segments towards the cell surface (Takizawa *et al.*, 2010; Chou *et al.*, 2013; Lakdawala *et al.*, 2014). In addition, neither HA nor M2 are required for co-localization of gene segments of different identities (Chou *et al.*, 2013) which indicates that vRNP sorting takes place prior to arrival at the budzone. It is not clear whether vRNPs are sorted following the delivery of vRNPs from the MTOC to Rab11-containing vesicles, during transport, or upon accumulation of vRNPs in Rab11-positive patches in the apical periphery (Eisfeld *et al.*, 2011a; Chou *et al.*, 2013). Nevertheless, Rab11-positive membranes may serve as a platform for the gathering of the distinct genome segments (often described as bundling), which could allow reassortment as well as assembly of vRNPs into packaging-ready bundles, which are then incorporated into budding particles (Eisfeld *et al.*, 2015).

For successful genome packaging, vRNPs need to be discriminated from other viral and cellular RNAs. In addition, the distinct genome segments are required to be identified and bundled in order to ensure packaging of a complete genome set. Many studies have reported that the information for these processes lies within the vRNA sequence: vRNP-specific genome sorting and bundling signals have been identified in the vRNAs (Hutchinson *et al.*, 2010; Gerber *et al.*, 2014). Concordantly, two vRNA-like molecules derived from the same gene segment but encoding different reporter genes were shown to compete for incorporation into virions (Inagaki *et al.*, 2012). In addition, the idea of packaging signals present in the vRNAs was strengthened by the finding that vRNA-derived defective interfering vRNAs containing deletions compete with their parental vRNAs for insertion into virions (Duhaut & McCauley, 1996; Odagiri & Tashiro, 1997; Duhaut & Dimmock, 2002). To date, many signals required for packaging have been mapped to different regions of the vRNA such as the highly conserved 3′ and 5′ UTR, the terminal part of the coding regions as well as the central part of the vRNA (Fujii *et al.*, 2003, 2009; Watanabe *et al.*, 2003; Dos Santos Afonso *et al.*, 2005; Liang *et al.*, 2005; Muramoto *et al.*, 2006; Gog *et al.*, 2007; Marsh *et al.*, 2007, 2008; Hutchinson *et al.*, 2008, 2009; Ozawa *et al.*, 2009; Wise *et al.*, 2011; Gavazzi *et al.*, 2013). These studies show that some packaging signals are universal for all vRNPs, while others appear to be segment- or even virus strain-specific. Such variations in packaging requirements between strains can lead to genomic incompatibilities and incomplete packaging. Indeed, reassortment occurs more frequently between closely related virus strains compared to more

distantly related viruses (Essere *et al.*, 2013; Marshall *et al.*, 2013).

For genome bundling, interactions between the different vRNPs are thought to be of importance. In fact, recent studies favour a model of selective and hierarchical bundling of genome segments into supramolecular complexes prior to incorporation into virions (Gerber *et al.*, 2014). The organization of vRNPs within virions predicts direct connections between the individual gene segments: vRNPs are organized in a so-called '7+1' pattern in which seven vRNPs are localized around one central segment (Harris *et al.*, 2006; Noda *et al.*, 2006; Fournier *et al.*, 2012b; Noda *et al.*, 2012). Indeed, a linear organization network between vRNPs has been described (Fournier *et al.*, 2012a, b). Mutations in packaging signals of one segment can affect the incorporation of other segments, which further supports the existence of interactions between individual vRNPs (Marsh *et al.*, 2007; Hutchinson *et al.*, 2008; Marsh *et al.*, 2008; Hutchinson *et al.*, 2009; Fournier *et al.*, 2012b). Interestingly, interaction networks of vRNPs have been visualized through 3D electron tomography and revealed the presence of a transition zone at the tip of the budding virion which indicates that vRNPs are incorporated as a supramolecular complex in which the gene segments directly interact with each other (Fournier *et al.*, 2012a, b). Furthermore, differences in vRNP interaction between virus strains were demonstrated (Gavazzi *et al.*, 2013), suggesting that sequences required for genome bundling might evolve independently in distantly related virus strains (Gerber *et al.*, 2014).

The 7+1 organization of the IAV genome is observed particularly in budding virions (Fournier *et al.,* 2012a, b; Noda *et al.*, 2012) and it is believed that one central gene segment mediates structural assembly of the vRNP bundle through interactions with the surrounding segments (Hutchinson *et al.*, 2010; Gerber *et al.*, 2014). In line with this model, many studies have shown that certain gene segments are of a higher regulatory order and more strongly affect genome bundling compared to other segments (Muramoto *et al.*, 2006; Marsh *et al.*, 2007, 2008; Hutchinson *et al.*, 2008, 2009; Gao *et al.*, 2012). This is supported by the finding that two to three vRNPs of different identities have been found to assemble already before nuclear export (Lakdawala *et al.*, 2014). Thus, for successful incorporation of all eight genome segments, a two-step bundling process is suggested, in which vRNPs of high hierarchical order form a complex first within the nucleus. Following export, the other vRNPs are added to the vRNP bundle in a second step, which could potentially take place during transport on Rab-11 platforms in recycling endosomes (Gerber *et al.*, 2014).

The efficiency and accuracy of vRNP packaging is still under debate: Some studies found that packaging of eight different segments is possible and that packaging of more than eight segments is uncommon (Noda *et al.*, 2006; Chou *et al.*, 2012). These data are indicative of efficient, regulated inclusion of eight distinct genome segments into virions. However, this has been questioned by the finding that at low MOI (multiplicity of infection) most infected cells were reported to lack expression of at least one major viral protein (Brooke *et al.*, 2013). This could potentially indicate that frequently genome segments are missing but it could also be explained by incorporation of damaged or mutated segments.

Budding and release of new virions

Different morphologies, ranging from spherical particles to long filaments, have been described for influenza virions (Palese & Shaw, 2007). Importantly, the particle morphology seems to change when adapting influenza viruses to tissue culture conditions: Laboratory-adapted strains typically produce mostly spherical particles with a diameter of about 100 nm as well as virions of pleomorphic shape (Fig. 3). Clinical isolates of influenza viruses in contrast display a filamentous morphology and their virions can be >1 μm in length (Mosley & Wyckoff, 1946; Choppin, 1963). In line with this difference between primary isolates and laboratory strains, a recent study found that upon passaging a laboratory-adapted, spherical virus strain in guinea pigs filamentous morphology was selected for. In contrast, passaging virus in embryonated chicken eggs, a method routinely used to grow virus in the laboratory, favoured spherical particles (Seladi-Schulman *et al.,* 2013).

While the different shapes of virions have been described structurally in detail, only little is known about the differences in assembly and budding for spherical versus filamentous viruses. It has been demonstrated that not only M1 has a major influence on the shape of the particle but also HA, NA, M2 and NP have been suggested to impact virus morphology (Bourmakina & Garcia-Sastre, 2003; Elleman & Barclay, 2004; Rossman *et al.*, 2010a; Bialas *et al.*, 2014; Chlanda *et al.*, 2015). Given that, most up-to-date studies on assembly and egress of influenza virus have been performed with laboratory-adapted spherical virions, this review will focus on budding of spherical virions.

Budding is a dynamic multistep process, which includes clustering of viral components at the apical cell surface, bud initiation, bud outgrowth, incorporation of the viral genome and scission of the bud in order to release the progeny virion. Studies on human broncheotracheal epithelial (HTBE) cells, a model for the human airway epithelium, revealed that virus budding occurs preferentially at the tips of epithelial microvilli (Kolesnikova *et al.*, 2013). It can be speculated that the lipid and/or protein composition of the membrane at these tips is particularly suitable for virus budding, but this hypothesis has not been analyzed yet. IAV envelopes are enriched for sphingolipids and cholesterol compared to the average lipid composition of the plasma membrane (Gerl *et al.*, 2012), supporting the idea of lipid raft-dependent virus budding.

Generally, all structural components of the virus need to be transported to the apical cell surface and clustered in lipid raft

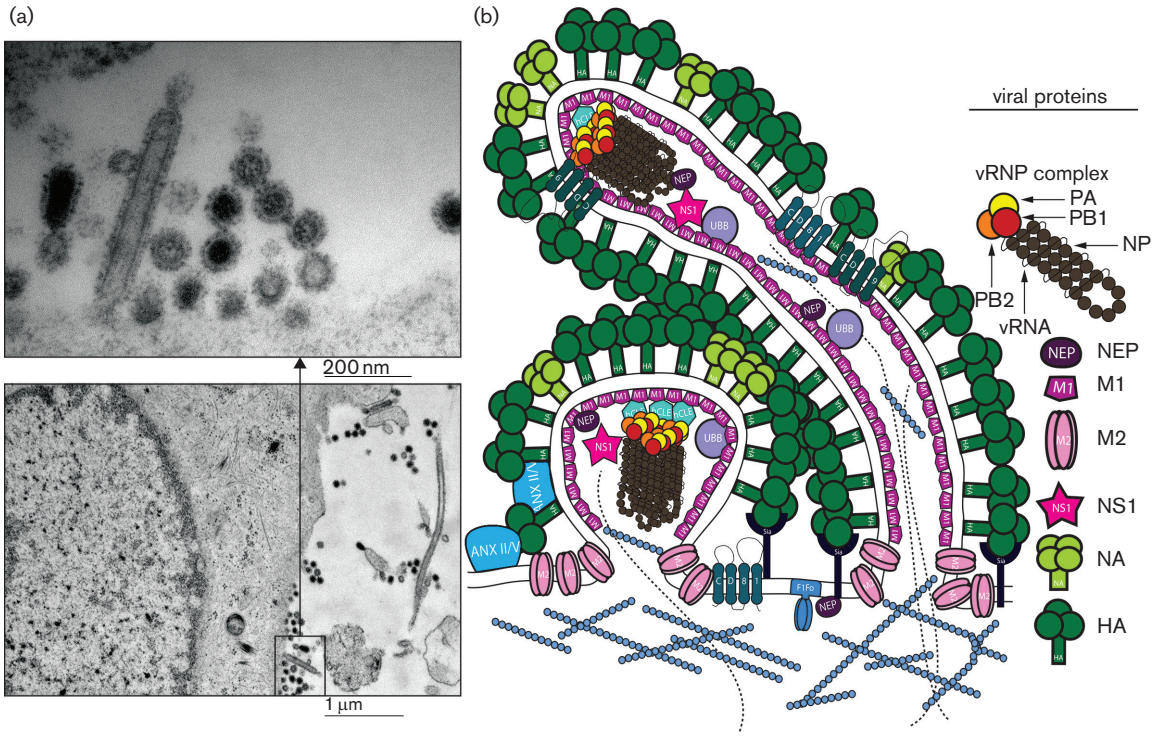

Fig. 3. IAV budding. (a) Electron micrograph of budding IAV. Viral particles can be of spherical, rod-like or filamentous shape. A549 cells were grown on 6 mm carbon-coated sapphire discs. Cells were infected with A/WSN/33 MOI=2 and 16 h post-infection, cells were fixed with 2.5 % glutaraldehyde in 0.1 M cacodylate buffer. Samples were processed for transmission electron microscopy (TEM) imaging using high pressure freezing. Images were acquired on a Phillips CM-100 TEM at the Center for Microscopy and Image Analysis of the University of Zurich. Shown are representative images (magnification: ×135 000 (upper image) and ×24 500 (lower image). (b) Cartoon. Viral particles form at budding sites on the apical cell surface. Accumulation of HA and NA on lipid rafts on the plasma membrane stimulates bud formation and outgrowth. M1 stabilizes the viral particles and might contribute to vRNP incorporation and recruitment of other viral components including M2. M2 plays an important role in scission of virions from the cell surface. For release of progeny viral particles, NA breaks interactions between HA and sialic acid-containing glycoproteins. Besides vRNP bundles and M1, also NEP and NS1 are components of IAV virions. In addition, cellular factors such as ubiquitin, hCLE, CD9, CD81, annexins or cytosceletal components are incorporated into viral particles.

domains to initiate the budding process. The accumulation of HA and NA at lipid raft microdomains in the plasma membrane results in the formation of larger functional raft domains for assembly and budding, the so-called budzone (Schmitt & Lamb, 2005; Rossman & Lamb, 2011). The trigger for bud formation is not known but most likely accumulation of viral glycoproteins starts the budding process. Studies investigating the budding of virus-like particles (VLPs) indicate that individual overexpression of HA, NA or M2 can mediate VLP formation (Chen *et al.*, 2007; Lai *et al.*, 2010). However, during virus infection HA is not sufficient to complete budding and therefore VLP budding appears not to mimic IAV budding accurately (Nayak *et al.*, 2009; Rossman & Lamb, 2011). A recent study showed that the generation of VLPs which morphologically resemble budding viral particles, requires at least the expression of either HA or NA together with M1 and M2 (Chlanda *et al.*, 2015).

Besides the glycoproteins, also M1 plays a critical role during budding. M1 is believed to interact with the plasma membrane and HA, NA, M2 and NEP as well as with vRNPs (Yasuda *et al.*, 1993; Ali *et al.*, 2000; Baudin *et al.*, 2001; Noton *et al.*, 2007; Chen *et al.*, 2008), which could be required for reciprocal recruitment and organization of the viral components in the budzone. M1 can form oligomers (Zhang *et al.*, 2012) and interactions of M1 with the plasma membrane have been shown to be required for multimerization (Hilsch *et al.*, 2014). Formation of M1 oligomers below the plasma membrane provides structure and sturdiness to viral particles (Harris *et al.*, 2001; Calder *et al.*, 2010) and could in addition be required for bud elongation (Rossman & Lamb, 2011). Furthermore, the interaction of M1 with the CT of HA and NA was shown to be of particular importance for virion morphogenesis (Jin *et al.*, 1997; Barman *et al.*, 2004).

The assembled vRNP complexes accumulate in Rab11-positive submembranous patches below the plasma membrane. The importance of Rab11 for virus budding has been demonstrated: knockdown of Rab11 and its effector FIP2 delays or stalls virus budding which is probably due to defects in vRNP transport to the cell surface as discussed above (Bruce *et al.*, 2010). Recruitment of the vRNP complex into the budzone could take place through interactions with other structural proteins that have already been inserted into the apical membrane. The CTs of HA and NA as well as that of M2 have been shown to be required for efficient genome packaging into budding virions (Zhang *et al.*, 2000a; McCown & Pekosz, 2005; Iwatsuki-Horimoto *et al.*, 2006). Also, the interaction between M1 and M2 is believed to be critical for the production of infectious viral particles (McCown & Pekosz, 2005; Iwatsuki-Horimoto *et al.*, 2006; Chen *et al.*, 2008; Grantham *et al.*, 2010). In the absence of other viral proteins, M2 is not part of lipid raft microdomains in the plasma membrane (Zhang *et al.*, 2000b; Leser & Lamb, 2005). However, in the presence of viral proteins, M2 is recruited to the site of budding and was shown to localize to the outer periphery of the budzone of infected cells (Rossman *et al.*, 2010a; Rossman & Lamb, 2011). Several possibilities for the recruitment of M2 to lipid raft domains harbouring the budzone have been suggested: The amphipathic helix, which is present in the CT of M2 is required for localization of M2 at the budzone (Roberts *et al.*, 2013). M2 has been shown to interact with cholesterol directly and to associate with cellular membranes (Schroeder *et al.*, 2005; Rossman *et al.*, 2010a; Thaa *et al.*, 2011), which indicates that association with cholesterol-rich domains might occur without the help of other recruitment factors. Indeed, M2 clusters with larger lipid raft domains, a process which was shown to be dependent on palmitoylation of the CT (Thaa *et al.*, 2011). In addition, M2 is known to interact with M1 and HA (Chen *et al.*, 2008; Thaa *et al.*, 2010), which might further promote re-localization of M2 to the lipid raft structure of the budzone. Importantly, M2 was reported to mediate pinching of virus particles off the plasma membrane (Rossman *et al.*, 2010b). For membrane scission, membrane curvature at the base of the budding virion needs to be induced and concordantly, M2 localizes primarily to the neck of budding virions (Rossman *et al.*, 2010a; Roberts *et al.*, 2013). The conserved amphipathic helix of M2 mediates completion of the budding process in a cholesterol-dependent manner through its insertion into the lipid bilayer (Rossman *et al.*, 2010b). Indeed, the amphipathic helix was shown to be capable of inducing a strong, negative Gaussian curvature at the base of the bud which is required for scission of viral particles (Schmidt *et al.*, 2013). Pinched off viral particles remain attached to the cell surface due to binding of HA to sialic acid-carrying proteins. For virion egress, NA cleaves off sialic acid residues on glycoproteins in proximity of the budzone (Palese *et al.*, 1974; Griffin *et al.*, 1983). Only few cellular factors have been identified to be required for IAV budding. For example, the tetraspanin CD81 was shown to be recruited to the budzone and to be incorporated into progeny virions (Shaw *et al.*, 2008; He *et al.*, 2013). Knockdown of CD81 results in altered virion morphology and stalled detachment of particles from the plasma membrane indicating that CD81 might be involved in the scission process (He *et al.*, 2013). Furthermore, the scaffolding protein receptor for protein C kinase 1 (Rack1) was shown to interact with a motif in the N-terminal part of M1 and this interaction was found to contribute to the release of virus buds from the cell surface (Demirov *et al.*, 2012). In addition, the ATPase activity of the cellular F1Fo-ATPase was shown to be important for the egress of budding virions (Gorai *et al.*, 2012). The F1Fo-ATPase associates with NEP and localizes to the budzone during late stages of infection (Gorai *et al.*, 2012). While it is not yet known how the F1Fo-ATPase supports budding, it can be hypothesized that it contributes to the induction of membrane curvature. For mitochondrial F1Fo-ATPase it could be demonstrated that the polymerization of dimers of the F1Fo-ATPase induces membrane budding, leading to cristae formation in the mitochondria (Allen, 1995). It is therefore tempting to speculate that a similar function of the F1Fo-ATPase at the plasma membrane is usurped by IAV to initiate virus budding.

In summary and according to the model proposed by Rossman and Lamb (2011), initiation of budding is mediated by HA and NA which fulfil redundant functions. Together with M1, recruitment of other viral proteins and the genome results in virion assembly and bud elongation. Inclusion of M2 to the neck of budding virions results in incorporation of M2 into the virions as well as scission of the viral particles. Therefore, budding is a much more complex process than suggested by earlier VLP studies. Likely, in the context of a viral infection, various interactions between different viral components as well as support of cellular factors are required to orchestrate budding.

Incorporation of cellular proteins into virions

For many viruses it has been shown that in addition to viral proteins, host-cell proteins can be incorporated into virus particles [reviewed in (Cantin *et al.*, 2005)]. It was found that most of those proteins are associated with lipid rafts, which are the budding sites for many viruses, such as IAV, human immunodeficiency virus (HIV)-1, respiratory syncytial virus (RSV) and others (Chazal & Gerlier, 2003). While some incorporated proteins have been described to be advantageous for the virus (e.g. cyclophilin A, a peptidyl prolyl isomerase incorporated into HIV-1 particles, which promotes capsid uncoating upon infection of the virus) (Franke *et al.*, 1994; Thali *et al.*, 1994), some have been found to decrease virus infectivity (e.g. APOBEC3G, a cytidine deaminase, which induces hypermutation of the HIV-1 genome) (Sheehy *et al.*, 2002; Mangeat *et al.*, 2003). However, for most of the cellular proteins incorporated into viruses, their functional significance remains to be determined.

The knowledge on cellular proteins which are incorporated into IAV virions is limited. First, a proteomics study was published in which cytoplasmic as well as envelope-associated proteins present in purified IAV were identified (Shaw *et al.*, 2008). The identified host-cell proteins were mostly cytoskeletal proteins, annexins, glycolytic enzymes and tetraspanins, but their function for the virus (or their antiviral role) has not been elucidated yet. However, for some members of the annexin family and the tetraspanins follow-up studies have addressed this question. Annexin II has been shown to be incorporated into IAV particles and to convert plasminogen into plasmin, enabling proteolytic activation of HA in the absence of suitable cellular proteases (LeBouder *et al.*, 2008). Recently, it was found that annexin V is upregulated and translocated to the cell surface upon IAV infection. Localizing to lipid rafts, annexin V gets incorporated into IAV particles and is associated with a decrease in γ-interferon signalling in newly infected cells, leading to an increase in viral replication (Berri *et al.,* 2014). Intriguingly, not only annexins but also other host-cell proteins described to be incorporated into IAV have been reported to be incorporated into other enveloped viruses. Shaw *et al.* (2008) distinguish between highly abundant cellular proteins that may be incorporated unspecifically (e.g. β-actin or tubulin) and proteins enriched at virus budding sites, such as lipid rafts. Whether the virus chooses its budding site because of the presence of specific beneficial proteins or whether incorporated proteins just happen to be present at the virus budding site remains elusive.

Hutchinson *et al.* (2014) added to the knowledge on cellular proteins incorporated into IAV by performing proteomics studies of IAV grown on either mammalian Madin–Darby canine kidney (MDCK) and Madin–Darby bovine kidney (MDBK) cells or in embryonated chicken eggs. They detected the incorporation of a myriad of host-cell proteins into IAV, many of which overlapped with previously described proteins, namely cytoskeletal proteins, annexins, glycolytic enzymes and ubiquitin (Franke *et al.*, 1994; Thali *et al.*, 1994; Shaw *et al.*, 2008). In addition, they described membrane proteins, small GTPases and other signalling proteins previously unaccounted for to be incorporated into IAV particles. Intriguingly, some host-cell proteins, such as ISG15, were uniquely found to be incorporated into IAV particles when the virus was grown on MDCK cells. Other proteins, such as the tetraspanin CD9, seemed to be functionally replaced by an avian substitute when the virus was grown in eggs. These data suggest that incorporation of certain host proteins is conserved and required across different species, whereas others might have species-specific roles.

Although some cellular proteins incorporated into IAV may be functionally irrelevant, many of them might harbour unanticipated functions and play important roles during infection, providing the virus with host factors needed at or shortly after viral entry into a susceptible target cell. In addition, as host factors stemming from one species may not be functional in another, they have the potential to determine the virus' host range, which is of great importance for IAV that is able to infect multiple species.

Table 1. Selected host factors with a described function during the late stages of IAV infection

Host factor	Function	Reference
Exportin	vRNP nuclear export	Pemberton *et al.* (1998)
CRM1/Ran-GTP	vRNP nuclear export	O'Neill *et al.* (1998), Neumann *et al.* (2000), Iwatsuki-Horimoto *et al.* (2004), Huang *et al.*(2013)
MAPK pathway	vRNP nuclear export	Pleschka *et al.* (2001)
Caspase 3	vRNP nuclear export	Wurzer *et al.* (2003)
AIMP2	vRNP nuclear export	Gao *et al.* (2015)
YB-1	vRNP trafficking	Kawaguchi *et al.* (2012)
HRB	vRNP trafficking	O'Neill *et al.* (1998), Eisfeld *et al.* (2011)
Staufen 1	vRNP trafficking	de Lucas *et al.* (2010)
microtubules	vRNP trafficking	Amorim *et al.* (2011), Avilov *et al.* (2012b)
Hsc70	vRNP trafficking	Watanabe *et al.* (2006, 2014a)
hCLE	vRNP trafficking	Rodriguez *et al.* (2011), Rodriguez-Frandsen *et al.* (2016)
Rab11	vRNP trafficking	Bruce *et al.* (2012), Hutchinson & Fodor (2013)
	M2 trafficking	Rossman *et al.* (2010b)
actin	M2 trafficking	Hughey *et al.* (1992), Thaa *et al.* (2010)
UBR4	Trafficking of HA, NA and M2	Tripathi *et al.* (2015)
COPI	Trafficking of HA, NA and M2	Sun *et al.* (2013)
Cdc42	NA trafficking	Wang *et al.* (2012)
cellular proteases	HA activation	Bottcher-Friebertshauser *et al.* (2013)
F1F0 ATPase	Virus budding	Gorai *et al.* (2012)
CD81	Virus budding	He *et al.* (2013)
Rack1	Virus release	Demirov *et al.* (2012)

Conclusions

In summary, the roles of viral proteins and vRNA during late stages of the infection have been studied in detail and we have made progress in understanding the processes leading to the release of new virions. Also with regards to cellular proteins involved, several host factors have been identified and characterized for their proviral function (Table 1). However, many open questions remain: despite tremendous progress and efforts we still only partially understand the mechanisms guiding packaging of the vRNPs. It is still unclear how M1 and NEP are transported to the assembly sites and it is not well understood how localization and assembly of the virion components at the budzone are regulated, timed and organized. Moreover, for technical reasons most studies have been performed with laboratory-adapted IAV strains which differ in their morphology from primary isolates and thus far, it is unclear how the assembly and budding processes differ between spherical and filamentous virions. It can also be assumed that many more cellular proteins are usurped by IAV for assembly and egress than currently known as hundreds of cellular factors have been identified as required for the virus but not been characterized yet (Stertz & Shaw, 2011; Tripathi *et al.*, 2015). Future studies are expected to reveal novel insights into the tight interplay between the virus and its host cell at late stages of the infection.

References

Akarsu, H., Burmeister, W. P., Petosa, C., Petit, I., Müller, C. W., Ruigrok, R. W. & Baudin, F. (2003). Crystal structure of the M1 protein-binding domain of the influenza A virus nuclear export protein (NEP/NS2). *EMBO J* **22**, 4646–4655.

Ali, A., Avalos, R. T., Ponimaskin, E. & Nayak, D. P. (2000). Influenza virus assembly: effect of influenza virus glycoproteins on the membrane association of M1 protein. *J Virol* **74**, 8709–8719.

Allen, R. D. (1995). Membrane tubulation and proton pumps. *Protoplasma* **189**, 1–8.

Amorim, M. J., Bruce, E. A., Read, E. K., Foeglein, A., Mahen, R., Stuart, A. D. & Digard, P. (2011). A Rab11- and microtubule-dependent mechanism for cytoplasmic transport of influenza A virus viral RNA. *J Virol* **85**, 4143–4156.

Avilov, S. V., Moisy, D., Munier, S., Schraidt, O., Naffakh, N. & Cusack, S. (2012a). Replication-competent influenza A virus that encodes a split-green fluorescent protein-tagged PB2 polymerase subunit allows live-cell imaging of the virus life cycle. *J Virol* **86**, 1433–1448.

Avilov, S. V., Moisy, D., Naffakh, N. & Cusack, S. (2012b). Influenza A virus progeny vRNP trafficking in live infected cells studied with the virus-encoded fluorescently tagged PB2 protein. *Vaccine* **30**, 7411–7417.

Babcock, H. P., Chen, C. & Zhuang, X. (2004). Using single-particle tracking to study nuclear trafficking of viral genes. *Biophys J* **87**, 2749–2758.

Barman, S. & Nayak, D. P. (2000). Analysis of the transmembrane domain of influenza virus neuraminidase, a type II transmembrane glycoprotein, for apical sorting and raft association. *J Virol* **74**, 6538–6545.

Barman, S., Adhikary, L., Chakrabarti, A. K., Bernas, C., Kawaoka, Y. & Nayak, D. P. (2004). Role of transmembrane domain and cytoplasmic tail amino acid sequences of influenza a virus neuraminidase in raft association and virus budding. *J Virol* **78**, 5258–5269.

Baudin, F., Petit, I., Weissenhorn, W. & Ruigrok, R. W. (2001). In vitro dissection of the membrane and RNP binding activities of influenza virus M1 protein. *Virology* **281**, 102–108.

Berri, F., Haffar, G., Lê, V. B., Sadewasser, A., Paki, K., Lina, B., Wolff, T. & Riteau, B. (2014). Annexin V incorporated into influenza virus particles inhibits gamma interferon signaling and promotes viral replication. *J Virol* **88**, 11215–11228.

Bialas, K. M., Bussey, K. A., Stone, R. L. & Takimoto, T. (2014). Specific nucleoprotein residues affect influenza virus morphology. *J Virol* **88**, 2227–2234.

Bourmakina, S. V. & García-Sastre, A. (2003). Reverse genetics studies on the filamentous morphology of influenza A virus. *J Gen Virol* **84**, 517–527.

Brooke, C. B., Ince, W. L., Wrammert, J., Ahmed, R., Wilson, P. C., Bennink, J. R. & Yewdell, J. W. (2013). Most influenza a virions fail to express at least one essential viral protein. *J Virol* **87**, 3155–3162.

Bruce, E. A., Digard, P. & Stuart, A. D. (2010). The Rab11 pathway is required for influenza A virus budding and filament formation. *J Virol* **84**, 5848–5859.

Bruce, E. A., Stuart, A., McCaffrey, M. W. & Digard, P. (2012). Role of the Rab11 pathway in negative-strand virus assembly. *Biochem Soc Trans* **40**, 1409–1415.

Brunotte, L., Flies, J., Bolte, H., Reuther, P., Vreede, F. & Schwemmle, M. (2014). The nuclear export protein of H5N1 influenza A viruses recruits Matrix 1 (M1) protein to the viral ribonucleoprotein to mediate nuclear export. *J Biol Chem* **289**, 20067–20077.

Bui, M., Wills, E. G., Helenius, A. & Whittaker, G. R. (2000). Role of the influenza virus M1 protein in nuclear export of viral ribonucleoproteins. *J Virol* **74**, 1781–1786.

Böttcher-Friebertshäuser, E., Klenk, H. D. & Garten, W. (2013). Activation of influenza viruses by proteases from host cells and bacteria in the human airway epithelium. *Pathog Dis* **69**, 87–100.

Calder, L. J., Wasilewski, S., Berriman, J. A. & Rosenthal, P. B. (2010). Structural organization of a filamentous influenza A virus. *Proc Natl Acad Sci U S A* **107**, 10685–10690.

Cantin, R., Méthot, S. & Tremblay, M. J. (2005). Plunder and stowaways: incorporation of cellular proteins by enveloped viruses. *J Virol* **79**, 6577–6587.

Cao, S., Liu, X., Yu, M., Li, J., Jia, X., Bi, Y., Sun, L., Gao, G. F. & Liu, W. (2012). A nuclear export signal in the matrix protein of Influenza A virus is required for efficient virus replication. *J Virol* **86**, 4883–4891.

Carrasco, M., Amorim, M. J. & Digard, P. (2004). Lipid raft-dependent targeting of the influenza A virus nucleoprotein to the apical plasma membrane. *Traffic* **5**, 979–992.

Chazal, N. & Gerlier, D. (2003). Virus entry, assembly, budding, and membrane rafts. *Microbiol Mol Biol Rev* **67**, 226–237, table of contents.

Chen, B. J., Takeda, M. & Lamb, R. A. (2005). Influenza virus hemagglutinin (H3 subtype) requires palmitoylation of its cytoplasmic tail for assembly: M1 proteins of two subtypes differ in their ability to support assembly. *J Virol* **79**, 13673–13684.

Chen, B. J., Leser, G. P., Morita, E. & Lamb, R. A. (2007). Influenza virus hemagglutinin and neuraminidase, but not the matrix protein, are required for assembly and budding of plasmid-derived virus-like particles. *J Virol* **81**, 7111–7123.

Chen, B. J., Leser, G. P., Jackson, D. & Lamb, R. A. (2008). The influenza virus M2 protein cytoplasmic tail interacts with the M1 protein and influences virus assembly at the site of virus budding. *J Virol* **82**, 10059–10070.

Chlanda, P., Schraidt, O., Kummer, S., Riches, J., Oberwinkler, H., Prinz, S., Kräusslich, H. G. & Briggs, J. A. (2015). Structural analysis of the roles of influenza a virus membrane-associated proteins in assembly and morphology. *J Virol* **89**, 8957–8966.

Choppin, P. W. (1963). On the emergence of influenza virus filaments from host cells. *Virology* **21**, 278–281.

Chou, Y. Y., Vafabakhsh, R., Doğanay, S., Gao, Q., Ha, T. & Palese, P. (2012). One influenza virus particle packages eight unique viral RNAs as shown by FISH analysis. *Proc Natl Acad Sci U S A* **109**, 9101–9106.

Chou, Y. Y., Heaton, N. S., Gao, Q., Palese, P., Singer, R. H., Singer, R. & Lionnet, T. (2013). Colocalization of different influenza viral RNA segments in the cytoplasm before viral budding as shown by single-molecule sensitivity FISH analysis. *PLoS Pathog* **9**, e1003358.

Chua, M. A., Schmid, S., Perez, J. T., Langlois, R. A. & Tenoever, B. R. (2013). Influenza A virus utilizes suboptimal splicing to coordinate the timing of infection. *Cell Rep* **3**, 23–29.

Ciampor, F., Bayley, P. M., Nermut, M. V., Hirst, E. M., Sugrue, R. J. & Hay, A. J. (1992). Evidence that the amantadine-induced, M2-mediated conversion of influenza A virus hemagglutinin to the low pH conformation occurs in an acidic trans Golgi compartment. *Virology* **188**, 14–24.

Cros, J. F. & Palese, P. (2003). Trafficking of viral genomic RNA into and out of the nucleus: influenza, Thogoto and Borna disease viruses. *Virus Res* **95**, 3–12.

de Lucas, S., Peredo, J., Marión, R. M., Sánchez, C. & Ortín, J. (2010). Human Staufen1 protein interacts with influenza virus ribonucleoproteins and is required for efficient virus multiplication. *J Virol* **84**, 7603–7612.

Demirov, D., Gabriel, G., Schneider, C., Hohenberg, H. & Ludwig, S. (2012). Interaction of influenza A virus matrix protein with RACK1 is required for virus release. *Cell Microbiol* **14**, 774–789.

Deom, C. M. & Schulze, I. T. (1985). Oligosaccharide composition of an influenza virus hemagglutinin with host-determined binding properties. *J Biol Chem* **260**, 14771–14774.

Domingues, P., Golebiowski, F., Tatham, M. H., Lopes, A. M., Taggart, A., Hay, R. T. & Hale, B. G. (2015). Global reprogramming of host SUMOylation during influenza virus infection. *Cell Rep* **13**, 1467–1480.

Doms, R. W., Lamb, R. A., Rose, J. K. & Helenius, A. (1993). Folding and assembly of viral membrane proteins. *Virology* **193**, 545–562.

Dos Santos Afonso, E., Escriou, N., Leclercq, I., van der Werf, S. & Naffakh, N. (2005). The generation of recombinant influenza A viruses expressing a PB2 fusion protein requires the conservation of a packaging signal overlapping the coding and noncoding regions at the 5′ end of the PB2 segment. *Virology* **341**, 34–46.

Duhaut, S. D. & McCauley, J. W. (1996). Defective RNAs inhibit the assembly of influenza virus genome segments in a segment-specific manner. *Virology* **216**, 326–337.

Duhaut, S. D. & Dimmock, N. J. (2002). Defective segment 1 RNAs that interfere with production of infectious influenza A virus require at least 150 nucleotides of 5′ sequence: evidence from a plasmid-driven system. *J Gen Virol* **83**, 403–411.

Eisfeld, A. J., Kawakami, E., Watanabe, T., Neumann, G. & Kawaoka, Y. (2011a). RAB11A is essential for transport of the influenza virus genome to the plasma membrane. *J Virol* **85**, 6117–6126.

Eisfeld, A. J., Neumann, G. & Kawaoka, Y. (2011b). Human immunodeficiency virus rev-binding protein is essential for influenza a virus replication and promotes genome trafficking in late-stage infection. *J Virol* **85**, 9588–9598.

Eisfeld, A. J., Neumann, G. & Kawaoka, Y. (2015). At the centre: influenza A virus ribonucleoproteins. *Nat Rev Microbiol* **13**, 28–41.

Elleman, C. J. & Barclay, W. S. (2004). The M1 matrix protein controls the filamentous phenotype of influenza A virus. *Virology* **321**, 144–153.

Elster, C., Larsen, K., Gagnon, J., Ruigrok, R. W. & Baudin, F. (1997). Influenza virus M1 protein binds to RNA through its nuclear localization signal. *J Gen Virol* **78**, 1589–1596.

Elton, D., Simpson-Holley, M., Archer, K., Medcalf, L., Hallam, R., McCauley, J. & Digard, P. (2001). Interaction of the influenza virus nucleoprotein with the cellular CRM1-mediated nuclear export pathway. *J Virol* **75**, 408–419.

Essere, B., Yver, M., Gavazzi, C., Terrier, O., Isel, C., Fournier, E., Giroux, F., Textoris, J., Julien, T. & other authors (2013). Critical role of segment-specific packaging signals in genetic reassortment of influenza A viruses. *Proc Natl Acad Sci U S A* **110**, E3840–3848.

Falcón, A. M., Fortes, P., Marión, R. M., Beloso, A. & Ortín, J. (1999). Interaction of influenza virus NS1 protein and the human homologue of Staufen *in vivo* and *in vitro*. *Nucleic Acids Res* **27**, 2241–2247.

Fournier, E., Moules, V., Essere, B., Paillart, J. C., Sirbat, J. D., Cavalier, A., Rolland, J. P., Thomas, D, Lina, B. & other authors (2012a). Interaction network linking the human H3N2 influenza A virus genomic RNA segments. *Vaccine* **30**, 7359–7367.

Fournier, E., Moules, V., Essere, B., Paillart, J. C., Sirbat, J. D., Isel, C., Cavalier, A., Rolland, J. P, Thomas, D. & other authors (2012b). A supramolecular assembly formed by influenza A virus genomic RNA segments. *Nucleic Acids Res* **40**, 2197–2209.

Franke, E. K., Yuan, H. E. & Luban, J. (1994). Specific incorporation of cyclophilin A into HIV-1 virions. *Nature* **372**, 359–362.

Fujii, Y., Goto, H., Watanabe, T., Yoshida, T. & Kawaoka, Y. (2003). Selective incorporation of influenza virus RNA segments into virions. *Proc Natl Acad Sci U S A* **100**, 2002–2007.

Fujii, K., Ozawa, M., Iwatsuki-Horimoto, K., Horimoto, T. & Kawaoka, Y. (2009). Incorporation of influenza A virus genome segments does not absolutely require wild-type sequences. *J Gen Virol* **90**, 1734–1740.

Fukuda, M., Asano, S., Nakamura, T., Adachi, M., Yoshida, M., Yanagida, M. & Nishida, E. (1997). CRM1 is responsible for intracellular transport mediated by the nuclear export signal. *Nature* **390**, 308–311.

Gao, Q., Chou, Y. Y., Doğanay, S., Vafabakhsh, R., Ha, T. & Palese, P. (2012). The influenza A virus PB2, PA, NP, and M segments play a pivotal role during genome packaging. *J Virol* **86**, 7043–7051.

Gao, S., Wu, J., Liu, R. Y., Li, J., Song, L., Teng, Y., Sheng, C., Liu, D., Yao, C. & other authors (2015). Interaction of NS2 with AIMP2 facilitates the switch from ubiquitination to SUMOylation of M1 in influenza A virus-infected cells. *J Virol* **89**, 300–311.

Gavazzi, C., Isel, C., Fournier, E., Moules, V., Cavalier, A., Thomas, D., Lina, B. & Marquet, R. (2013). An *in vitro* network of intermolecular interactions between viral RNA segments of an avian H5N2 influenza A virus: comparison with a human H3N2 virus. *Nucleic Acids Res* **41**, 1241–1254.

Gerber, M., Isel, C., Moules, V. & Marquet, R. (2014). Selective packaging of the influenza A genome and consequences for genetic reassortment. *Trends Microbiol* **22**, 446–455.

Gerl, M. J., Sampaio, J. L., Urban, S., Kalvodova, L., Verbavatz, J. M., Binnington, B., Lindemann, D., Lingwood, C. A, Shevchenko, A. & other authors (2012). Quantitative analysis of the lipidomes of the influenza virus envelope and MDCK cell apical. *Membrane. J Cell Biol* **196**, 213–221.

Gog, J. R., Afonso Edos, S., Dalton, R. M., Leclercq, I., Tiley, L., Elton, D., von Kirchbach, J. C., Naffakh, N., Escriou, N. & other authors (2007). Codon conservation in the influenza A virus genome defines RNA packaging signals. *Nucleic Acids Res* **35**, 1897–1907.

Gorai, T., Goto, H., Noda, T., Watanabe, T., Kozuka-Hata, H., Oyama, M., Takano, R., Neumann, G., Watanabe, S. & other authors (2012). F1Fo-ATPase, F-type proton-translocating ATPase, at the plasma membrane is critical for efficient influenza virus budding. *Proc Natl Acad Sci U S A* **109**, 4615–4620.

Grambas, S. & Hay, A. J. (1992). Maturation of influenza A virus hemagglutinin – estimates of the pH encountered during transport and its regulation by the M2 protein. *Virology* **190**, 11–18.

Grantham, M. L., Stewart, S. M., Lalime, E. N. & Pekosz, A. (2010). Tyrosines in the influenza A virus M2 protein cytoplasmic tail are critical for production of infectious virus particles. *J Virol* **84**, 8765–8776.

Griffin, J. A., Basak, S. & Compans, R. W. (1983). Effects of hexose starvation and the role of sialic acid in influenza virus release. *Virology* **125**, 324–334.

Harris, A., Forouhar, F., Qiu, S., Sha, B. & Luo, M. (2001). The crystal structure of the influenza matrix protein M1 at neutral pH: M1-M1 protein interfaces can rotate in the oligomeric structures of M1. *Virology* **289**, 34–44.

Harris, A., Cardone, G., Winkler, D. C., Heymann, J. B., Brecher, M., White, J. M. & Steven, A. C. (2006). Influenza virus pleiomorphy characterized by cryoelectron tomography. *Proc Natl Acad Sci U S A* **103**, 19123–19127.

He, J., Sun, E., Bujny, M. V., Kim, D., Davidson, M. W. & Zhuang, X. (2013). Dual function of CD81 in influenza virus uncoating and budding. *PLoS Pathog* **9**, e1003701.

Hilsch, M., Goldenbogen, B., Sieben, C., Höfer, C. T., Rabe, J. P., Klipp, E., Herrmann, A. & Chiantia, S. (2014). Influenza A matrix protein M1 multimerizes upon binding to lipid membranes. *Biophys J* **107**, 912–923.

Huang, S., Chen, J., Chen, Q., Wang, H., Yao, Y., Chen, J. & Chen, Z. (2013). A second CRM1-dependent nuclear export signal in the influenza A virus NS2 protein contributes to the nuclear export of viral ribonucleoproteins. *J Virol* **87**, 767–778.

Huarte, M., Sanz-Ezquerro, J. J., Roncal, F., Ortín, J. & Nieto, A. (2001). PA subunit from influenza virus polymerase complex interacts with a cellular protein with homology to a family of transcriptional activators. *J Virol* **75**, 8597–8604.

Hughey, P. G., Compans, R. W., Zebedee, S. L. & Lamb, R. A. (1992). Expression of the influenza A virus M2 protein is restricted to apical surfaces of polarized epithelial cells. *J Virol* **66**, 5542–5552.

Hutchinson, E. C., Curran, M. D., Read, E. K., Gog, J. R. & Digard, P. (2008). Mutational analysis of cis-acting RNA signals in segment 7 of influenza A virus. *J Virol* **82**, 11869–11879.

Hutchinson, E. C., Wise, H. M., Kudryavtseva, K., Curran, M. D. & Digard, P. (2009). Characterisation of influenza A viruses with mutations in segment 5 packaging signals. *Vaccine* **27**, 6270–6275.

Hutchinson, E. C., von Kirchbach, J. C., Gog, J. R. & Digard, P. (2010). Genome packaging in influenza A virus. *J Gen Virol* **91**, 313–328.

Hutchinson, E. C. & Fodor, E. (2013). Transport of the influenza virus genome from nucleus to nucleus. *Viruses* **5**, 2424–2446.

Hutchinson, E. C., Charles, P. D., Hester, S. S., Thomas, B., Trudgian, D., Martínez-Alonso, M. & Fodor, E. (2014). Conserved and host-specific features of influenza virion architecture. *Nat Commun* **5**, 4816.

Inagaki, A., Goto, H., Kakugawa, S., Ozawa, M. & Kawaoka, Y. (2012). Competitive incorporation of homologous gene segments of influenza A virus into virions. *J Virol* **86**, 10200–10202.

Iwatsuki-Horimoto, K., Horimoto, T., Fujii, Y. & Kawaoka, Y. (2004). Generation of influenza A virus NS2 (NEP) mutants with an altered nuclear export signal sequence. *J Virol* **78**, 10149–10155.

Iwatsuki-Horimoto, K., Horimoto, T., Noda, T., Kiso, M., Maeda, J., Watanabe, S., Muramoto, Y., Fujii, K. & Kawaoka, Y. (2006). The cytoplasmic tail of the influenza A virus M2 protein plays a role in viral assembly. *J Virol* **80**, 5233–5240.

Jin, H., Leser, G. P., Zhang, J. & Lamb, R. A. (1997). Influenza virus hemagglutinin and neuraminidase cytoplasmic tails control particle shape. *EMBO J* **16**, 1236–1247.

Jo, S., Kawaguchi, A., Takizawa, N., Morikawa, Y., Momose, F. & Nagata, K. (2010). Involvement of vesicular trafficking system in membrane targeting of the progeny influenza virus genome. *Microbes Infect* **12**, 1079–1084.

Kawaguchi, A., Matsumoto, K. & Nagata, K. (2012). YB-1 functions as a porter to lead influenza virus ribonucleoprotein complexes to microtubules. *J Virol* **86**, 11086–11095.

Keller, P. & Simons, K. (1998). Cholesterol is required for surface transport of influenza virus hemagglutinin. *J Cell Biol* **140**, 1357–1367.

Kolesnikova, L., Heck, S., Matrosovich, T., Klenk, H. D., Becker, S. & Matrosovich, M. (2013). Influenza virus budding from the tips of cellular microvilli in differentiated human airway epithelial cells. *J Gen Virol* **94**, 971–976.

Kundu, A., Avalos, R. T., Sanderson, C. M. & Nayak, D. P. (1996). Transmembrane domain of influenza virus neuraminidase, a type II protein, possesses an apical sorting signal in polarized MDCK cells. *J Virol* **70**, 6508–6515.

Lai, J. C., Chan, W. W., Kien, F., Nicholls, J. M., Peiris, J. S. & Garcia, J. M. (2010). Formation of virus-like particles from human cell lines exclusively expressing influenza neuraminidase. *J Gen Virol* **91**, 2322–2330.

Lakdawala, S. S., Wu, Y., Wawrzusin, P., Kabat, J., Broadbent, A. J., Lamirande, E. W., Fodor, E., Altan-Bonnet, N., Shroff, H. & other authors (2014). Influenza A virus assembly intermediates fuse in the cytoplasm. *PLoS Pathog* **10**, e1003971.

LeBouder, F., Morello, E., Rimmelzwaan, G. F., Bosse, F., Péchoux, C., Delmas, B. & Riteau, B. (2008). Annexin II incorporated into influenza virus particles supports virus replication by converting plasminogen into plasmin. *J Virol* **82**, 6820–6828.

Leser, G. P. & Lamb, R. A. (2005). Influenza virus assembly and budding in raft-derived microdomains: a quantitative analysis of the surface distribution of HA, NA and M2 proteins. *Virology* **342**, 215–227.

Liang, Y., Hong, Y. & Parslow, T. G. (2005). cis-Acting packaging signals in the influenza virus PB1, PB2 and PA genomic RNA segments. *J Virol* **79**, 10348–10355.

Lin, S., Naim, H. Y., Rodriguez, A. C. & Roth, M. G. (1998). Mutations in the middle of the transmembrane domain reverse the polarity of transport of the influenza virus hemagglutinin in MDCK epithelial cells. *J Cell Biol* **142**, 51–57.

Ma, K., Roy, A. M. & Whittaker, G. R. (2001). Nuclear export of influenza virus ribonucleoproteins: identification of an export intermediate at the nuclear periphery. *Virology* **282**, 215–220.

Mangeat, B., Turelli, P., Caron, G., Friedli, M., Perrin, L. & Trono, D. (2003). Broad antiretroviral defence by human APOBEC3G through lethal editing of nascent reverse transcripts. *Nature* **424**, 99–103.

Marión, R. M., Fortes, P., Beloso, A., Dotti, C. & Ortín, J. (1999). A human sequence homologue of Staufen is an RNA-binding protein that is associated with polysomes and localizes to the rough endoplasmic reticulum. *Mol Cell Biol* **19**, 2212–2219.

Marsh, G. A., Hatami, R. & Palese, P. (2007). Specific residues of the influenza A virus hemagglutinin viral RNA are important for efficient packaging into budding virions. *J Virol* **81**, 9727–9736.

Marsh, G. A., Rabadán, R., Levine, A. J. & Palese, P. (2008). Highly conserved regions of influenza a virus polymerase gene segments are critical for efficient viral RNA packaging. *J Virol* **82**, 2295–2304.

Marshall, N., Priyamvada, L., Ende, Z., Steel, J. & Lowen, A. C. (2013). Influenza virus reassortment occurs with high frequency in the absence of segment mismatch. *PLoS Pathog* **9**, e1003421.

Martin, K. & Helenius, A. (1991). Nuclear transport of influenza virus ribonucleoproteins: the viral matrix protein (M1) promotes export and inhibits import. *Cell* **67**, 117–130.

McCown, M. F. & Pekosz, A. (2005). The influenza A virus M2 cytoplasmic tail is required for infectious virus production and efficient genome packaging. *J Virol* **79**, 3595–3605.

Momose, F., Kikuchi, Y., Komase, K. & Morikawa, Y. (2007). Visualization of microtubule-mediated transport of influenza viral progeny ribonucleoprotein. *Microbes Infect* **9**, 1422–1433.

Momose, F., Sekimoto, T., Ohkura, T., Jo, S., Kawaguchi, A., Nagata, K. & Morikawa, Y. (2011). Apical transport of influenza A virus ribonucleoprotein requires Rab11-positive recycling endosome. *PLoS One* **6**, e21123.

Mosley, V. M. & Wyckoff, R. W. (1946). Electron micrography of the virus of influenza. *Nature* **157**, 263.

Muramoto, Y., Takada, A., Fujii, K., Noda, T., Iwatsuki-Horimoto, K., Watanabe, S., Horimoto, T., Kida, H. & Kawaoka, Y. (2006). Hierarchy among viral RNA (vRNA) segments in their role in vRNA incorporation into influenza A virions. *J Virol* **80**, 2318–2325.

Nayak, D. P., Balogun, R. A., Yamada, H., Zhou, Z. H. & Barman, S. (2009). Influenza virus morphogenesis and budding. *Virus Res* **143**, 147–161.

Neumann, G., Hughes, M. T. & Kawaoka, Y. (2000). Influenza A virus NS2 protein mediates vRNP nuclear export through NES-independent interaction with hCRM1. *EMBO J* **19**, 6751–6758.

Noda, T., Sagara, H., Yen, A., Takada, A., Kida, H., Cheng, R. H. & Kawaoka, Y. (2006). Architecture of ribonucleoprotein complexes in influenza A virus particles. *Nature* **439**, 490–492.

Noda, T., Sugita, Y., Aoyama, K., Hirase, A., Kawakami, E., Miyazawa, A., Sagara, H. & Kawaoka, Y. (2012). Three-dimensional analysis of ribonucleoprotein complexes in influenza A virus. *Nat Commun* **3**, 639.

Noton, S. L., Medcalf, E., Fisher, D., Mullin, A. E., Elton, D. & Digard, P. (2007). Identification of the domains of the influenza A virus M1 matrix protein required for NP binding, oligomerization and incorporation into virions. *J Gen Virol* **88**, 2280–2290.

O'Neill, R. E., Talon, J. & Palese, P. (1998). The influenza virus NEP (NS2 protein) mediates the nuclear export of viral ribonucleoproteins. *EMBO J* **17**, 288–296.

Odagiri, T. & Tashiro, M. (1997). Segment-specific noncoding sequences of the influenza virus genome RNA are involved in the specific competition between defective interfering RNA and its progenitor RNA segment at the virion assembly step. *J Virol* **71**, 2138–2145.

Ohkura, T., Momose, F., Ichikawa, R., Takeuchi, K. & Morikawa, Y. (2014). Influenza A virus hemagglutinin and neuraminidase mutually accelerate their apical targeting through clustering of lipid rafts. *J Virol* **88**, 10039–10055.

Ozawa, M., Maeda, J., Iwatsuki-Horimoto, K., Watanabe, S., Goto, H., Horimoto, T. & Kawaoka, Y. (2009). Nucleotide sequence requirements at the 5′ end of the influenza A virus M RNA segment for efficient virus replication. *J Virol* **83**, 3384–3388.

Palese, P., Tobita, K., Ueda, M. & Compans, R. W. (1974). Characterization of temperature sensitive influenza virus mutants defective in neuraminidase. *Virology* **61**, 397–410.

Palese, P. & Shaw, M. L. (2007). Orthomyxoviridae: the viruses and their replication. *Fields Virology* **2**, 1647–1689.

Paterson, D. & Fodor, E. (2012). Emerging roles for the influenza A virus nuclear export protein (NEP). *PLoS Pathog* **8**, e1003019.

Pemberton, L. F., Blobel, G. & Rosenblum, J. S. (1998). Transport routes through the nuclear pore complex. *Curr Opin Cell Biol* **10**, 392–399.

Pleschka, S., Wolff, T., Ehrhardt, C., Hobom, G., Planz, O., Rapp, U. R. & Ludwig, S. (2001). Influenza virus propagation is impaired by inhibition of the Raf/MEK/ERK signalling cascade. *Nat Cell Biol* **3**, 301–305.

Richardson, J. C. & Akkina, R. K. (1991). NS2 protein of influenza virus is found in purified virus and phosphorylated in infected cells. *Arch Virol* **116**, 69–80.

Roberts, K. L., Leser, G. P., Ma, C. & Lamb, R. A. (2013). The amphipathic helix of influenza A virus M2 protein is required for filamentous bud formation and scission of filamentous and spherical particles. *J Virol* **87**, 9973–9982.

Rodriguez, A., Pérez-González, A. & Nieto, A. (2011). Cellular human CLE/C14orf166 protein interacts with influenza virus polymerase and is required for viral replication. *J Virol* **85**, 12062–12066.

Rodriguez-Frandsen, A., de Lucas, S., Pérez-González, A., Pérez-Cidoncha, M., Roldan-Gomendio, A., Pazo, A., Marcos-Villar, L., Landeras-Bueno, S., Ortín, J. & other authors (2016). hCLE/C14orf166, a cellular protein required for viral replication, is incorporated into influenza virus particles. *Sci Rep* **6**, 20744.

Rossman, J. S. & Lamb, R. A. (2011). Influenza virus assembly and budding. *Virology* **411**, 229–236.

Rossman, J. S., Jing, X., Leser, G. P., Balannik, V., Pinto, L. H. & Lamb, R. A. (2010a). Influenza virus m2 ion channel protein is necessary for filamentous virion formation. *J Virol* **84**, 5078–5088.

Rossman, J. S., Jing, X., Leser, G. P. & Lamb, R. A. (2010b). Influenza virus M2 protein mediates ESCRT-independent membrane scission. *Cell* **142**, 902–913.

Sakaguchi, T., Leser, G. P. & Lamb, R. A. (1996). The ion channel activity of the influenza virus M2 protein affects transport through the Golgi apparatus. *J Cell Biol* **133**, 733–747.

Scheiffele, P., Roth, M. G. & Simons, K. (1997). Interaction of influenza virus haemagglutinin with sphingolipid-cholesterol membrane domains via its transmembrane domain. *EMBO J* **16**, 5501–5508.

Schmidt, N. W., Mishra, A., Wang, J., DeGrado, W. F. & Wong, G. C. (2013). Influenza virus A M2 protein generates negative Gaussian membrane curvature necessary for budding and scission. *J Am Chem Soc* **135**, 13710–13719.

Schmitt, A. P. & Lamb, R. A. (2005). Influenza virus assembly and budding at the viral budozone. *Adv Virus Res* **64**, 383–416.

Schroeder, C., Heider, H., Möncke-Buchner, E. & Lin, T. I. (2005). The influenza virus ion channel and maturation cofactor M2 is a cholesterol-binding protein. *Eur Biophys J* **34**, 52–66.

Seladi-Schulman, J., Steel, J. & Lowen, A. C. (2013). Spherical influenza viruses have a fitness advantage in embryonated eggs, while filament-producing strains are selected *in vivo*. *J Virol* **87**, 13343–13353.

Shapira, S. D., Gat-Viks, I., Shum, B. O., Dricot, A., de Grace, M. M., Wu, L., Gupta, P. B., Hao, T., Silver, S. J. & other authors (2009). A physical and regulatory map of host-influenza interactions reveals pathways in H1N1 infection. *Cell* **139**, 1255–1267.

Shaw, M. L., Stone, K. L., Colangelo, C. M., Gulcicek, E. E. & Palese, P. (2008). Cellular proteins in influenza virus particles. *PLoS Pathog* **4**, e1000085.

Sheehy, A. M., Gaddis, N. C., Choi, J. D. & Malim, M. H. (2002). Isolation of a human gene that inhibits HIV-1 infection and is suppressed by the viral Vif protein. *Nature* **418**, 646–650.

Shimizu, T., Takizawa, N., Watanabe, K., Nagata, K. & Kobayashi, N. (2011). Crucial role of the influenza virus NS2 (NEP) C-terminal domain in M1 binding and nuclear export of vRNP. *FEBS Lett* **585**, 41–46.

Simons, K. & Ikonen, E. (1997). Functional rafts in cell membranes. *Nature* **387**, 569–572.

Simpson, D. A. & Lamb, R. A. (1992). Alterations to influenza virus hemagglutinin cytoplasmic tail modulate virus infectivity. *J Virol* **66**, 790–803.

Stertz, S. & Shaw, M. L. (2011). Uncovering the global host cell requirements for influenza virus replication via RNAi screening. *Microbes Infect* **13**, 516–525.

Sun, E., He, J. & Zhuang, X. (2013). Dissecting the role of COPI complexes in influenza virus infection. *J Virol* **87**, 2673–2685.

Takeda, M., Leser, G. P., Russell, C. J. & Lamb, R. A. (2003). Influenza virus hemagglutinin concentrates in lipid raft microdomains for efficient viral fusion. *Proc Natl Acad Sci U S A* **100**, 14610–14617.

Takizawa, N., Kumakura, M., Takeuchi, K., Kobayashi, N. & Nagata, K. (2010). Sorting of influenza A virus RNA genome segments after nuclear export. *Virology* **401**, 248–256.

Tchatalbachev, S., Flick, R. & Hobom, G. (2001). The packaging signal of influenza viral RNA molecules. *RNA* **7**, 979–989.

Thaa, B., Herrmann, A. & Veit, M. (2010). Intrinsic cytoskeleton-dependent clustering of influenza virus M2 protein with hemagglutinin assessed by FLIM-FRET. *J Virol* **84**, 12445–12449.

Thaa, B., Levental, I., Herrmann, A. & Veit, M. (2011). Intrinsic membrane association of the cytoplasmic tail of influenza virus M2 protein and lateral membrane sorting regulated by cholesterol binding and palmitoylation. *Biochem J* **437**, 389–397.

Thali, M., Bukovsky, A., Kondo, E., Rosenwirth, B., Walsh, C. T., Sodroski, J. & Göttlinger, H. G. (1994). Functional association of cyclophilin A with HIV-1 virions. *Nature* **372**, 363–365.

Tripathi, S., Pohl, M. O., Zhou, Y., Rodriguez-Frandsen, A., Wang, G., Stein, D. A., Moulton, H. M., DeJesus, P., Che, J. & other authors (2015). Meta- and Orthogonal integration of influenza 'OMICs' data defines a role for ubr4 in virus budding. *Cell Host Microbe* **18**, 723–735.

Tsukahara, F. & Maru, Y. (2004). Identification of novel nuclear export and nuclear localization-related signals in human heat shock cognate protein 70. *J Biol Chem* **279**, 8867–8872.

Wang, S., Li, H., Chen, Y., Wei, H., Gao, G. F., Liu, H., Huang, S. & Chen, J. L. (2012). Transport of influenza virus neuraminidase (NA) to host cell surface is regulated by ARHGAP21 and Cdc42 proteins. *J Biol Chem* **287**, 9804–9816.

Watanabe, K., Takizawa, N., Katoh, M., Hoshida, K., Kobayashi, N. & Nagata, K. (2001). Inhibition of nuclear export of ribonucleoprotein complexes of influenza virus by leptomycin B. *Virus Res* **77**, 31–42.

Watanabe, T., Watanabe, S., Noda, T., Fujii, Y. & Kawaoka, Y. (2003). Exploitation of nucleic acid packaging signals to generate a novel influenza virus-based vector stably expressing two foreign genes. *J Virol* **77**, 10575–10583.

Watanabe, K., Fuse, T., Asano, I., Tsukahara, F., Maru, Y., Nagata, K., Kitazato, K. & Kobayashi, N. (2006). Identification of Hsc70 as an influenza virus matrix protein (M1) binding factor involved in the virus life cycle. *FEBS Lett* **580**, 5785–5790.

Watanabe, K., Takizawa, N., Noda, S., Tsukahara, F., Maru, Y. & Kobayashi, N. (2008). Hsc70 regulates the nuclear export but not the import of influenza viral RNP: A possible target for the development of anti-influenza virus drugs. *Drug Discov Ther* **2**, 77–84.

Watanabe, K., Shimizu, T., Noda, S., Tsukahara, F., Maru, Y. & Kobayashi, N. (2014a). Nuclear export of the influenza virus ribonucleoprotein complex: Interaction of Hsc70 with viral proteins M1 and NS2. *FEBS Open Bio* **4**, 683–688.

Watanabe, T., Kawakami, E., Shoemaker, J. E., Lopes, T. J., Matsuoka, Y., Tomita, Y., Kozuka-Hata, H., Gorai, T., Kuwahara, T. & other authors (2014b). Influenza virus-host interactome screen as a platform for antiviral drug development. *Cell Host Microbe* **16**, 795–805.

Whittaker, G., Bui, M. & Helenius, A. (1996). The role of nuclear import and export in influenza virus infection. *Trends Cell Biol* **6**, 67–71.

Wise, H. M., Barbezange, C., Jagger, B. W., Dalton, R. M., Gog, J. R., Curran, M. D., Taubenberger, J. K., Anderson, E. C. & Digard, P. (2011). Overlapping signals for translational regulation and packaging of influenza A virus segment 2. *Nucleic Acids Res* **39**, 7775–7790.

Wu, C. Y., Jeng, K. S. & Lai, M. M. (2011). The SUMOylation of matrix protein M1 modulates the assembly and morphogenesis of influenza A virus. *J Virol* **85**, 6618–6628.

Wurzer, W. J., Planz, O., Ehrhardt, C., Giner, M., Silberzahn, T., Pleschka, S. & Ludwig, S. (2003). Caspase 3 activation is essential for efficient influenza virus propagation. *EMBO J* **22**, 2717–2728.

Yasuda, J., Nakada, S., Kato, A., Toyoda, T. & Ishihama, A. (1993). Molecular assembly of influenza virus: association of the NS2 protein with virion matrix. *Virology* **196**, 249–255.

Ye, Z., Liu, T., Offringa, D. P., McInnis, J. & Levandowski, R. A. (1999). Association of influenza virus matrix protein with ribonucleoproteins. *J Virol* **73**, 7467–7473.

Yu, M., Liu, X., Cao, S., Zhao, Z., Zhang, K., Xie, Q., Chen, C., Gao, S., Bi, Y. & other authors (2012). Identification and characterization of three novel nuclear export signals in the influenza A virus nucleoprotein. *J Virol* **86**, 4970–4980.

Zhang, J., Leser, G. P., Pekosz, A. & Lamb, R. A. (2000a). The cytoplasmic tails of the influenza virus spike glycoproteins are required for normal genome packaging. *Virology* **269**, 325–334.

Zhang, J., Pekosz, A. & Lamb, R. A. (2000b). Influenza virus assembly and lipid raft microdomains: a role for the cytoplasmic tails of the spike glycoproteins. *J Virol* **74**, 4634–4644.

Zhang, K., Wang, Z., Liu, X., Yin, C., Basit, Z., Xia, B. & Liu, W. (2012). Dissection of influenza A virus M1 protein: pH-dependent oligomerization of N-terminal domain and dimerization of C-terminal domain. *PLoS One* **7**, e37786.

REFERENCES

1. Webster, R.G., et al., *Evolution and ecology of influenza A viruses.* Microbiol Rev, 1992. **56**(1): p. 152-79.
2. Morens, D.M. and J.K. Taubenberger, *Historical thoughts on influenza viral ecosystems, or behold a pale horse, dead dogs, failing fowl, and sick swine.* Influenza Other Respir Viruses, 2010. **4**(6): p. 327-37.
3. Neumann, G., T. Noda, and Y. Kawaoka, *Emergence and pandemic potential of swine-origin H1N1 influenza virus.* Nature, 2009. **459**(7249): p. 931-9.
4. Vemula, S.V., et al., *Current Approaches for Diagnosis of Influenza Virus Infections in Humans.* Viruses, 2016. **8**(4): p. 96.
5. Horimoto, T. and Y. Kawaoka, *Influenza: lessons from past pandemics, warnings from current incidents.* Nat Rev Microbiol, 2005. **3**(8): p. 591-600.
6. Schneider, W.M., M.D. Chevillotte, and C.M. Rice, *Interferon-stimulated genes: a complex web of host defenses.* Annu Rev Immunol, 2014. **32**: p. 513-45.
7. Ozawa, M. and Y. Kawaoka, *Cross talk between animal and human influenza viruses.* Annu Rev Anim Biosci, 2013. **1**: p. 21-42.
8. Fouchier, R.A., et al., *Characterization of a novel influenza A virus hemagglutinin subtype (H16) obtained from black-headed gulls.* J Virol, 2005. **79**(5): p. 2814-22.
9. Tong, S., et al., *A distinct lineage of influenza A virus from bats.* Proc Natl Acad Sci U S A, 2012. **109**(11): p. 4269-74.
10. Tong, S., et al., *New world bats harbor diverse influenza A viruses.* PLoS Pathog, 2013. **9**(10): p. e1003657.
11. Wu, Y., et al., *Bat-derived influenza-like viruses H17N10 and H18N11.* Trends Microbiol, 2014. **22**(4): p. 183-91.
12. Moreira, E.A., et al., *Synthetically derived bat influenza A-like viruses reveal a cell type- but not species-specific tropism.* Proc Natl Acad Sci U S A, 2016.
13. Juozapaitis, M., et al., *An infectious bat-derived chimeric influenza virus harbouring the entry machinery of an influenza A virus.* Nat Commun, 2014. **5**: p. 4448.
14. Naesens, L., A. Stevaert, and E. Vanderlinden, *Antiviral therapies on the horizon for influenza.* Curr Opin Pharmacol, 2016. **30**: p. 106-115.
15. Peter Palese, M.L.S., *Orthomyxoviridae: The Viruses and Their Replication*, in *Fields Virology, 5th Edition*, D.M.H. Knipe, Peter M., Editor. 2007, Lippincott Williams & Wilkins.

16. Herz, C., et al., *Influenza virus, an RNA virus, synthesizes its messenger RNA in the nucleus of infected cells.* Cell, 1981. **26**(3 Pt 1): p. 391-400.
17. Jackson, D.A., et al., *Influenza virus RNA is synthesized at fixed sites in the nucleus.* Nature, 1982. **296**(5855): p. 366-8.
18. Shapiro, G.I., T. Gurney, Jr., and R.M. Krug, *Influenza virus gene expression: control mechanisms at early and late times of infection and nuclear-cytoplasmic transport of virus-specific RNAs.* J Virol, 1987. **61**(3): p. 764-73.
19. Hutchinson, E.C. and E. Fodor, *Nuclear import of the influenza A virus transcriptional machinery.* Vaccine, 2012. **30**(51): p. 7353-8.
20. Te Velthuis, A.J. and E. Fodor, *Influenza virus RNA polymerase: insights into the mechanisms of viral RNA synthesis.* Nat Rev Microbiol, 2016. **14**(8): p. 479-93.
21. Helenius, A., *Unpacking the incoming influenza virus.* Cell, 1992. **69**(4): p. 577-8.
22. Pielak, R.M. and J.J. Chou, *Influenza M2 proton channels.* Biochim Biophys Acta, 2011. **1808**(2): p. 522-9.
23. Hale, B.G., et al., *The multifunctional NS1 protein of influenza A viruses.* J Gen Virol, 2008. **89**(Pt 10): p. 2359-76.
24. O'Neill, R.E., J. Talon, and P. Palese, *The influenza virus NEP (NS2 protein) mediates the nuclear export of viral ribonucleoproteins.* EMBO J, 1998. **17**(1): p. 288-96.
25. Paterson, D. and E. Fodor, *Emerging roles for the influenza A virus nuclear export protein (NEP).* PLoS Pathog, 2012. **8**(12): p. e1003019.
26. Chen, W., et al., *A novel influenza A virus mitochondrial protein that induces cell death.* Nat Med, 2001. **7**(12): p. 1306-12.
27. Zamarin, D., et al., *Influenza virus PB1-F2 protein induces cell death through mitochondrial ANT3 and VDAC1.* PLoS Pathog, 2005. **1**(1): p. e4.
28. McAuley, J.L., et al., *Expression of the 1918 influenza A virus PB1-F2 enhances the pathogenesis of viral and secondary bacterial pneumonia.* Cell Host Microbe, 2007. **2**(4): p. 240-9.
29. Wise, H.M., et al., *A complicated message: Identification of a novel PB1-related protein translated from influenza A virus segment 2 mRNA.* J Virol, 2009. **83**(16): p. 8021-31.
30. Yamayoshi, S., et al., *Identification of a Novel Viral Protein Expressed from the PB2 Segment of Influenza A Virus.* J Virol, 2015. **90**(1): p. 444-56.
31. Jagger, B.W., et al., *An overlapping protein-coding region in influenza A virus segment 3 modulates the host response.* Science, 2012. **337**(6091): p. 199-204.
32. Muramoto, Y., et al., *Identification of novel influenza A virus proteins translated from PA mRNA.* J Virol, 2013. **87**(5): p. 2455-62.

33. Klenk, E., H. Faillard, and H. Lempfrid, *[Enzymatic effect of the influenza virus].* Hoppe Seylers Z Physiol Chem, 1955. **301**(4-6): p. 235-46.
34. Varki, A., *Essentials of glycobiology*. 2nd ed. 2009, Cold Spring Harbor, N.Y.: Cold Spring Harbor Laboratory Press. xxix, 784 p.
35. Rogers, G.N. and J.C. Paulson, *Receptor determinants of human and animal influenza virus isolates: differences in receptor specificity of the H3 hemagglutinin based on species of origin.* Virology, 1983. **127**(2): p. 361-73.
36. Shinya, K., et al., *Avian flu: influenza virus receptors in the human airway.* Nature, 2006. **440**(7083): p. 435-6.
37. Connor, R.J., et al., *Receptor specificity in human, avian, and equine H2 and H3 influenza virus isolates.* Virology, 1994. **205**(1): p. 17-23.
38. Webster, R.G., et al., *Intestinal influenza: replication and characterization of influenza viruses in ducks.* Virology, 1978. **84**(2): p. 268-78.
39. Skehel, J.J. and D.C. Wiley, *Receptor binding and membrane fusion in virus entry: the influenza hemagglutinin.* Annu Rev Biochem, 2000. **69**: p. 531-69.
40. Steinhauer, D.A., *Role of hemagglutinin cleavage for the pathogenicity of influenza virus.* Virology, 1999. **258**(1): p. 1-20.
41. Bottcher-Friebertshauser, E., H.D. Klenk, and W. Garten, *Activation of influenza viruses by proteases from host cells and bacteria in the human airway epithelium.* Pathog Dis, 2013. **69**(2): p. 87-100.
42. Conner, S.D. and S.L. Schmid, *Regulated portals of entry into the cell.* Nature, 2003. **422**(6927): p. 37-44.
43. Alberts, B., *Molecular biology of the cell*. 5th ed. 2008, New York: Garland Science.
44. Lajoie, P. and I.R. Nabi, *Lipid rafts, caveolae, and their endocytosis.* Int Rev Cell Mol Biol, 2010. **282**: p. 135-63.
45. Henley, J.R., H. Cao, and M.A. McNiven, *Participation of dynamin in the biogenesis of cytoplasmic vesicles.* FASEB J, 1999. **13 Suppl 2**: p. S243-7.
46. Merrifield, C.J., et al., *Imaging actin and dynamin recruitment during invagination of single clathrin-coated pits.* Nat Cell Biol, 2002. **4**(9): p. 691-8.
47. Lakadamyali, M., M.J. Rust, and X. Zhuang, *Endocytosis of influenza viruses.* Microbes Infect, 2004. **6**(10): p. 929-36.
48. Matlin, K.S., et al., *Infectious entry pathway of influenza virus in a canine kidney cell line.* J Cell Biol, 1981. **91**(3 Pt 1): p. 601-13.
49. Sieczkarski, S.B. and G.R. Whittaker, *Influenza virus can enter and infect cells in the absence of clathrin-mediated endocytosis.* J Virol, 2002. **76**(20): p. 10455-64.

50. de Vries, E., et al., *Dissection of the influenza A virus endocytic routes reveals macropinocytosis as an alternative entry pathway.* PLoS Pathog, 2011. **7**(3): p. e1001329.
51. Rust, M.J., et al., *Assembly of endocytic machinery around individual influenza viruses during viral entry.* Nat Struct Mol Biol, 2004. **11**(6): p. 567-73.
52. Chen, C. and X. Zhuang, *Epsin 1 is a cargo-specific adaptor for the clathrin-mediated endocytosis of the influenza virus.* Proc Natl Acad Sci U S A, 2008. **105**(33): p. 11790-5.
53. Ehrhardt, C., et al., *Bivalent role of the phosphatidylinositol-3-kinase (PI3K) during influenza virus infection and host cell defence.* Cell Microbiol, 2006. **8**(8): p. 1336-48.
54. Eierhoff, T., et al., *The epidermal growth factor receptor (EGFR) promotes uptake of influenza A viruses (IAV) into host cells.* PLoS Pathog, 2010. **6**(9): p. e1001099.
55. Mellman, I., *Endocytosis and molecular sorting.* Annu Rev Cell Dev Biol, 1996. **12**: p. 575-625.
56. Sieczkarski, S.B. and G.R. Whittaker, *Differential requirements of Rab5 and Rab7 for endocytosis of influenza and other enveloped viruses.* Traffic, 2003. **4**(5): p. 333-43.
57. Huotari, J. and A. Helenius, *Endosome maturation.* EMBO J, 2011. **30**(17): p. 3481-500.
58. Yoshimura, A. and S. Ohnishi, *Uncoating of influenza virus in endosomes.* J Virol, 1984. **51**(2): p. 497-504.
59. White, J., J. Kartenbeck, and A. Helenius, *Membrane fusion activity of influenza virus.* EMBO J, 1982. **1**(2): p. 217-22.
60. Carr, C.M. and P.S. Kim, *A spring-loaded mechanism for the conformational change of influenza hemagglutinin.* Cell, 1993. **73**(4): p. 823-32.
61. Stegmann, T., et al., *The HA2 subunit of influenza hemagglutinin inserts into the target membrane prior to fusion.* J Biol Chem, 1991. **266**(27): p. 18404-10.
62. Durrer, P., et al., *H+-induced membrane insertion of influenza virus hemagglutinin involves the HA2 amino-terminal fusion peptide but not the coiled coil region.* J Biol Chem, 1996. **271**(23): p. 13417-21.
63. Tatulian, S.A., et al., *Influenza hemagglutinin assumes a tilted conformation during membrane fusion as determined by attenuated total reflection FTIR spectroscopy.* EMBO J, 1995. **14**(22): p. 5514-23.
64. Chernomordik, L.V., et al., *The pathway of membrane fusion catalyzed by influenza hemagglutinin: restriction of lipids, hemifusion, and lipidic fusion pore formation.* J Cell Biol, 1998. **140**(6): p. 1369-82.
65. Fontana, J. and A.C. Steven, *At low pH, influenza virus matrix protein M1 undergoes a conformational change prior to dissociating from the membrane.* J Virol, 2013. **87**(10): p. 5621-8.

66. Greber, U.F., *Virus and Host Mechanics Support Membrane Penetration and Cell Entry.* J Virol, 2016. **90**(8): p. 3802-5.

67. Li, S., et al., *pH-Controlled two-step uncoating of influenza virus.* Biophys J, 2014. **106**(7): p. 1447-56.

68. Martin, K. and A. Helenius, *Nuclear transport of influenza virus ribonucleoproteins: the viral matrix protein (M1) promotes export and inhibits import.* Cell, 1991. **67**(1): p. 117-30.

69. O'Neill, R.E., et al., *Nuclear import of influenza virus RNA can be mediated by viral nucleoprotein and transport factors required for protein import.* J Biol Chem, 1995. **270**(39): p. 22701-4.

70. Akkina, R.K., et al., *Intracellular localization of the viral polymerase proteins in cells infected with influenza virus and cells expressing PB1 protein from cloned cDNA.* J Virol, 1987. **61**(7): p. 2217-24.

71. Jones, I.M., P.A. Reay, and K.L. Philpott, *Nuclear location of all three influenza polymerase proteins and a nuclear signal in polymerase PB2.* EMBO J, 1986. **5**(9): p. 2371-6.

72. Nieto, A., et al., *Complex structure of the nuclear translocation signal of influenza virus polymerase PA subunit.* J Gen Virol, 1994. **75 (Pt 1)**: p. 29-36.

73. Fodor, E., *The RNA polymerase of influenza a virus: mechanisms of viral transcription and replication.* Acta Virol, 2013. **57**(2): p. 113-22.

74. Plotch, S.J., M. Bouloy, and R.M. Krug, *Transfer of 5'-terminal cap of globin mRNA to influenza viral complementary RNA during transcription in vitro.* Proc Natl Acad Sci U S A, 1979. **76**(4): p. 1618-22.

75. Dias, A., et al., *The cap-snatching endonuclease of influenza virus polymerase resides in the PA subunit.* Nature, 2009. **458**(7240): p. 914-8.

76. Ulmanen, I., B.A. Broni, and R.M. Krug, *Role of two of the influenza virus core P proteins in recognizing cap 1 structures (m7GpppNm) on RNAs and in initiating viral RNA transcription.* Proc Natl Acad Sci U S A, 1981. **78**(12): p. 7355-9.

77. Bier, K., A. York, and E. Fodor, *Cellular cap-binding proteins associate with influenza virus mRNAs.* J Gen Virol, 2011. **92**(Pt 7): p. 1627-34.

78. Jorba, N., R. Coloma, and J. Ortin, *Genetic trans-complementation establishes a new model for influenza virus RNA transcription and replication.* PLoS Pathog, 2009. **5**(5): p. e1000462.

79. Moeller, A., et al., *Organization of the influenza virus replication machinery.* Science, 2012. **338**(6114): p. 1631-4.

80. Mark, G.E., et al., *Nuclear accumulation of influenza viral RNA transcripts and the effects of cycloheximide, actinomycin D, and alpha-amanitin.* J Virol, 1979. **29**(2): p. 744-52.

81. Vreede, F.T., T.E. Jung, and G.G. Brownlee, *Model suggesting that replication of influenza virus is regulated by stabilization of replicative intermediates.* J Virol, 2004. **78**(17): p. 9568-72.
82. Pohl, M.O., C. Lanz, and S. Stertz, *Late stages of the influenza A virus replication cycle-a tight interplay between virus and host.* J Gen Virol, 2016. **97**(9): p. 2058-72.
83. Capua, I. and O. Munoz, *Emergence of influenza viruses with zoonotic potential: open issues which need to be addressed. A review.* Vet Microbiol, 2013. **165**(1-2): p. 7-12.
84. Lubeck, M.D., P. Palese, and J.L. Schulman, *Nonrandom association of parental genes in influenza A virus recombinants.* Virology, 1979. **95**(1): p. 269-74.
85. Ince, W.L., et al., *Reassortment complements spontaneous mutation in influenza A virus NP and M1 genes to accelerate adaptation to a new host.* J Virol, 2013. **87**(8): p. 4330-8.
86. Brown, I.H., *The epidemiology and evolution of influenza viruses in pigs.* Vet Microbiol, 2000. **74**(1-2): p. 29-46.
87. Drake, J.W., *Rates of spontaneous mutation among RNA viruses.* Proc Natl Acad Sci U S A, 1993. **90**(9): p. 4171-5.
88. Ito, T., et al., *Molecular basis for the generation in pigs of influenza A viruses with pandemic potential.* J Virol, 1998. **72**(9): p. 7367-73.
89. Subbarao, K., et al., *Characterization of an avian influenza A (H5N1) virus isolated from a child with a fatal respiratory illness.* Science, 1998. **279**(5349): p. 393-6.
90. Claas, E.C., et al., *Human influenza A H5N1 virus related to a highly pathogenic avian influenza virus.* Lancet, 1998. **351**(9101): p. 472-7.
91. Claas, E.C., et al., *Human influenza virus A/HongKong/156/97 (H5N1) infection.* Vaccine, 1998. **16**(9-10): p. 977-8.
92. DeLay, P.D., H.L. Casey, and H.S. Tubiash, *Comparative study of fowl plague virus and a virus isolated from man.* Public Health Rep, 1967. **82**(7): p. 615-20.
93. Taylor, H.R. and A.J. Turner, *A case report of fowl plague keratoconjunctivitis.* Br J Ophthalmol, 1977. **61**(2): p. 86-8.
94. Myers, K.P., C.W. Olsen, and G.C. Gray, *Cases of swine influenza in humans: a review of the literature.* Clin Infect Dis, 2007. **44**(8): p. 1084-8.
95. Russell, C.A., et al., *Improving pandemic influenza risk assessment.* Elife, 2014. **3**: p. e03883.
96. Girard, M.P., et al., *Report on the first WHO integrated meeting on development and clinical trials of influenza vaccines that induce broadly protective and long-lasting immune responses: Hong Kong SAR, China, 24-26 January 2013.* Vaccine, 2013. **31**(37): p. 3766-71.
97. Henle, W., *Interference phenomena between animal viruses; a review.* J Immunol, 1950. **64**(3): p. 203-36.

98. Isaacs, A. and J. Lindenmann, *Virus interference. I. The interferon.* Proc R Soc Lond B Biol Sci, 1957. **147**(927): p. 258-67.

99. Isaacs, A., J. Lindenmann, and R.C. Valentine, *Virus interference. II. Some properties of interferon.* Proc R Soc Lond B Biol Sci, 1957. **147**(927): p. 268-73.

100. Lengyel, P., *Biochemistry of interferons and their actions.* Annu Rev Biochem, 1982. **51**: p. 251-82.

101. Mogensen, T.H., *Pathogen recognition and inflammatory signaling in innate immune defenses.* Clin Microbiol Rev, 2009. **22**(2): p. 240-73, Table of Contents.

102. Jaitin, D.A., et al., *Inquiring into the differential action of interferons (IFNs): an IFN-alpha2 mutant with enhanced affinity to IFNAR1 is functionally similar to IFN-beta.* Mol Cell Biol, 2006. **26**(5): p. 1888-97.

103. Kalie, E., et al., *The stability of the ternary interferon-receptor complex rather than the affinity to the individual subunits dictates differential biological activities.* J Biol Chem, 2008. **283**(47): p. 32925-36.

104. Valente, G., et al., *Distribution of interferon-gamma receptor in human tissues.* Eur J Immunol, 1992. **22**(9): p. 2403-12.

105. Kotenko, S.V., et al., *IFN-lambdas mediate antiviral protection through a distinct class II cytokine receptor complex.* Nat Immunol, 2003. **4**(1): p. 69-77.

106. Sheppard, P., et al., *IL-28, IL-29 and their class II cytokine receptor IL-28R.* Nat Immunol, 2003. **4**(1): p. 63-8.

107. Prokunina-Olsson, L., et al., *A variant upstream of IFNL3 (IL28B) creating a new interferon gene IFNL4 is associated with impaired clearance of hepatitis C virus.* Nat Genet, 2013. **45**(2): p. 164-71.

108. Sommereyns, C., et al., *IFN-lambda (IFN-lambda) is expressed in a tissue-dependent fashion and primarily acts on epithelial cells in vivo.* PLoS Pathog, 2008. **4**(3): p. e1000017.

109. Levy, D.E. and J.E. Darnell, Jr., *Stats: transcriptional control and biological impact.* Nat Rev Mol Cell Biol, 2002. **3**(9): p. 651-62.

110. Darnell, J.E., Jr., I.M. Kerr, and G.R. Stark, *Jak-STAT pathways and transcriptional activation in response to IFNs and other extracellular signaling proteins.* Science, 1994. **264**(5164): p. 1415-21.

111. Krishnan, K., et al., *Dimerization of a chimeric CD4-interferon-alpha receptor reconstitutes the signaling events preceding STAT phosphorylation.* Oncogene, 1996. **13**(1): p. 125-33.

112. Heim, M.H., et al., *Contribution of STAT SH2 groups to specific interferon signaling by the Jak-STAT pathway.* Science, 1995. **267**(5202): p. 1347-9.

113. Ivashkiv, L.B. and L.T. Donlin, *Regulation of type I interferon responses.* Nat Rev Immunol, 2014. **14**(1): p. 36-49.

114. Wilkins, C. and M. Gale, Jr., *Recognition of viruses by cytoplasmic sensors.* Curr Opin Immunol, 2010. **22**(1): p. 41-7.

115. Jiang, F., et al., *Structural basis of RNA recognition and activation by innate immune receptor RIG-I.* Nature, 2011. **479**(7373): p. 423-7.

116. Ray, A., et al., *Bacterial cell wall macroamphiphiles: pathogen-/microbe-associated molecular patterns detected by mammalian innate immune system.* Biochimie, 2013. **95**(1): p. 33-42.

117. Botos, I., D.M. Segal, and D.R. Davies, *The structural biology of Toll-like receptors.* Structure, 2011. **19**(4): p. 447-59.

118. Nishiya, T. and A.L. DeFranco, *Ligand-regulated chimeric receptor approach reveals distinctive subcellular localization and signaling properties of the Toll-like receptors.* J Biol Chem, 2004. **279**(18): p. 19008-17.

119. Alexopoulou, L., et al., *Recognition of double-stranded RNA and activation of NF-kappaB by Toll-like receptor 3.* Nature, 2001. **413**(6857): p. 732-8.

120. Schulz, O., et al., *Toll-like receptor 3 promotes cross-priming to virus-infected cells.* Nature, 2005. **433**(7028): p. 887-92.

121. Iwasaki, A. and P.S. Pillai, *Innate immunity to influenza virus infection.* Nat Rev Immunol, 2014. **14**(5): p. 315-28.

122. Diebold, S.S., et al., *Innate antiviral responses by means of TLR7-mediated recognition of single-stranded RNA.* Science, 2004. **303**(5663): p. 1529-31.

123. Lund, J.M., et al., *Recognition of single-stranded RNA viruses by Toll-like receptor 7.* Proc Natl Acad Sci U S A, 2004. **101**(15): p. 5598-603.

124. Kato, H., et al., *Cell type-specific involvement of RIG-I in antiviral response.* Immunity, 2005. **23**(1): p. 19-28.

125. Pichlmair, A., et al., *RIG-I-mediated antiviral responses to single-stranded RNA bearing 5'-phosphates.* Science, 2006. **314**(5801): p. 997-1001.

126. Hornung, V., et al., *5'-Triphosphate RNA is the ligand for RIG-I.* Science, 2006. **314**(5801): p. 994-7.

127. Rehwinkel, J., et al., *RIG-I detects viral genomic RNA during negative-strand RNA virus infection.* Cell, 2010. **140**(3): p. 397-408.

128. Yoneyama, M., et al., *The RNA helicase RIG-I has an essential function in double-stranded RNA-induced innate antiviral responses.* Nat Immunol, 2004. **5**(7): p. 730-7.

129. Saito, T., et al., *Innate immunity induced by composition-dependent RIG-I recognition of hepatitis C virus RNA.* Nature, 2008. **454**(7203): p. 523-7.

130. Uzri, D. and L. Gehrke, *Nucleotide sequences and modifications that determine RIG-I/RNA binding and signaling activities.* J Virol, 2009. **83**(9): p. 4174-84.

131. Kowalinski, E., et al., *Structural basis for the activation of innate immune pattern-recognition receptor RIG-I by viral RNA.* Cell, 2011. **147**(2): p. 423-35.

132. Luo, D., et al., *Structural insights into RNA recognition by RIG-I.* Cell, 2011. **147**(2): p. 409-22.

133. Belgnaoui, S.M., S. Paz, and J. Hiscott, *Orchestrating the interferon antiviral response through the mitochondrial antiviral signaling (MAVS) adapter.* Curr Opin Immunol, 2011. **23**(5): p. 564-72.

134. Franchi, L., et al., *Function of Nod-like receptors in microbial recognition and host defense.* Immunol Rev, 2009. **227**(1): p. 106-28.

135. Schroder, K. and J. Tschopp, *The inflammasomes.* Cell, 2010. **140**(6): p. 821-32.

136. Amin, J., D. Boche, and S. Rakic, *What do we know about the inflammasome in humans?* Brain Pathol, 2016.

137. Kanneganti, T.D., et al., *Critical role for Cryopyrin/Nalp3 in activation of caspase-1 in response to viral infection and double-stranded RNA.* J Biol Chem, 2006. **281**(48): p. 36560-8.

138. Thomas, P.G., et al., *The intracellular sensor NLRP3 mediates key innate and healing responses to influenza A virus via the regulation of caspase-1.* Immunity, 2009. **30**(4): p. 566-75.

139. McAuley, J.L., et al., *Activation of the NLRP3 inflammasome by IAV virulence protein PB1-F2 contributes to severe pathophysiology and disease.* PLoS Pathog, 2013. **9**(5): p. e1003392.

140. Ichinohe, T., I.K. Pang, and A. Iwasaki, *Influenza virus activates inflammasomes via its intracellular M2 ion channel.* Nat Immunol, 2010. **11**(5): p. 404-10.

141. Allen, I.C., et al., *The NLRP3 inflammasome mediates in vivo innate immunity to influenza A virus through recognition of viral RNA.* Immunity, 2009. **30**(4): p. 556-65.

142. Lindenmann, J., *Resistance of mice to mouse-adapted influenza A virus.* Virology, 1962. **16**: p. 203-4.

143. Haller, O., M. Acklin, and P. Staeheli, *Influenza virus resistance of wild mice: wild-type and mutant Mx alleles occur at comparable frequencies.* J Interferon Res, 1987. **7**(5): p. 647-56.

144. Staeheli, P., et al., *Influenza virus-susceptible mice carry Mx genes with a large deletion or a nonsense mutation.* Mol Cell Biol, 1988. **8**(10): p. 4518-23.

145. Haller, O. and G. Kochs, *Interferon-induced mx proteins: dynamin-like GTPases with antiviral activity.* Traffic, 2002. **3**(10): p. 710-7.

146. Verhelst, J., P. Hulpiau, and X. Saelens, *Mx proteins: antiviral gatekeepers that restrain the uninvited.* Microbiol Mol Biol Rev, 2013. **77**(4): p. 551-66.

147. Staeheli, P. and O. Haller, *Interferon-induced human protein with homology to protein Mx of influenza virus-resistant mice.* Mol Cell Biol, 1985. **5**(8): p. 2150-3.

148. Aebi, M., et al., *cDNA structures and regulation of two interferon-induced human Mx proteins.* Mol Cell Biol, 1989. **9**(11): p. 5062-72.

149. King, M.C., G. Raposo, and M.A. Lemmon, *Inhibition of nuclear import and cell-cycle progression by mutated forms of the dynamin-like GTPase MxB.* Proc Natl Acad Sci U S A, 2004. **101**(24): p. 8957-62.

150. Liu, Z., et al., *The interferon-inducible MxB protein inhibits HIV-1 infection.* Cell Host Microbe, 2013. **14**(4): p. 398-410.

151. Goujon, C., et al., *Human MX2 is an interferon-induced post-entry inhibitor of HIV-1 infection.* Nature, 2013. **502**(7472): p. 559-62.

152. Pavlovic, J., O. Haller, and P. Staeheli, *Human and mouse Mx proteins inhibit different steps of the influenza virus multiplication cycle.* J Virol, 1992. **66**(4): p. 2564-9.

153. Gao, S., et al., *Structure of myxovirus resistance protein a reveals intra- and intermolecular domain interactions required for the antiviral function.* Immunity, 2011. **35**(4): p. 514-25.

154. Nigg, P.E. and J. Pavlovic, *Oligomerization and GTP-binding Requirements of MxA for Viral Target Recognition and Antiviral Activity against Influenza A Virus.* J Biol Chem, 2015. **290**(50): p. 29893-906.

155. Zimmermann, P., et al., *The viral nucleoprotein determines Mx sensitivity of influenza A viruses.* J Virol, 2011. **85**(16): p. 8133-40.

156. Manz, B., et al., *Pandemic influenza A viruses escape from restriction by human MxA through adaptive mutations in the nucleoprotein.* PLoS Pathog, 2013. **9**(3): p. e1003279.

157. Dauber, B. and T. Wolff, *Activation of the Antiviral Kinase PKR and Viral Countermeasures.* Viruses, 2009. **1**(3): p. 523-44.

158. Dauber, B., et al., *Influenza B virus ribonucleoprotein is a potent activator of the antiviral kinase PKR.* PLoS Pathog, 2009. **5**(6): p. e1000473.

159. Galabru, J. and A. Hovanessian, *Autophosphorylation of the protein kinase dependent on double-stranded RNA.* J Biol Chem, 1987. **262**(32): p. 15538-44.

160. Chong, K.L., et al., *Human p68 kinase exhibits growth suppression in yeast and homology to the translational regulator GCN2.* EMBO J, 1992. **11**(4): p. 1553-62.

161. Hershey, J.W., *Translational control in mammalian cells.* Annu Rev Biochem, 1991. **60**: p. 717-55.

162. Kumar, A., et al., *Double-stranded RNA-dependent protein kinase activates transcription factor NF-kappa B by phosphorylating I kappa B.* Proc Natl Acad Sci U S A, 1994. **91**(14): p. 6288-92.

163. Balachandran, S., et al., *Essential role for the dsRNA-dependent protein kinase PKR in innate immunity to viral infection.* Immunity, 2000. **13**(1): p. 129-41.

164. Min, J.Y., et al., *A site on the influenza A virus NS1 protein mediates both inhibition of PKR activation and temporal regulation of viral RNA synthesis.* Virology, 2007. **363**(1): p. 236-43.

165. Hovanessian, A.G. and J. Justesen, *The human 2'-5'oligoadenylate synthetase family: unique interferon-inducible enzymes catalyzing 2'-5' instead of 3'-5' phosphodiester bond formation.* Biochimie, 2007. **89**(6-7): p. 779-88.

166. Hovanessian, A.G., *Interferon-induced and double-stranded RNA-activated enzymes: a specific protein kinase and 2',5'-oligoadenylate synthetases.* J Interferon Res, 1991. **11**(4): p. 199-205.

167. Min, J.Y. and R.M. Krug, *The primary function of RNA binding by the influenza A virus NS1 protein in infected cells: Inhibiting the 2'-5' oligo (A) synthetase/RNase L pathway.* Proc Natl Acad Sci U S A, 2006. **103**(18): p. 7100-5.

168. Bauman, D.R., et al., *25-Hydroxycholesterol secreted by macrophages in response to Toll-like receptor activation suppresses immunoglobulin A production.* Proc Natl Acad Sci U S A, 2009. **106**(39): p. 16764-9.

169. Park, K. and A.L. Scott, *Cholesterol 25-hydroxylase production by dendritic cells and macrophages is regulated by type I interferons.* J Leukoc Biol, 2010. **88**(6): p. 1081-7.

170. Holmes, R.S., J.L. Vandeberg, and L.A. Cox, *Genomics and proteomics of vertebrate cholesterol ester lipase (LIPA) and cholesterol 25-hydroxylase (CH25H).* 3 Biotech, 2011. **1**(2): p. 99-109.

171. Liu, S.Y., et al., *Interferon-inducible cholesterol-25-hydroxylase broadly inhibits viral entry by production of 25-hydroxycholesterol.* Immunity, 2013. **38**(1): p. 92-105.

172. Blanc, M., et al., *The transcription factor STAT-1 couples macrophage synthesis of 25-hydroxycholesterol to the interferon antiviral response.* Immunity, 2013. **38**(1): p. 106-18.

173. Gold, E.S., et al., *25-Hydroxycholesterol acts as an amplifier of inflammatory signaling.* Proc Natl Acad Sci U S A, 2014. **111**(29): p. 10666-71.

174. Friedman, R.L., et al., *Transcriptional and posttranscriptional regulation of interferon-induced gene expression in human cells.* Cell, 1984. **38**(3): p. 745-55.

175. Reid, L.E., et al., *A single DNA response element can confer inducibility by both alpha- and gamma-interferons.* Proc Natl Acad Sci U S A, 1989. **86**(3): p. 840-4.

176. Lange, U.C., et al., *The fragilis interferon-inducible gene family of transmembrane proteins is associated with germ cell specification in mice.* BMC Dev Biol, 2003. **3**: p. 1.

177. Takahashi, S., et al., *TAPA-1, the target of an antiproliferative antibody, is associated on the cell surface with the Leu-13 antigen.* J Immunol, 1990. **145**(7): p. 2207-13.

178. Deblandre, G.A., et al., *Expression cloning of an interferon-inducible 17-kDa membrane protein implicated in the control of cell growth.* J Biol Chem, 1995. **270**(40): p. 23860-6.

179. Chen, Y.X., et al., *Induction of T cell aggregation by antibody to a 16kd human leukocyte surface antigen.* J Immunol, 1984. **133**(5): p. 2496-501.

180. Evans, S.S., et al., *Monoclonal antibody to the interferon-inducible protein Leu-13 triggers aggregation and inhibits proliferation of leukemic B cells.* Blood, 1990. **76**(12): p. 2583-93.

181. Matsumoto, A.K., et al., *Functional dissection of the CD21/CD19/TAPA-1/Leu-13 complex of B lymphocytes.* J Exp Med, 1993. **178**(4): p. 1407-17.

182. Alber, D. and P. Staeheli, *Partial inhibition of vesicular stomatitis virus by the interferon-induced human 9-27 protein.* J Interferon Cytokine Res, 1996. **16**(5): p. 375-80.

183. Zhu, H. and C. Liu, *Interleukin-1 inhibits hepatitis C virus subgenomic RNA replication by activation of extracellular regulated kinase pathway.* J Virol, 2003. **77**(9): p. 5493-8.

184. Brass, A.L., et al., *The IFITM proteins mediate cellular resistance to influenza A H1N1 virus, West Nile virus, and dengue virus.* Cell, 2009. **139**(7): p. 1243-54.

185. Bailey, C.C., et al., *Ifitm3 limits the severity of acute influenza in mice.* PLoS Pathog, 2012. **8**(9): p. e1002909.

186. Everitt, A.R., et al., *IFITM3 restricts the morbidity and mortality associated with influenza.* Nature, 2012. **484**(7395): p. 519-23.

187. Yang, X., et al., *Interferon-Inducible Transmembrane Protein 3 Genetic Variant rs12252 and Influenza Susceptibility and Severity: A Meta-Analysis.* PLoS One, 2015. **10**(5): p. e0124985.

188. Williams, D.E., et al., *IFITM3 polymorphism rs12252-C restricts influenza A viruses.* PLoS One, 2014. **9**(10): p. e110096.

189. Wilkins, J., et al., *Nonhuman Primate IFITM Proteins Are Potent Inhibitors of HIV and SIV.* PLoS One, 2016. **11**(6): p. e0156739.

190. Lu, J., et al., *The IFITM proteins inhibit HIV-1 infection.* J Virol, 2011. **85**(5): p. 2126-37.

191. Weidner, J.M., et al., *Interferon-induced cell membrane proteins, IFITM3 and tetherin, inhibit vesicular stomatitis virus infection via distinct mechanisms.* J Virol, 2010. **84**(24): p. 12646-57.

192. Savidis, G., et al., *The IFITMs Inhibit Zika Virus Replication.* Cell Rep, 2016. **15**(11): p. 2323-30.

193. Huang, I.C., et al., *Distinct patterns of IFITM-mediated restriction of filoviruses, SARS coronavirus, and influenza A virus.* PLoS Pathog, 2011. **7**(1): p. e1001258.

194. Mudhasani, R., et al., *IFITM-2 and IFITM-3 but not IFITM-1 restrict Rift Valley fever virus.* J Virol, 2013. **87**(15): p. 8451-64.

195. Zhang, Z., et al., *Evolutionary dynamics of the interferon-induced transmembrane gene family in vertebrates.* PLoS One, 2012. **7**(11): p. e49265.

196. Moffatt, P., et al., *Bril: a novel bone-specific modulator of mineralization.* J Bone Miner Res, 2008. **23**(9): p. 1497-508.

197. Sallman Almen, M., et al., *The dispanins: a novel gene family of ancient origin that contains 14 human members.* PLoS One, 2012. **7**(2): p. e31961.

198. Li, K., et al., *IFITM proteins restrict viral membrane hemifusion.* PLoS Pathog, 2013. **9**(1): p. e1003124.

199. Yount, J.S., R.A. Karssemeijer, and H.C. Hang, *S-palmitoylation and ubiquitination differentially regulate interferon-induced transmembrane protein 3 (IFITM3)-mediated resistance to influenza virus.* J Biol Chem, 2012. **287**(23): p. 19631-41.

200. Jia, R., et al., *The N-terminal region of IFITM3 modulates its antiviral activity by regulating IFITM3 cellular localization.* J Virol, 2012. **86**(24): p. 13697-707.

201. Bailey, C.C., et al., *Interferon-induced transmembrane protein 3 is a type II transmembrane protein.* J Biol Chem, 2013. **288**(45): p. 32184-93.

202. Bailey, C.C., et al., *IFITM-Family Proteins: The Cell's First Line of Antiviral Defense.* Annu Rev Virol, 2014. **1**: p. 261-283.

203. Feeley, E.M., et al., *IFITM3 inhibits influenza A virus infection by preventing cytosolic entry.* PLoS Pathog, 2011. **7**(10): p. e1002337.

204. Wakim, L.M., et al., *Enhanced survival of lung tissue-resident memory CD8(+) T cells during infection with influenza virus due to selective expression of IFITM3.* Nat Immunol, 2013. **14**(3): p. 238-45.

205. Yount, J.S., et al., *Palmitoylome profiling reveals S-palmitoylation-dependent antiviral activity of IFITM3.* Nat Chem Biol, 2010. **6**(8): p. 610-4.

206. Chesarino, N.M., T.M. McMichael, and J.S. Yount, *E3 Ubiquitin Ligase NEDD4 Promotes Influenza Virus Infection by Decreasing Levels of the Antiviral Protein IFITM3.* PLoS Pathog, 2015. **11**(8): p. e1005095.

207. Malakhova, O.A. and D.E. Zhang, *ISG15 inhibits Nedd4 ubiquitin E3 activity and enhances the innate antiviral response.* J Biol Chem, 2008. **283**(14): p. 8783-7.

208. Shan, Z., et al., *Negative regulation of interferon-induced transmembrane protein 3 by SET7-mediated lysine monomethylation.* J Biol Chem, 2013. **288**(49): p. 35093-103.

209. Jia, R., et al., *Identification of an endocytic signal essential for the antiviral action of IFITM3.* Cell Microbiol, 2014. **16**(7): p. 1080-93.

210. Desai, T.M., et al., *IFITM3 restricts influenza A virus entry by blocking the formation of fusion pores following virus-endosome hemifusion.* PLoS Pathog, 2014. **10**(4): p. e1004048.

211. Lin, T.Y., et al., *Amphotericin B increases influenza A virus infection by preventing IFITM3-mediated restriction.* Cell Rep, 2013. **5**(4): p. 895-908.

212. Parasassi, T., et al., *Two-photon fluorescence microscopy of laurdan generalized polarization domains in model and natural membranes.* Biophys J, 1997. **72**(6): p. 2413-29.

213. John, S.P., et al., *The CD225 domain of IFITM3 is required for both IFITM protein association and inhibition of influenza A virus and dengue virus replication.* J Virol, 2013. **87**(14): p. 7837-52.

214. Amini-Bavil-Olyaee, S., et al., *The antiviral effector IFITM3 disrupts intracellular cholesterol homeostasis to block viral entry.* Cell Host Microbe, 2013. **13**(4): p. 452-64.

215. Compton, A.A., et al., *IFITM proteins incorporated into HIV-1 virions impair viral fusion and spread.* Cell Host Microbe, 2014. **16**(6): p. 736-47.

216. Tartour, K., et al., *IFITM proteins are incorporated onto HIV-1 virion particles and negatively imprint their infectivity.* Retrovirology, 2014. **11**: p. 103.

217. Yu, J., et al., *IFITM Proteins Restrict HIV-1 Infection by Antagonizing the Envelope Glycoprotein.* Cell Rep, 2015. **13**(1): p. 145-56.

218. Rojek, J.M. and S. Kunz, *Cell entry by human pathogenic arenaviruses.* Cell Microbiol, 2008. **10**(4): p. 828-35.

219. Diamond, M.S. and M. Farzan, *The broad-spectrum antiviral functions of IFIT and IFITM proteins.* Nat Rev Immunol, 2013. **13**(1): p. 46-57.

220. Tanaka, S.S. and Y. Matsui, *Developmentally regulated expression of mil-1 and mil-2, mouse interferon-induced transmembrane protein like genes, during formation and differentiation of primordial germ cells.* Mech Dev, 2002. **119 Suppl 1**: p. S261-7.

221. Tanaka, S.S., et al., *IFITM/Mil/fragilis family proteins IFITM1 and IFITM3 play distinct roles in mouse primordial germ cell homing and repulsion.* Dev Cell, 2005. **9**(6): p. 745-56.

222. Saitou, M., S.C. Barton, and M.A. Surani, *A molecular programme for the specification of germ cell fate in mice.* Nature, 2002. **418**(6895): p. 293-300.

223. Compton, A.A., et al., *Natural mutations in IFITM3 modulate post-translational regulation and toggle antiviral specificity.* EMBO Rep, 2016. **17**(11): p. 1657-1671.

224. Anafu, A.A., et al., *Interferon-inducible transmembrane protein 3 (IFITM3) restricts reovirus cell entry.* J Biol Chem, 2013. **288**(24): p. 17261-71.

225. Xie, M., et al., *Human cytomegalovirus exploits interferon-induced transmembrane proteins to facilitate morphogenesis of the virion assembly compartment.* J Virol, 2015. **89**(6): p. 3049-61.

226. Zhao, X., et al., *Interferon induction of IFITM proteins promotes infection by human coronavirus OC43.* Proc Natl Acad Sci U S A, 2014. **111**(18): p. 6756-61.

227. Bradbury, L.E., et al., *The CD19/CD21 signal transducing complex of human B lymphocytes includes the target of antiproliferative antibody-1 and Leu-13 molecules.* J Immunol, 1992. **149**(9): p. 2841-50.

228. Warren, C.J., et al., *The antiviral restriction factors IFITM1, 2 and 3 do not inhibit infection of human papillomavirus, cytomegalovirus and adenovirus.* PLoS One, 2014. **9**(5): p. e96579.

229. Miller, L.C., et al., *Evolutionary characterization of pig interferon-inducible transmembrane gene family and member expression dynamics in tracheobronchial lymph nodes of pigs infected with swine respiratory disease viruses.* Vet Immunol Immunopathol, 2014. **159**(3-4): p. 180-91.

230. Jia, R., et al., *The C-terminal sequence of IFITM1 regulates its anti-HIV-1 activity.* PLoS One, 2015. **10**(3): p. e0118794.

231. Hoffmann, H.H., P. Palese, and M.L. Shaw, *Modulation of influenza virus replication by alteration of sodium ion transport and protein kinase C activity.* Antiviral Res, 2008. **80**(2): p. 124-34.

232. Dittmann, J., et al., *Influenza A virus strains differ in sensitivity to the antiviral action of Mx-GTPase.* J Virol, 2008. **82**(7): p. 3624-31.

233. Reed, M.L., et al., *The pH of activation of the hemagglutinin protein regulates H5N1 influenza virus pathogenicity and transmissibility in ducks.* J Virol, 2010. **84**(3): p. 1527-35.

234. Brown, J.D., et al., *Persistence of H5 and H7 avian influenza viruses in water.* Avian Dis, 2007. **51**(1 Suppl): p. 285-9.

235. Alexander, D.J., *A review of avian influenza in different bird species.* Vet Microbiol, 2000. **74**(1-2): p. 3-13.

236. Cornelissen, J.B., et al., *Differences in highly pathogenic avian influenza viral pathogenesis and associated early inflammatory response in chickens and ducks.* Avian Pathol, 2013. **42**(4): p. 347-64.

237. Smith, J., et al., *A comparative analysis of host responses to avian influenza infection in ducks and chickens highlights a role for the interferon-induced transmembrane proteins in viral resistance.* BMC Genomics, 2015. **16**: p. 574.

238. Blyth, G.A., et al., *Duck Interferon-Inducible Transmembrane Protein 3 Mediates Restriction of Influenza Viruses.* J Virol, 2015. **90**(1): p. 103-16.

239. Barber, M.R., et al., *Association of RIG-I with innate immunity of ducks to influenza.* Proc Natl Acad Sci U S A, 2010. **107**(13): p. 5913-8.

240. Smith, S.E., et al., *Chicken interferon-inducible transmembrane protein 3 restricts influenza viruses and lyssaviruses in vitro.* J Virol, 2013. **87**(23): p. 12957-66.

241. Benfield, C.T., et al., *Bat and pig IFN-induced transmembrane protein 3 restrict cell entry by influenza virus and lyssaviruses.* J Gen Virol, 2015. **96**(Pt 5): p. 991-1005.

242. Schoggins, J.W. and C.M. Rice, *Interferon-stimulated genes and their antiviral effector functions.* Curr Opin Virol, 2011. **1**(6): p. 519-25.

243. Schoggins, J.W., et al., *A diverse range of gene products are effectors of the type I interferon antiviral response.* Nature, 2011. **472**(7344): p. 481-5.

244. Neil, S.J., T. Zang, and P.D. Bieniasz, *Tetherin inhibits retrovirus release and is antagonized by HIV-1 Vpu.* Nature, 2008. **451**(7177): p. 425-30.

245. McNatt, M.W., T. Zang, and P.D. Bieniasz, *Vpu binds directly to tetherin and displaces it from nascent virions.* PLoS Pathog, 2013. **9**(4): p. e1003299.

246. Perez-Caballero, D., et al., *Tetherin inhibits HIV-1 release by directly tethering virions to cells.* Cell, 2009. **139**(3): p. 499-511.

247. Ohtomo, T., et al., *Molecular cloning and characterization of a surface antigen preferentially overexpressed on multiple myeloma cells.* Biochem Biophys Res Commun, 1999. **258**(3): p. 583-91.

248. Yondola, M.A., et al., *Budding capability of the influenza virus neuraminidase can be modulated by tetherin.* J Virol, 2011. **85**(6): p. 2480-91.

249. Watanabe, R., G.P. Leser, and R.A. Lamb, *Influenza virus is not restricted by tetherin whereas influenza VLP production is restricted by tetherin.* Virology, 2011. **417**(1): p. 50-6.

250. Bruce, E.A., et al., *Release of filamentous and spherical influenza A virus is not restricted by tetherin.* J Gen Virol, 2012. **93**(Pt 5): p. 963-9.

251. Winkler, M., et al., *Influenza A virus does not encode a tetherin antagonist with Vpu-like activity and induces IFN-dependent tetherin expression in infected cells.* PLoS One, 2012. **7**(8): p. e43337.

252. Gnirss, K., et al., *Tetherin Sensitivity of Influenza A Viruses Is Strain Specific: Role of Hemagglutinin and Neuraminidase.* J Virol, 2015. **89**(18): p. 9178-88.

253. Moules, V., et al., *Importance of viral genomic composition in modulating glycoprotein content on the surface of influenza virus particles.* Virology, 2011. **414**(1): p. 51-62.

254. Helbig, K.J., et al., *Viperin is induced following dengue virus type-2 (DENV-2) infection and has anti-viral actions requiring the C-terminal end of viperin.* PLoS Negl Trop Dis, 2013. **7**(4): p. e2178.

255. Nasr, N., et al., *HIV-1 infection of human macrophages directly induces viperin which inhibits viral production.* Blood, 2012. **120**(4): p. 778-88.

256. Wang, X., E.R. Hinson, and P. Cresswell, *The interferon-inducible protein viperin inhibits influenza virus release by perturbing lipid rafts.* Cell Host Microbe, 2007. **2**(2): p. 96-105.

257. Tan, K.S., et al., *In vivo and in vitro studies on the antiviral activities of viperin against influenza H1N1 virus infection.* J Gen Virol, 2012. **93**(Pt 6): p. 1269-77.

258. Billcliff, P.G., et al., *CD317/tetherin is an organiser of membrane microdomains.* J Cell Sci, 2013. **126**(Pt 7): p. 1553-64.

Acknowledgments

My PhD was a very happy time I was fortunate to enjoy at the Institute of Medical Virology in a nice atmosphere under great supervision with colleagues who have become friends.
In particular I would like to thank:

Silke: Thank you for the opportunity to do my PhD in your lab, for your great supervision and support. I really appreciated how you always had time for me whenever I needed help. Thank you for your trust and the freedom you gave me.

The Stertz lab (past & present): Marie, Emilio, Umut, Thomas, Eva, Annika and Dario, thank you for the great time, the nice working atmosphere, your help, funny conversations & lab lunch. Eva, Emilio and Dario, thank you for your help with the IFITM projects.
Eva, I was very fortunate to have had you as a master student and I'm happy you've become a friend.
Marie, my PhD would have been half as much fun without you, thanks for your help and advice and most of all for your friendship.

The Hale & the Pavlovic lab (past & present): Thank you for your help and input regarding science, but also for the nice atmosphere in our office, the chats, the Perplexus Epic challenge, the girl's nights and the Mario Kart dinners.

The Trkola lab: Thank you for the nice working and coffee room atmosphere and your input during progress meetings. Lucie: thank you for all the social activities you organized, I really appreciated it and enjoyed it a lot.

Fabienne & Hanna: Thank you for our jogging rounds that I came to love not only for jogging, but also for our conversations and the nice time we've spent.

My PhD Committee: Silke, Alexandra, Nicolas and Christian, thank you for accompanying me during the course of my PhD with helpful discussions, encouragement and input during my Committee meetings.

Eva, Nick, Monika, Jacqueline, Therese, Jothi, Slavi, Burcu and Flo: thank you for your readiness to help and make the IMV such a pleasant place to work in.

My family & friends: Mami, Papi, Nati and Roger, thank you for always being there for me no matter what, for your constant support, understanding and love. I'm incredibly grateful for having you.

Curriculum Vitae

Personal Details

Name:	LANZ
First Name:	Caroline
Date of Birth:	November 21st 1987
Place of citizenship:	Rütschelen BE

Education

January 2013 – May 2017	**PhD programme in Microbiology & Immunology** University of Zurich, Switzerland Group of Prof. Dr. Silke Stertz, Institute of Medical Virology "Characterization of Human and Swine IFITM-Mediated Restriction of Influenza A Virus"
January 2011 – December 2012	**Master of Science (MSc) ETH in Biology** ETH Zurich, Switzerland Specialization: Microbiology and Immunology
Masterthesis:	Group of Prof. Dr. Alexandra Trkola, Institute of Medical Virology, University of Zurich, Switzerland "Characterization of the HIV-2/SIV entry process in comparison to HIV-1"
Research Internship I:	Group of Prof. Dr. M. Aebi, Institute of Microbiology, ETH Zurich, Switzerland "Enrichment of glycoproteins from *Caenorhabditis elegans* binding to the fungal lectins RedA and CGL2 / Cloning and characterization of the RedA homolog present in *Laccaria bicolor*"

Research Project II:	Group of Prof. Dr. W.-D. Hardt, Institute of Microbiology, ETH Zurich, Switzerland "The host cell factor Vasp and its impact on *Salmonella Typhimurium* docking/invasion"
September 2007 – September 2010	**Bachelor of Science (BSc) ETH in Food Science** ETH Zurich, Switzerland
August 2002 – August 2006	**General Qualification for University Entrance (Matura)** Kantonsschule Zürcher Oberland, Switzerland Major: English & Italian

Work Experience / Internships

January 2013 – May 2017	**University of Zurich, Switzerland** Institute of Medical Virology: **Doctoral Candidate** in the laboratory of **Prof. Dr. Silke Stertz** Characterization of the IFITM-mediated restriction of Influenza A Viruses.
October 2010 – December 2010	**Zentrallabor Coop, Basel, Switzerland** **Internship** on gas chromatography (GC) and tandem mass spectrometry (MS/MS) Characterization and validation of fragments generated from two fungicides (Captan and Folpet) extracted from fruit and vegetable samples.
July 2009	**ETH Zurich, Switzerland** **Teaching assistant** for the Chemistry revision course for 1st year students

Conference Presentations

LS2 annual meeting 2017	Zurich, Switzerland, 2017 poster presentation
Swiss Society for Microbiology annual meeting 2016	Bern, Switzerland, 2016 oral presentation
6th Swiss Virology Meeting	Thun, Switzerland, 2016 poster presentation
Viruses 2016 – At the Forefront of Virus-Host Interactions	Basel, Switzerland, 2016 poster presentation
16th Negative Strand Viruses Meeting	Siena, Italy, 2015 poster presentation
4th International Influenza Meeting	Münster, Germany, 2014 poster presentation
Society for General Microbiology Annual Conference 2014	Liverpool, United Kingdom oral presentation

Grants

January 2016	Travel grant to attend the "Viruses 2016 – At the Fore-Front of Virus-Host Interactions" in Basel, Switzerland issued by the PhD programme in Microbiology & Immunology (MIM)
June 2015	Travel grant to attend the "16th Negative Strand Viruses Meeting" in Siena, Italy issued by the Hartmann-Müller Foundation

Publications

Pohl MO, **Lanz C**, Stertz S. (2016). Late stages of the influenza A virus replication cycle – a tight interplay between virus and host. *Journal of General Virology; 97(9):2058-72, doi: 10.1099/jgv.0.000562*

Lanz C, Yángüez E, Andenmatten D, Stertz S. (2015). Swine interferon-inducible transmembrane proteins potently inhibit influenza A virus replication. *Journal of Virology; 89(1):863-9; doi: 10.1128//JVI.02516-14*